Stony Brook University

Developmental and Receptor-Mediated Pathways Define Acinar Cell Plasticity

A Dissertation Presented

by

Christopher James Halbrook

to

The Graduate School

in Partial Fulfillment of the

Requirements

for the Degree of

Doctor of Philosophy

in

Chemistry

(Chemical Biology)

Stony Brook University

May 2015

Stony Brook University

The Graduate School

Christopher James Halbrook

We, the dissertation committee for the above candidate for the

Doctor of Philosophy degree, hereby recommend

acceptance of this dissertation.

Dr. Isaac Carrico – Dissertation Advisor
Associate Professor - Department of Chemistry

Dr. Nicole Sampson - Chairperson of Defense
Professor – Department of Chemistry

Dr. Wei-Xing Zong
Professor – Department of Molecular Genetics and Microbiology

Dr. Howard Crawford
Professor – Department of Molecular and Integrative Physiology
University of Michigan, Ann Arbor MI

This dissertation is accepted by the Graduate School

Charles Taber
Dean of the Graduate School

Abstract of the Dissertation

Developmental and Receptor-Mediated Pathways Define Acinar Cell Plasticity

by

Christopher James Halbrook

Doctor of Philosophy

in

Chemistry

(Chemical Biology)

Stony Brook University

2015

Pancreatic cancer is the fourth leading cause of cancer related death in the United States with most patients succumbing to the disease within a year of diagnosis. Kras mutations are present in the vast majority of pancreatic cancers, though the full mechanism behind Kras induced tumorigenesis is not well defined. Both the EGFR and Notch signaling pathways have been implicated in the formation of precursor lesions from normal acinar cells in a process known as acinar to ductal metaplasia (ADM). Inhibition of MEK kinase downstream of either EGFR or mutant Kras has been shown to be required for ADM formation and subsequent tumorigenesis in a mouse model of pancreatic cancer. However, pharmacological inhibition of MEK prevents the interrogation of individual MEK isoforms, MEK1 and MEK2. In this study, I describe the generation of two novel mouse models using RNA interference to selectively knockdown MEK1, MEK2, or a combination of both. I then investigated the contributions of MEK kinases in pancreatitis, an inflammatory disease which is a risk factor for pancreatic cancer, and Kras initiated tumorigenesis. I have found that combined knockdown of both MEK1 and MEK2, but not knockdown of either alone, confer protection against chronic pancreatitis, and a partial protection against Kras driven tumorigenesis. I next investigated the roles of EGFR and Notch in ADM using primary acinar explants in an ex vivo transdifferentiation assay, as Notch has been described as a downstream target of EGFR and Ras signaling. Notch induced ADM was blocked by genetic ablation of EGFR in acinar cells, which could be rescued by the expression of oncogenic Kras. Additionally inhibition of MEK kinase was able to block Notch induced ADM in WT acinar cells, and well as the acinar cells lacking EGFR and expressing oncogenic Kras. I further investigated the connection of EGFR and Notch pathway components and found a requirement for MEK signaling in both Notch and Kras driven ADM. Taken together, these results demonstrate a central role of MEK kinase in driving the process of ADM and subsequent development of pancreatic cancer.

Table of Contents

List of Figures:

List of Abbreviations

ADAM	A Disintegrin and Metalloproteinase
ADM	Acinar-to-Ductal-Metaplasia
AP	Acute Pancreatitis
BrdU	Bromodeoxyuridine
cDNA	Complementary DNA
CM	Conditioned Media
CP	Chronic Pancreatitis
CPE	Cytopathic Effect
DMEM	Dulbecco's Modified Eagle Medium
DNA	Deoxyribonucleic Acid
Dox	Doxycycline
DPBS	Dulbecco's Phosphate-Buffered Saline
dsRNA	Double stranded RNA
DUSP	Dual-specificity Phosphatase
ECD	Extra-cellular domain
ES	Embryonic Stem-cell
FBS	Fetal Bovine Serum
GAP	GTPase-Activating Protein
gDNA	Genomic DNA
GEF	Guanine Nucleotide Exchange Factor
GFP	Green Fluorescent Protein
HBSS	Hank's Balanced Salt Solution
ICD	Intercellular domain
IPMN	Intraductal Papillary Mucinous Neoplasm
IRES	Internal Ribosome Entry Site
LN2	Liquid Nitrogen
LPS	Lipopolysaccharide
LSL	Lox-stop-lox
MAPK	Mitogen-activated Protein Kinase
MAPKK	Mitogen-activated Protein Kinase Kinase
MAPKKK	Mitogen-activated Protein Kinase Kinase Kinase
MCN	Mucinous Cystic Neoplasm
miRNA	MicroRNA
MLB	Magnesium Containing Lysis Buffer
MMP	Matrix Metalloproteinase
O/N	Overnight
PAGE	Polyacrylamide Gel Electrophoresis
PanIN	Pancreatic Intraepithelial Neoplasia
PDA	Pancreatic Ductal Adenocarcinoma
PI3K	Phosphoinositide 3-Kinase
PVDF	Polyvinylidene Fluoride

RFP	Red Fluorescent Protein
RIPA	Radioimmunoprecipitation Assay
RNA	Ribonucleic acid
RNAi	RNA interference
μshRNA	Short hairpin RNA
TBS	Tris-Buffered Saline
Tet	Tetracycline
TGF-α	Transforming Growth Factor alpha
TNF-α	Tumor Necrosis Factor Alpha
tTA	Tetracycline transactivator
WT	Wild-type
YFP	Yellow Fluorescent Protein

Acknowledgments

First and foremost, I would like to thank Dr. Howard Crawford for the opportunity to train under his guidance. In the past four years Howard has been a role model as a scientist, not only in terms of success in his field, but also as a person who genuinely cares about his cause. Besides serving as my scientific mentor, Howard has also taught me that no amount of knowledge is trivial, as evidenced by the staggering amount of prize money we have accumulated as a trivia team.

I would also like to thank Dr. Ken Takeuchi, who has proven to be an indispensable ally in the both the lab as well as the home brewery operation. I also need to thank the rest of the people who worked alongside me in Crawford Lab during the past four years, Dr. Hui-Ju Wen, Dr. Jason Hall, Meggie Hoffman, Jeanine Ruggeri, Joshua "Mc"Knight, Gangadaar Thotakura, Louise Peverly, Alex Coomes, Dr. Eileen So-Carpenter, Leslie Scudder, Dr. Christine Ardito, and Dr. Kathleen Delgiorno. Each person in the lab has helped shaped my career by providing me with help, advice, scientifically relevant (and occasionally irrelevant) conversation, as well as life experiences to learn from.

Last but not least, I would also like to thank my friends and family. You have all been a very important support structure to me and I never would have made it to the end of my graduate career, or to my graduate career for that matter, without all of you.

Vita, Publications and/or Fields of Study

Ardito, C.M., Gruner, B.M., Takeuchi, K.K., Lubeseder-Martellato, C., Teichmann, N., Mazur, P.K., Delgiorno, K.E., Carpenter, E.S., **Halbrook, C.J**., Hall, J.C., et al. (2012). **EGF receptor is required for KRAS-induced pancreatic tumorigenesis**. Cancer Cell 22, 304-317.

Delgiorno, K.E., Hall, J.C., Takeuchi, K.K., Pan, F.C., **Halbrook, C.J**., Washington, M.K., Olive, K.P., Spence, J.R., Sipos, B., Wright, C.V., et al. (2014). **Identification and manipulation of biliary metaplasia in pancreatic tumors**. Gastroenterology 146, 233-244 e235.

Wu, C.Y., Carpenter, E.S., Takeuchi, K.K., **Halbrook, C.J**., Peverley, L.V., Bien, H., Hall, J.C., DelGiorno, K.E., Pal, D., Song, Y., et al. (2014). **PI3K Regulation of RAC1 Is Required for KRAS-Induced Pancreatic Tumorigenesis in Mice**. Gastroenterology 147, 1405-1416 e1407.

Chapter 1: Background

Biology of the pancreas

The pancreas is a dual function organ that contains two distinct populations of cells, each providing an important biological function. The first population makes up the pancreatic endocrine system which is responsible for the maintenance of glucose homeostasis. There are five different hormone producing cells types in the pancreatic endocrine system; α cells (glucagon), β cells (insulin), δ cells (somatostatin), ε cells (ghrelin), and PP-cells (pancreatic polypeptide). All five types of cells aggregate to form the islets of Langerhans, although β cells make up the majority of the islet. The islets are tightly associated with blood vessels and neurons, allowing the cells in the islets to secrete the appropriate hormones based on metabolite levels in the blood.

The second function of the pancreas is the production and transport of digestive enzymes to the duodenum. The exocrine system of the pancreas consists of enzyme-secreting acinar cell clusters situated on ductal system which transports digestive enzymes into the main pancreatic duct. Centroacinar cells are located at the junction of the duct terminus and the acinar clusters. The main pancreatic duct joins with the common bile duct to form the hepato-pancreatic duct, which empties into the duodenum to aid in digestion. In humans, the hepato-pancreatic duct junction occurs at the duodenum, whereas in mice the hepato-pancreatic duct junction occurs inside the head of the pancreas. In addition to forming a distribution network for acinar secreted digestive enzymes, the ductal epithelial cells also produce bicarbonates that are important in digestion to neutralize the acidic chyme produced by the stomach, which provides a proper pH for the digestive enzymes to work.

Mouse Pancreas Development

Pancreatic organogenesis

Pancreas development is conserved among mammals, birds, reptiles and amphibians[1]. The pancreas starts as two separate buds, one each on the ventral and dorsal side of the duodenum. In the mouse, pancreas development is first evident around day E9.5, where the dorsal bud forms off the endodermal foregut and protrudes into the mesenchyme. Around day E10, the ventral bud is formed from the ventral foregut. At approximately day E11.5, the gut tube rotates and the ventral bud is brought into contact with the dorsal bud, allowing the two buds to fuse together. Around day E12.5 the epithelial precursor cells become segregated into a "tip" and "trunk" domain, which will go on to an acinar lineage or an endocrine-duct bi-progenitor pool, respectively[2]. At ~E13.5 a differentiation wave occurs, and the mature acinar, ductal, and endocrine lineages all begin to appear and expand.

Transcriptional drivers of pancreas development

Molecular profiling of each stage of pancreas development has led to the discovery of several transcription factors required for the formation of a normal pancreas. Pancreatic and duodenal homeobox 1 (Pdx1) is a transcription factor that is first expressed around E8.5, and is required for pancreas development [3]. In adult mice, Pdx1 expression is seen largely in the beta cells, although a much lower level of expression is also observed in acinar and duct cells (unpublished data). However, lineage tracing has shown that $Pdx1^{+}$ progenitor cells give rise to all three pancreatic cell lineages [4], further demonstrating a central role that Pdx1 plays in pancreatic organogenesis.

Pancreas specific transcription factor 1a (Ptf1a) is expressed around day E9.5 and is required for the development of the exocrine pancreas[5]. Mature endocrine cells are still found in Ptf1a-null embryos, localized in the spleen, however the mice die shortly after birth. The postnatal death of Ptf1a null mice may not be entirely due to exocrine pancreas deficiency, as Ptf1a has also been shown to play a critical role in cerebellar development[6]. Similar to Pdx1, Ptf1a lineage tracing also demonstrates that $Ptf1a^{+}$ progenitor cells give rise to all three pancreatic cell lineages[7]. In the adult mouse, Ptf1a expression is restricted to acinar cells.

Ptf1a is part of the trimeric pancreas specific transcription factor 1 complex (PTF1), which in addition to Ptf1a contains a ubiquitous transcription factor HEB or E2A, and either RBP-J or RBP-JL. It has been shown that in early development, the PTF1 complex contains RBP-J which is gradually replaced with RBP-JL during acinar maturation[8]. The PTF1-RBP-J complex drives the transcription of RBP-JL, which is believed to be part of the mechanism leading to the replacement RBP-J with RBP-JL in the PTF1 complex.

Sox9 is another transcription factor which has been demonstrated to be important in pancreatic development. Sox9 is co-localized with Pdx1 starting at day E9 and the overlap continues until day E12.5[9]. Conditional deletion of Sox9 using a Pdx1 promoter-driven Cre-recombinase generated embryos with impaired pancreas development which were not viable after birth. In adult mice, Sox9 expression is localized to the centroacinar cells and ducts.

The Notch signaling pathway as a repressor of progenitor differentiation

The Notch signaling path consists of four transmembrane receptors (Notch1-4), which are activated by Delta and Jagged extracellular ligands. After activation, the extra-cellular domain (ECD) of the Notch receptor is cleaved by an α-secretase such as ADAM10 or ADAM17. ECD

cleavage exposes a transmembrane binding site for gamma-secretase, which results in an intramembrane cleavage releasing the Notch intracellular domain (NICD) into the cytoplasm. NICD then forms a transcriptional complex with RBP-J and MAML1 in the nucleus. In pancreas development, Notch signaling has been shown to repress progenitor cell differentiation when activated by epithelial expression of FGF10 driven by a Pdx1 promoter[10] or by Notch1-ICD overexpression[11]. Conversely, impairment of Notch signaling in mice deficient for the Notch ligand delta-like 1 (Dll1) or the transcriptional binding partner RBP-J resulted in increased differentiation of endocrine cells[12]. In both genotypes there was with no evidence of exocrine differentiation, although it is likely a result of the early stage of development in which the embryos arrested, E12 for the Dll1 null mice and E9 for the RBP-J null mice. In both mice and zebrafish, Notch has been shown to actively repress acinar differentiation during development[13].

Pancreatitis

Pancreatitis is inflammation of the pancreas. Pancreatitis is classified as either acute pancreatitis or chronic pancreatitis. Acute pancreatitis is a sudden bout of inflammation from which the pancreas is able to recover. In chronic pancreatitis, the inflammation is persistent and causes irreversible damage to the pancreas. Acute pancreatitis is the most common reason for digestive system related hospitalization, with heavy alcohol abuse or the presence of gallstones being most common causes of acute pancreatitis[14]. Acute pancreatitis can also be divided into mild acute pancreatitis where the main pathology is interstitial edema, or severe acute pancreatitis in which the edema is accompanied by pancreatic necrosis which can lead to organ failure[15].

A hallmark of pancreatitis is the inappropriate activation of zymogens inside the pancreas, which results in active digestive enzymes being released inside the pancreas. Because

of this, elevated levels of amylase and lipase in the blood serum can be used as diagnostic biomarkers for patients with acute pancreatitis[16]. Missense mutations in the PRSS1 gene which cause inappropriate trypsin activation have also been linked to hereditary pancreatitis, and expression of an R122H mutant Prss1 in mouse acinar cells is sufficient to induce pancreatitis[17]. Several other methods have been successfully employed to induce pancreatitis in mice including pancreatic ductal ligation[18] and administration of the cholecystokinin analogue cerulein[19]. Administration of ethanol alone does not appear to cause pancreatitis[20], however it has been found that ethanol exposure sensitizes rats to pancreatitis caused by systemic inflammation caused by either lipopolysaccharide (LPS) injection[21] or administration of a high fat diet[22]. LPS injection alone does not appear to cause pancreatitis in mice despite the infiltration of immune cells into the pancreas (unpublished data); however chronic systemic infection with Salmonella enterica serovar Typhimurium bacteria is sufficient to induce chronic pancreatitis[23].

Pancreatic Cancer

Epidemiology of pancreatic cancer

Pancreatic cancer is estimated to be the ninth most commonly diagnosed cancer in the United States, with ~46,000 new cases expected in 2014. However, 40,000 people are estimated to die in the same year from pancreatic cancer, making pancreas cancer the fourth leading cause of cancer related death in the United States[24]. Pancreatic cancer carries a dismal prognosis with the majority of the patients succumbing to the disease within a year of diagnosis, which is reflected in the mortality rate nearly equaling the incidence rate. A recent clinical trial combining nab-paclitaxel and gemcitabine was considered a success compared to the original standard of care, gemcitabine alone, when the median survival of patients in the combination treatment group was extended to 8.5 months from 6.7 months in the gemcitabine alone group[25].

This success story still leaves us with a median survival well under a year, demonstrating the urgent need for advances in the treatment of patients.

A major factor contributing to the high mortality rate of pancreatic cancer is lack of early detection. The disease is often symptomless until it has already spread and begins to interfere with the function of other organs. There are also relatively few risk factors identified, the most prevalent being smoking, long standing diabetes, chronic pancreatitis, and obesity. Each of these conditions carries around a 2% relative risk factor[26]. Approximately 5-10% of pancreatic cancer is thought to be hereditary, however the genetic mechanism of the inherited risk is not usually known.

Precursors to pancreatic cancer

Pancreatic ductal adenocarcinoma (PDA) is the most common and aggressive type of pancreatic cancer, making up about 85% of pancreas cancers. Careful molecular profiling has allowed for the pathological identification of a progression model to pancreatic cancer, beginning with precursor lesions called Pancreatic Intraepithelial Neoplasia (PanINs) which progress into invasive adenocarcinomas. PanINs are benign tumors graded histologically according to morphological characteristics and level of dysplasia. PanIN-1 lesions are characterized by columnar epithelial cells, with basally-oriented round nuclei. PanIN-2 lesions have a loss of nuclear polarity, nuclear crowding, and variation in nuclear size. Besides having enlarged and poorly oriented nuclei, PanIN-3 lesions also have the formation of papillae and cribiform structures, and cells may bud off the epithelium into the lumen of the duct[27]. PanINs are common benign lesions found in most normal pancreata, and lesion incidence increases with age. More PanINs are seen in chronic pancreatitis and PDA patients compared to normal pancreata, and these lesions are of a higher average grade. Patients with PDA are also observed

to have a much higher incidence of PanIN-3 lesions compared to chronic pancreatitis patients[28], which has led to the idea that the presence of PanIN3 lesions are a strong indicator of progression to PDA.

Besides PanINs, two other less common types of precursor lesions have also been identified, Intraductal Papillary Mucinous Neoplasms (IPMNs) and Mucinous Cystic Neoplasm (MCNs). IPMNs are formed from either the main pancreatic duct or a branching side duct, whereas MCNs have no obvious connection to the main duct. MCNs are typically resected and have a very good prognosis, whereas IPMNs are either monitored or resected based on the judgment of the clinician[29].

Genetic drivers of pancreatic cancer

In contrast to the risk factors of pancreatic cancer which are largely unknown, the genetic driver of pancreatic cancer is well characterized, as v-Ki-ras2 Kirsten rat sarcoma viral oncogene homolog (Kras) mutations are found in over 90% of pancreatic cancer patient samples[30]. Approximately 40% of all PanIN-1 lesions harbor a Kras mutation, the frequency of which increases to 87% in PanIN2 and PanIN3 lesions[31]. Since Kras mutations are so found frequently in early precursor lesions, activating Kras mutations are thought to be an initiating event in pancreatic cancer. Another genetic feature thought to occur early in tumor progression is telomere shortening, which is found at a frequency of 96% in all PanIN lesions, including 91% in the lowest grade PanIN-1 lesions. The loci containing the $p16^{Ink4A}$ tumor suppressor gene is found to be inactivated in about 13% of low grade PanINs and around 90% of high grade PanINs, demonstrating that the loss of p16 tumor suppressor protein typically occurs later than Kras mutations in PanIN progression[32]. The activity of tumor suppressor proteins p53 and DPC4 is frequently lost in high grade PanINs, either through loss of expression or mutation. This loss

of function of p53 or DPC4 is not seen in PanIN-1 lesions, again indicating that these mutations are also typically lost later in PanIN progression[33].

Ras signaling

Ras proteins

Besides Kras, there are two other major Ras proteins which have been implicated in cancer, Hras and Nras. There is very little structural difference between Hras, Nras, and Kras, with the exception of the posttranslational modifications to the C-terminal domain. All three isoforms are membrane targeted by the addition of two targeting groups, the first being the addition of a farnesyl group by a farnesyl transferase, however the second targeting signal of Hras and Nras differs from Kras. Kras contains a polybasic region, which automatically results in trafficking primarily to the plasma membrane after farnesylation, whereas Hras and Nras must be palmitoylated to permit targeting to the plasma membrane, and are otherwise located in the Golgi membrane prior to palmitoylation. Palmitoylation is a reversible posttranslational modification, and results in a palmitoylation-depalmitoylation cycle which generates a constant shuffling of Hras and Nras from the plasma membrane to the Golgi[34]. Kras is also the only of one of the three major Ras isoforms required in development. Deletion of Kras results in embryonic lethality where Hras and Nras mice are viable and display no obvious abnormalities[35].

The Ras proteins are small GTPase proteins which act as on-off switches for cellular signaling based on which guanine nucleotide they are bound to. They are in an active state when bound to GTP, which Ras proteins can hydrolyze very slowly to GDP to change to a conformationally inactive state. The hydrolysis process is typically assisted by a the binding of a GTPase-activating protein (GAP) to the GTP bound Ras, which helps stabilize the transition

state intermediate and results in efficient hydrolysis and release of both the nucleotide and the GAP. GDP-bound Ras is locked in a conformationally inactive state until the binding of a guanine nucleotide exchange factors (GEF), usually stimulated by growth factor signaling, reduces the affinity of Ras for the bound nucleotide and leads to release of the nucleotide. After GEF dissociation, Ras then binds a free guanine nucleotide from the cytosol, which is most likely to be GTP due to a ten times higher concentration in the cytosol than GDP[36].

Ras mutations

Oncogenic Ras mutations interrupt the ability of Ras to either hydrolyze the GTP by mutation to the catalytic glutamine-61, or most commonly through mutation to the GAP binding region in codon 12 or 13. Due to the picomolar affinity of Ras for GTP[37] and the nearly millimolar concentration of intercellular GTP[38], inhibition of the enzymatic activity of Ras is highly unlikely. Initial attempts to target Ras with small molecule inhibitors aimed at blocking the posttranslational addition of the farnesyl group required for Ras membrane targeting. However cancer cells challenged in this manner responded by instead substituting the farnesyl modification for a geranylgeranyl modification which was sufficient to restore Ras membrane localization[39]. It has been possible to utilize the cysteine mutation in a $Kras^{G12C}$ mutant to allosterically inhibit binding of the downstream Ras effector Raf *in vitro*[40], providing some evidence that Ras may not be as undruggable as once feared.

Additional work has shown that the Ras GEF Son of sevenless (SOS) may contain an allosteric binding site for mutant RAS which allows for the binding and activation of wild-type Hras and Nras[41]. In line with these observations, Kras mutant cells lines have recently also been shown to have a requirement for other wild-type Ras isoforms to drive proliferation in cancer cells as well. In pancreatic cancer cell lines expressing mutant Kras, the cells also appear to

require the expression of wild-type Hras and Nras isoforms in order to progress through cell cycle checkpoints and avoid DNA damage[42], demonstrating a non-redundant role for Ras isoforms even in a cancer context.

Ras in the EGFR pathway

Ras proteins are typically activated in response to receptor tyrosine kinase binding of growth factors or other signaling molecules. Of particular importance is the epidermal growth factor receptor (EGFR) pathway (Figure 1a). EGFR is one of the four members of the ErbB receptor family. Prior to ligand binding, EGFR (ErbB1) is found as an inactive membrane bound monomer and undergoes a conformational change upon ligand binding which exposes a dimerization domain. The ligand-bound EGFR monomer can interact with another ligand bound EGFR monomer, to create a homodimer, or with another member of the ErbB family to create a heterodimer[43]. All the ErbB family undergo a similar activation for dimerization upon ligand binding in their extracellular domain, with the exception of ErbB2 (Her2/Neu) which lacks an extracellular ligand binding domain. Interestingly, ErbB2 is the preferred binding partner for all the other ErbB receptors despite having no extracellular activation domain[44].

The dimerization of EGFR stimulates the autophosphorylation of several tyrosine residues in the C-terminal domain, which recruits several proteins based on their SH2 domains, including growth factor –receptor bound protein 2 (Grb2). Grb2 is an adapter protein which can then bind the SOS, a Ras GEF capable of stimulating Kras activation. Once activated, Kras can activate the mitogen activated protein kinase (MAPK) cascade by binding to and activating Raf kinase, also known as mitogen activated protein kinase kinase kinase (MAPKKK), which exists in 3 isoforms; a-Raf, b-Raf, and c-Raf. Once activated Raf can then phosphorylate and activate the mitogen activated protein kinase kinase (MAPKK) MEK, which has two isoforms: MEK1

and MEK2. Once stimulated, MEK1/2 can activate the mitogen activated protein kinase (MAPK) protein ERK by phosphorylation, which is also present in two isoforms: ERK1 and ERK2. ERK1/2, once activated, initiates a program of cell growth and proliferation.

Modeling pancreatic cancer in the mouse

As Kras mutations are nearly ubiquitous in pancreatic cancer, mouse models expressing mutant Kras in the pancreas were created in an effort to recapitulate the human disease. The first mouse model to successfully mimic human pancreatic cancer was generated by knocking a $Kras^{G12D}$ cassette into the endogenous Kras locus. The cassette also contained a stop sequence which flanked by two LoxP sites preceding the start codon of the $Kras^{G12D}$ gene, which prevents the expression of mutant Ras unless the stop sequence is recombined out by Cre-recombinase (LSL-$Kras^{G12D}$). Crossing the $Kras^{+/LSL\text{-}G12D}$ mouse with a $Ptf1a^{+/Cre}$ or transgenic Cre under the PDX1 promoter (PDX-Cre) allowed the pancreas specific expression of $Kras^{G12D}$, which generated spontaneous tumorigenesis and displayed the full range of progression from PanIN-1 through PanIN-3 lesions as well as occasional invasive PDA[45].

Consistent with molecular profiling with human PDA, introduction of a p53 mutation by crossing a $p53^{+/R172H}$ allele in the $Kras^{+/G12D}$;$PDX1^{+/Cre}$ to recapitulate later stage PanINs and PDA resulted in a significantly more aggressive and invasive cancer model[46]. Models combining mutant Kras expression with the loss of the tumor suppressor proteins trp53[47] and $p16^{Ink4}$ [48], or dysregulation of SMAD4 signaling either by SMAD4 deletion[49] or TGFBRII deletion[50], also results in a more aggressive model than expression of mutant Kras alone, which is again consistent with these genes being altered in later stages of tumor progression in human patients.

Acinar cells as the cell of origin for pancreatic cancer

Because of the histologically ductal appearance of PanIN precursors to PDA, as well as the presence of ductal differentiation markers such as Sox9 and cytokeratin-19 (CK19) in PDA, the ductal epithelium was assumed to be the origin of PDA. However, transgenic mice targeting the expression of mutant Kras to the ducts of the adult pancreas by fusing a duct-cell specific CK-19 promoter to a mutant Kras expression vector failed to induce neoplasia in the mice[51]. Centroacinar cells, which lie at the junction of acinar and ductal components of the pancreas, have also been proposed to be a potential source of PDA from a study using a mouse model which had a pancreas specific deletion of the PTEN tumor suppressor gene[52], however the pan-pancreatic deletion of PTEN did not allow for an identification of a specific cell lineage as the source of PDA.

A first attempt at more specifically addressing this was done by creating a Kras $^{+/LSLG12Vgeo}$ mouse with both a tetracycline transactivator (tTA) fused to an elastase promoter and a Cre-recombinase under the control of a tet-O operator[53]. The *Elas*-tTA/*tetO*-Cre would allow for prenatal recombination of the LSL-Kras allele in the absence of doxycycline or allow for temporal activation of the mutation Kras allele by removal of doxycycline at a specific time point. By using the elastase promoter, the tTA induced expression of Cre recombinase would be also limited to acinar and centroacinar cells if doxycycline was administered after the pancreas has matured. This model was able to generate a full spectrum of PanINs and PDA originating from the acinar/centroacinar cell compartment when recombination was allowed to occur prenatally. Using this model, it was also observed that mutant Kras activation in adult acinar/centroacinar cells was not sufficient to induce tumorigenesis without the additional stimulus of pancreatitis.

The ability of adult acinar cells to spontaneously generate PanIN lesions without the additional requirement of pancreatitis was done using Cre-ERT recombinase which requires tamoxifen treatment in order to allow Cre-recombinase activity. Using a Cre-ERT^2 fused with either the elastase promoter or the adult acinar cell-specific transcription factor Mist1 to drive Kras$^{+/LSL-G12D}$ recombination in adult acinar cells, spontaneous tumorigenesis was readily observed[54,55]. It is also interesting to note that using the elastase-ERT system to induce mutant Kras in adult acinar cells was able to induce tumorigenesis, however when the same system was used to delete PTEN from adult acinar cells it had no effect[52].

To further investigate the susceptibility of the acinar compartment versus the centroacinar/ductal compartment to transformation by oncogenic Kras, Kopp et. al. targeted mutant Kras to the adult acinar compartment or ductal/centroacinar compartment by crossing the Kras$^{+/LSL-G12D}$ allele into Ptf1a$^{+/CreERT2}$ or Sox9$^{+/CreERT2}$ mice, respectively. Recombination was then induced in the respective compartments by administration of tamoxifen at postnatal day ten, and the addition of a ROSA26$^{LSL-YFP}$ to allow lineage tracing of recombined cells[56]. When mutant Kras^{G12D} was targeted to the acinar compartment, all mice were observed to have abundant PanINs which were YFP positive, indicating acinar cell origin. In contrast, very few PanINs were observed in the Kras$^{+/G12D}$;Sox9$^{+/CreERT2}$ mice of the same age, suggesting that the ductal and centroacinar cells are resistant to Kras induced transformation, whereas acinar cells are readily transformed by mutant Kras. This observation has led the view of the acinar cells as a more likely source of human PDA.

Acinar to ductal metaplasia

Characterization of Acinar to Ductal Metaplasia

While it was originally thought that most epithelial cells were terminally differentiated and derived from lineage specific stem cells, the concept of de-differentiation and transdifferentiation has become more widely accepted[57]. The lack of a defined stem-cell compartment in the pancreas has also raised the possibility of the restorative capability of the normal epithelial cells within the pancreas, including the acinar cells. The observation that acinar cells were capable of undergoing a metaplastic change into duct-like structures was first noted using a mouse model overexpressing TGF-α under a metallothionein promoter or an Elastase promoter[58]. The mechanism of the acinar-to-ductal metaplasia (ADM) event was carefully dissected by Jensen et. al., who observed that amylase RNA expression was lost by acinar cells during cerulein-induced pancreatitis. The normal exocrine programming was replaced by the expression of genes normally seen in embryonic pancreatic precursors such as PDX1 and Notch signaling pathway components[59] as well as elevation of the MAPK pathway. Primary acinar cell explants embedded in collagen have also been shown to undergo ADM in response to recombinant TGF-α treatment, in a gamma-secretase dependent manner[60]. Using the same *in vitro,* methods it was also demonstrated that ductal cysts arise directly from acinar cells using lineage tracing, and that ADM was a direct result of a cell-to-cell conversion since there was less than 10% BrdU incorporation during the transdifferentiation process, which would be insufficient to account for the number of cell in the ductal cysts[61].

In response to pancreatic damage, normal acinar cells undergo ADM, which have been shown to highly proliferative by BrdU incorporation after cerulein treatment[62]. Using lineage tracing it has also been shown that acinar cells which have regenerated after pancreatic damage

due to cerulein or partial pancreatectomy are derived from pre-existing acinar cells[63]. This regenerative capacity of acinar cells was limited to new acinar cells, as no endocrine cells were found to have been regenerated from pre-existing acinar cells. Importantly, ADM lesions in the normal pancreas are transient, and revert back to normal acinar cells by a mechanism that requires the expression of Beta-Catenin. However, when acinar cells contain oncogenic Kras, ADM is unable to re-differentiate back into normal acinar cells and is instead locked into a de-differentiated state, which is able to progress into PanIN lesions[64].

Loss of acinar drivers sensitizes acinar cells to ADM

The process of ADM involves the loss of acinar differentiation and a gain of expression of ductal markers, the loss of expression of genes involved in the maintenance of acinar programming can prime acinar cells for ADM. Acinar cells lacking the expression of Mist1, an acinar-specific transcription factor required to maintain acinar identity[13], undergo TGF-α induced ADM in *in-vitro* assays at a rate much faster than WT acinar cells that express Mist1. As the absence of Mist1 expression creates an easier route to a de-differentiated state, coupling the loss of Mist1 expression with concurrent expression of oncogenic Kras predictably led to significantly increased rate of tumorigenesis in mice[54]. Conversely, forced expression of transgenic Mist1 prevents the conversion of acinar cells into ductal cysts in Matrigel cultures, and also significantly attenuates mutant Kras induced PanIN formation in mice[65].

A similar phenomenon is observed with the nuclear receptor protein Nr5a2. Genetic deletion of Nr5a2 in mice results in a normal pancreas at birth, but leads to the loss of acinar integrity as the mice age. Cultured acinar cells from these mice undergo more rapid ADM than wild type mice, and co-expression of mutant Kras leads to significantly faster tumorigenesis. Additionally, induction of pancreatitis in the mice lacking Nr5a2 resulted in an impaired ability

to resolve the pancreatitis by acinar cell regeneration[64]. It has also been shown that normal levels of Nr5a2 expression are required to maintain acinar homeostasis, as a reduced dose of Nr5a2 by heterozygous deletion of Nr5a2 in mice is sufficient to sensitize the acinar cells to ADM, pancreatitis, and Kras induced tumorigenesis[66].

ADM requires the gain of specific ductal programming

As acinar cells undergo ADM, they begin to express transcription factors present in differentiated ductal epithelial cells such as HNF6 and Sox9. Acinar cells of mice lacking both HNF6 and SOX9 have been shown to be more resistant to pancreatitis induced by pancreatic ductal ligation[67]. Ectopic expression of HNF6, but not Sox9, was then shown to repress acinar markers and induce the expression of ductal markers in an immortalized mouse acinar cell line. *In vivo*, overexpression of Sox9 in acinar cells lead to the induction of ductal genes which was able to sensitize acinar cells to cerulein induced pancreatitis, however overexpression of Sox9 alone was insufficient to fully reprogram acinar cells into a ADM fate[56]. Interestingly, deletion of Sox9 in adult mouse acinar cells is sufficient to block TGF-α induced ADM[68]. Furthermore, deletion of Sox9 coupled with activation of mutant Kras results in a block in tumorigenesis[56,68].

Notch signaling in pancreatic cancer

Activation of Notch pathway components is seen in ADM and throughout PanIN progression, as well as in PDA[60]. The elucidation of the role of Notch signaling in the adult pancreas as well as its role in tumorigenesis and PDA has not been straightforward. Notch signaling, in particular Notch1 receptor, has been shown to be required for exocrine regeneration after cerulein induced pancreatitis[69]. This is relatively consistent with the observation that the concurrent activation of constitutively active Notch signaling by the transgenic expression of Notch1-ICD with mutant Kras leads to a significantly increased rate of tumorigenesis[55], as Notch

signaling is known to be important in the repression of acinar differentiation[13]. However, genetic ablation of the Notch1 receptor in mice with oncogenic Kras also lead to increased and higher grade PanIN formation, implicating Notch1 receptor as a tumor suppressor in pancreatic cancer[70]. Deletion of the Notch2 receptor had the opposite effect when coupled with the expression of oncogenic Kras. Mice still developed tumors, however, they survived significantly longer than mice expressing mutant Kras alone[71]. Again, this contrasted from Notch1 knockout mice with mutant Kras which had a significantly shorter survival timeframe than mice with mutant Kras alone. Using lineage tracing models, Notch1 and Notch2 receptors were found to be localized to the acinar and ductal/centroacinar compartments of the adult pancreas, respectively, while PanIN lesions displayed Notch2 expression but not Notch1 expression[71]. The Notch2 expression but lack of Notch 1 expression could also account for the differences in the phenotypes of the Notch1 versus the Notch2 knockout mice.

EGFR pathway in pancreatic cancer

Ras activity threshold is required for tumorigenesis

As Kras is considered the main driver of pancreatic cancer, much work has been done to elucidate the mechanism by which Kras can induce pancreatic tumorigenesis (Figure 1b). Since Kras appears sufficient to induce pancreatic cancer, it is surprising that mice harboring an allele of mutant Kras are born with grossly normal pancreata, and slowly develop focal lesions over time[45]. Ji et. al. attempted to explain this by levels of Ras activity and subsequent ERK activity as the important factor in driving tumorigenesis. Using a mouse model expressing a conditional transgenic $KRas^{G12V}$ under a human CMV fused with a chicken-β-actin promoter resulted in a higher level of Ras-GTP loading and Ras activity, as measured by ERK phosphorylation, than

$Kras^{G12D}$ driven from the endogenous Kras promoter. As a result, they saw and increase in the rate of tumorigenesis.

The importance of Ras GTP loading, and therefore activity of Ras, was also demonstrated in mice expressing mutant Kras in the absence of EGFR[72,73]. The mice showed a complete lack of tumorigenesis from cells lacking EGFR, as well as significantly lower Ras-GTP and phosphorylated ERK levels. It is important to note that the assay used to determine Ras-GTP levels is unable to distinguish between the WT Kras protein and mutant Kras protein, so while the ablation of EGFR expression resulted in lowered levels of Ras-GTP level, it is still unclear if EGFR signaling results in activation of WT Kras or $Kras^{G12D}$, or both. It was observed that the block in tumorigenesis was unique to the pancreas, as models of mutant Kras tumorigenesis in both the colon and the lung develop tumors in the absence of EGFR expression[73]. However, deletion of the tumor suppressor protein p53 was sufficient to overcome the EGFR-null block in tumorigenesis, demonstrating a role for wild-type p53 for determining the Kras activity and subsequent ERK activation level necessary to transform pancreatic epithelial cells.

The ability to form tumors in the pancreas of the mouse by hyper-activation of MAPK signaling is not a unique property of mutant Kras. Activation of a constitutively active $Braf^{V600E}$ in the pancreas led to PanIN lesions that were morphologically indistinguishable from PanINs in $Kras^{G12D}$ mice generated in the same fashion[74]. Consistent with mutant Ras activation, mutant Braf expression resulted in significantly elevated ERK signaling, again demonstrating the central role of ERK in pancreatic tumorigenesis.

Maintenance of RAS-MEK-ERK signaling is required to maintain PanIN lesions

Kras mutations are sufficient to drive tumorigenesis in mice; however it was unclear if mutant Kras expression was required to maintain tumors after formation. Using an shRNA approach to knockdown Kras in pancreatic cancer cell lines expressing mutant Kras revealed that a subset of cancer was indeed dependent on the maintained expression of mutant Kras[75]. To model this in the mouse, transgenic mice containing a $Kras^{G12D}$ under the control of a tet-O operator were utilized[76,77]. When Kras was expressed, tumors were readily formed in the mice, however once the expression of the transgenic Kras was extinguished, the tumors underwent complete regression. Cell lines created from inducible Kras mice were occasionally able to continue to proliferate after withdrawal of doxycycline from the media. The mechanism of survival in the absence of doxycycline induced expression of mutant Kras appeared to be either driven by loss of doxycycline dependence of the mutant Kras transgene expression, or over expression of the transcription factor YAP1[78]. Importantly, as the tumor lesions regressed, there was a loss of ERK signaling, again demonstrating the central role of ERK activation in PanIN formation and maintenance.

MEK kinase activity is required for pancreatic tumor formation and maintenance

Given the central role of upregulated ERK signaling, starting in early ADM and maintained throughout pancreatic tumorigenesis, inhibition of MEK should have a large impact on the ability of mutant Kras to generate and sustain tumors. In practice, the use of pharmacological inhibitors to block MEK prior to induction of pancreatitis in mice harboring oncogenic Kras does indeed result in a near complete block in tumorigenesis[72,79]. Administration of MEK inhibitors after the establishment of tumors in Kras mice resulted in a regression in the tumor lesions, which, after careful analysis, were revealed to re-differentiate back into acinar

cells[79]. This differed from cells in which oncogenic Kras was withdrawn, which underwent extensive cell death[76].

PI3K signaling in pancreatic cancer

Phosphatidylinositol-3-kinases (PI3K) are a family of enzymes that catalyze the phosphorylation of phosphoinositides in the plasma membrane in response to activation by receptor tyrosine kinases such as EGFR, including the conversion of phosphatidylinositol 4,5-bisphosphate phosphatidylinositol 3-phosphate (PIP_2) to phosphatidylinositol (3,4,5)-trisphosphate (PIP_3) by phosphorylation of the 5' position of the inositol ring. PIP_3 can then recruit proteins containing pleckstrin homology (PH) domains to the cytoplasmic face of the plasma membrane such as AKT kinases and GEFS (Figure 2). Once recruited to the membrane, AKT can be activated by phosphorylation by phosphoinositide dependent kinase 1 (PDPK1) on serine 308 and mammalian target of rapamycin complex 2 (mTORC2) on threonine 473 , both of which are required for activation. After phosphorylation, AKT can then activate a number of pathways which can promote cell survival, growth, and division. PIP_3 can be de-phosphorylated to PIP_2 by the tumor suppressor protein PTEN, which results in dissociation and subsequent loss of signaling of AKT[80].

Hyper-activation of the PI3K pathway by genetic ablation of the tumor suppressor PTEN has been shown to be sufficient for tumorigenesis in the mouse pancreas[52]. Similarly, expression of a constitutively active form of the class I PI3K isoform p110-α, $p110\alpha^{H1047R}$, has also been demonstrated to drive pancreatic tumorigenesis[81]. Mechanistically, this was shown to be through activation of PDPK1, knocking PDPK1 out of both $Kras^{G12D}$ driven and $p110\alpha^{H1047R}$ driven tumor models was sufficient to block ADM and subsequent tumorigenesis. Furthermore, the authors noted that inhibition of AKT downstream of PDPK1 was able to block the formation of

ADM *in vitro*, implicating AKT signaling as the critical node for tumorigenesis. The concept of AKT activation promoting ADM is reinforced by the demonstration that transgenic expression of a constitutively active AKT in the pancreas leads to ADM and tumor formation[82]. It is also important to note that a similar mouse model of $p110\alpha^{H1047R}$ expression in the mouse pancreas failed to induce any discernible phenotype[74]; however the differences in the method of transgene expression might be changing the copy number of $p110\alpha^{H1047R}$ levels, which could partially explain these contrasting observations.

Besides PDPK1 and AKT, PIP_3 can also recruit GEFs responsible for the activation of the small GTPase Ras-related C3 botulinum toxin substrate 1 (RAC1). RAC1 signaling is implicated in many cell signaling processes such as cell cycle, adhesion, and motility[83]. RAC1 is also important in cytoskeletal rearrangement processes. Genetic ablation of RAC1 in the $Kras^{+/G12D}$;$Ptf1a^{+/Cre}$ mouse tumorigenesis model revealed a complete block in tumorigenesis, which was shown to be due to an inability of acinar cells to initiate an actin rearrangement required for stable ADM[84]. PIP_3 initiated RAC-GEF activation has also been tied specifically to RAC1 activity as, knockout of the class I PI3K isoform p110-α phenocopied the loss of RAC1 in preventing $Kras^{G12D}$ induced tumorigenesis[85]. The loss of production of PIP_3 in the p110-α knockout mice corresponded to a loss of activation of the RAC-GEFs VAV1, TIAM1, and DOCK10 which lead to a significantly lower amount of active Rac1 and impaired actin-rearrangement preventing the formation of stable ADM.

RNA interference

The ability of a gene that encodes an RNA sequence with the potential to influence the transcript levels of other RNAs was first described in *Caenorhabditis elegans* (*C. elegans*) with

the discovery that a 22 nucleotide section of the lin-4 transcript contained a sequence complementary to a repeated sequence in the 3' untranslated region of the lin-14, and the RNA-RNA interaction negatively regulated lin-14 translation[86]. The idea of RNA interference (RNAi) was better clarified with the observation that although sense and antisense strands of RNA were capable of causing interference[87], double stranded RNA (dsRNA) was significantly more effective in modulating transcript levels of the target RNA[88]. It was also noted that there did not appear to be a stoichiometric relationship between the amount of dsRNA injected and the amount of transcript it was able affect, which would prove to be an important observation in the development of the mechanism of RNAi.

Small RNAs have since been largely divided into two classes; microRNAs (miRNA) like lin-4 which are present in the genome of an organism and serve to regulate endogenous genes, and small interfering RNAs (siRNA) which are primarily introduced exogenously to cells and thought to serve as genome defense[89]. In human cells, dsRNA strands are bound to the RISC-loader complex, which is a trimeric complex consisting of the Dicer, TRBP, and Ago-2 proteins. Once loaded, the dsRNA strands are cleaved by Dicer to the 21-23 nucleotide double stranded siRNA sequence. The double stranded siRNA is the unwound and then one side of the duplex known as the guide strand is then loaded into Ago-2, while the second "passenger strand" is discarded. The preference of one strand over the other appears to be thermodynamically driven, as introduction of thermodynamic instability in the 5' end of one siRNA strand has been shown to lead to preferential accumulation of that strand in the RISC complex[90]. The RISC complex can then use the guide strand to base pair with mRNA transcripts. Binding of mRNA by the RISC-complex induces cleavage of the mRNA by Ago-2. The cleaved mRNA is the dissociated and the RISC-complex can bind a new mRNA transcript, leading to the non-stoichiometric level

of transcript regulation. The siRNA cleavage of a gene resulting in the loss of the target mRNA transcript has been termed gene knockdown.

miRNAs are produced as a primary miRNA and undergo several levels of processing to produce a mature miRNA. The primary miRNA folds into a stem-loop structure which is first cleaved by the enzyme Drosha. The cleavage product is the transported to the cytoplasm and further cleaved to the 21-23 nucleotide mature miRNA by Dicer-TBRP- Ago-2 RISC loading complex. The double stranded miRNA is then unwound and loaded onto Ago-2, again in a manner favoring the more thermodynamically unstable strand. In contrast to siRNA-RISC complexes, miRNA-RISC complexes can regulate mRNA targets on multiple levels. A perfect match of the miRNA guide strand can result in Ago-2 cleavage, similar to siRNA-RISC cleavage, however miRNA-RISC complexes are capable of binding mRNAs with mismatches as well. This can lead to alternate methods of mRNA cleavage, or the miRNA-RISC complex can lead to a block in translation[89].

In molecular biology, siRNA duplexes are often introduced into cells by transfection to induce transient knockdown of a gene target. In order to create a system where siRNA knockdown could be retained for a sustained period, short hairpin RNAs (shRNA) were designed using the *C. elegans* miRNA *Let-7* as a template[91]. shRNA is then processed by Dicer to generate the siRNA duplex which could then initiate gene knockdown. Further optimization of shRNA technology has led to the observation that the expression of a siRNA sequence from the stem sequence of the human mirR-30 miRNA can result in an 80% increase in the efficacy of gene knockdown as compared to a short hairpin of the same sequence[92]. It has also been demonstrated that a single copy insertion of an optimized miR-30 shRNA is sufficient to induce strong knockdown of gene targets in a doxycycline regulated system[93].

Figures for Chapter 1: Background

a.

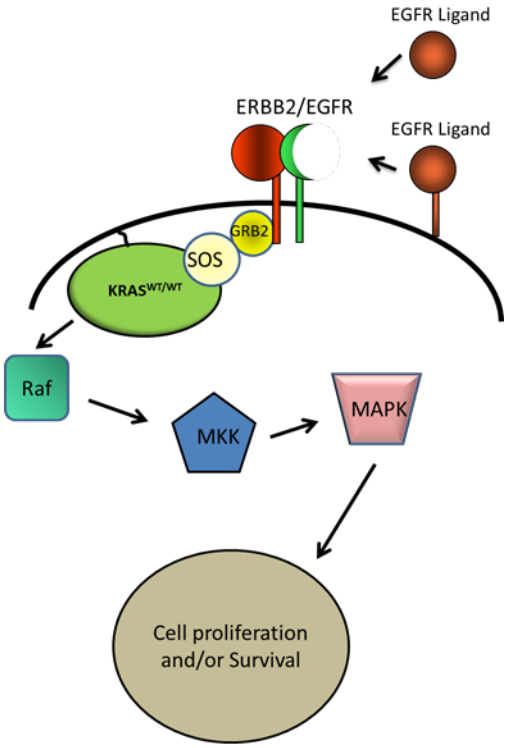
EGFR Ligand
ERBB2/EGFR
EGFR Ligand
GRB2
SOS
KRASWT/WT
Raf
MKK
MAPK
Cell proliferation
and/or Survival

b.

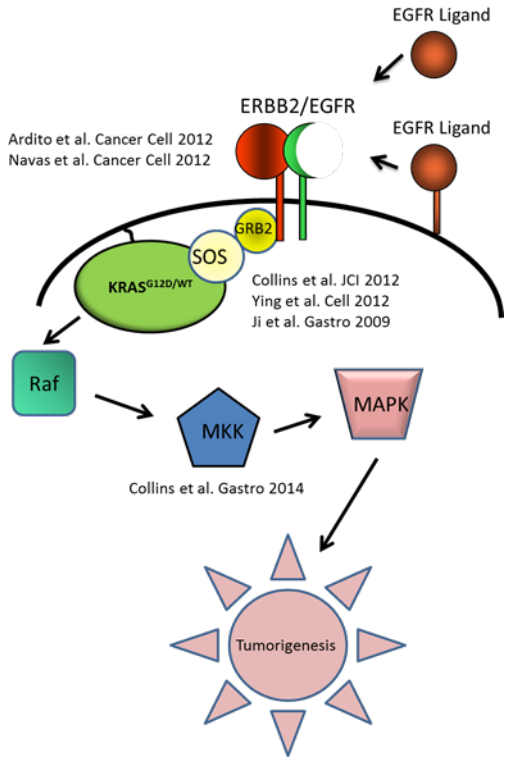
EGFR Ligand
ERBB2/EGFR
Ardito et al. Cancer Cell 2012
Navas et al. Cancer Cell 2012
EGFR Ligand
GRB2
SOS
KRASG12D/WT
Collins et al. JCI 2012
Ying et al. Cell 2012
Ji et al. Gastro 2009
Raf
MKK
MAPK
Collins et al. Gastro 2014
Tumorigenesis

Figure 1: EGFR-RAS-MAPK pathway diagram. a. EGFR is activated by extracellular ligands, or ligands released from the extracellular membrane by proteolytic cleavage. Once activated, EGFR autophosphorylation recruits the adapter protein GRB2 which allows the binding of the Kras GEF SOS. SOS stimulates the replacement of GDP to GTP in Kras which results in a conformation change that will allow for binding and activation of Raf by Kras. When activated, Raf will then phosphorylate MAPKK (MKK), which subsequently phosphorylates MAPK. Phosphorylation of MAPK results in the activation of many downstream signaling pathways which regulate cell growth and survival. **b.** Kras mutations such as $Kras^{G12D}$ results in increased levels of RAS activity and subsequent ERK activation which leads to tumorigenesis in the pancreas. In the absence of EGFR expression, Ras activity levels are decreased even in the presence of $Kras^{G12D}$ mutation, although it is unknown if this effect is due to EGFR mediated activation of WT or mutant Kras protein, or both. $Kras^{G12D}$ expression and MEK activity are required to sustain tumors that form in the pancreas.

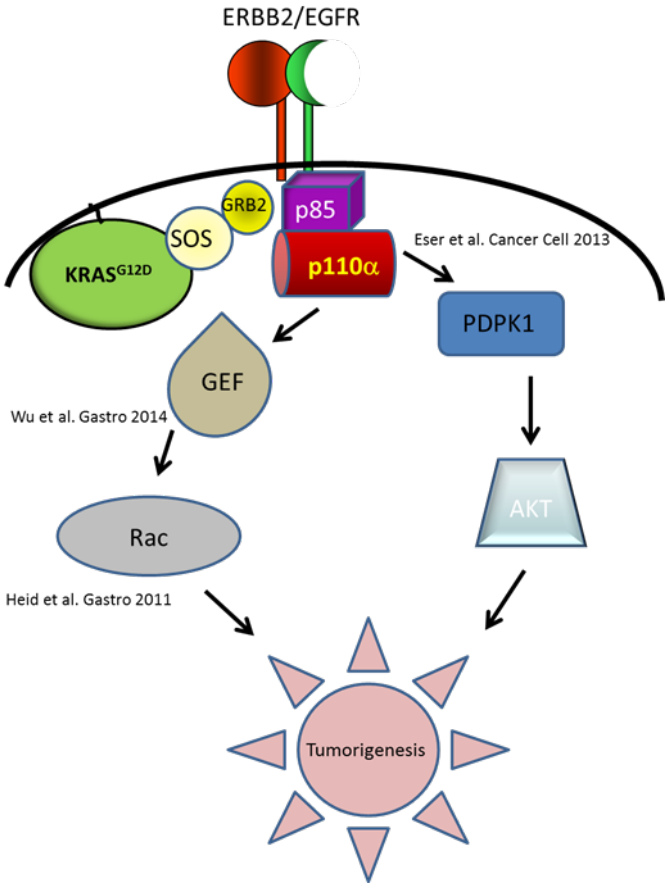
ERBB2/EGFR
GRB2
p85
SOS
KRASG12D
p110α
Eser et al. Cancer Cell 2013
PDPK1
GEF
Wu et al. Gastro 2014
AKT
Rac
Heid et al. Gastro 2011
Tumorigenesis

Figure 2: p110α signaling has multiple roles in Kras induced tumorigenesis. p110α has been demonstrated to have two indispensable role in pancreatic tumorigenesis. First, PIP_3 production recruits PDPK1 to the cytoplasmic surface of the cell membrane where it can activate AKT. Genetic loss of PDPK1 results in a block in AKT activation and tumorigenesis. Second, PIP_3 production leads to the membrane recruitment of Rac GEFs, which facilitate the GDP to GTP exchange of RAC. Once activated, Rac can mediate cytoskeletal rearrangement which is required for tumorigenesis, as genetic deletion of Rac1 can block tumorigenesis. Accordingly, genetic ablation of p110α results in a loss of $Kras^{G12D}$ induced Rac activation, which also prevents tumorigenesis.

Chapter 2: Materials and Methods

Mouse strains: Kras$^{+/LSL-G12D}$, Ptf1a$^{+/Cre}$, EGFR$^{f/f}$, trp53$^{+/R172H}$, p110α$^{f/f}$, and shRen713 mice have all been previously described [7,45,72,94,85,95]. shMEK1-2338, shMEK1-2268, shMEK2-404 mice were all generated by Mirimus Inc. in a KH3 ES cell line that contained a Rosa26-M2rtTA , or a D34 ES cell line which contained a ROSA26-CAG-LSL-rtTA^{3}-IRES-mKate2[96]. Experiments were conducted in accordance with the Office of Laboratory Animal Welfare and approved by the Institutional Animal Care and Use Committees of Stony Brook University and Mayo Clinic, and University Animal Care and Use Committee of the University of Michigan. All mice were genotyped using primers listed below.

Gene	Direction	Primer Sequence
CAG-rtTA	5'	GTTCGGCTTCTGGCGTGTGA
CAG-rtTA	3'	CGCTTGTTCTTCACGTGCGA
CAG-rtTA (LSL)	5'	AAAAACTCCCACACCTCCC
Cre	5'	TCGCGATTATCTTCTATATCTTCAG
Cre	3'	GCTCGACCAGTTTAGTTACCC
EGFR	5'	CTTTGGAGAACCTGCAGATC
EGFR	3'	CTGCTACTGGCTCAAGTTTC
KRAS	5'	CGCAGACTGTAGAGCAGCG
KRAS	3'	CCATGGCTTGAGTAAGTCTGC
Map2k1_2338	5'	AAGCCACAGATGTATTAGATTTGAT
Map2k2_404	5'	AAGCCACAGATGTATATCCTCTCAA
p53 Common	3'	CTTGGAGACATAGCCACACTG
p53 Mutant	5'	AGCTAGCCACCATGGCTTGAGTAAGTCT
p53 WT	5'	TTACACATCCAGCCTCTGTGG
Rosa Common	3'	AAAGTCGCTCTGAGTTGTTAT
Rosa Transgene	5'	GCGAAGAGTTTGTCCTCAACC
Rosa WT	5'	GGAGCGGGAGAAATGGATATG
shCommon Rev	3'	GAAAGAACAATCAAGGGTCC
p110 alpha	5'	CTGAGCTATAGAACTTCGTAACG
p110 alpha	3'	CTACACAGAGAAACCCTGTCTTG

Cerulein induced pancreatitis: Cerulein (American Peptide Company Inc.) was dissolved in sterile saline at a stock concentration of 500µg/mL stored at -20°C. For chronic pancreatitis a fresh 1:100 dilution of cerulein was prepared and administered to mice twice a day at a concentration of 250µg/kg body weight via intraperitoneal injection. For acute pancreatitis a fresh 1:500 dilution of cerulein was prepared, and mice were given hourly injections of cerulein for 7 hours at a concentration of 50µg/kg body weight. Sterile saline was used as control and injected in equal volume amounts.

Formalin fixed paraffin embedded tissue: Mice were sacrificed by CO_2 asphyxiation then tissue was quickly harvested and fixed overnight at room temperature with Z-fix solution (Anatech LTD). The tissue was then washed in 70% ethanol and stepwise dehydrated and embedded in paraffin blocks. 5µm sections were cut from blocks onto InkJet+ slides (Thermo Fisher Scientific Inc.). Immunohistochemistry was performed on either an Autostainer Plus (Dako North America Inc.), or a Discovery XT autostainer (Ventana Medical Systems Inc.).

Frozen tissue: Mice were sacrificed by CO2 asphyxiation then tissue was quickly harvested and fixed for 3 hours in Z-fix solution (Anatech LTD) at room temperature. Tissue was then transferred to a 30% sucrose solution and equilibrated overnight at 4°C. Tissue was then transferred to a 1:1 mixture of 30% sucrose: OCT compound (Thermo Fisher Scientific Inc.) for 15 minutes, then embedded in OCT by freezing in a petri dish floated on LN_2. 7µm sections were cut with a cryostat (Leica Microsystems) onto InkJet+ slides (Thermo Fisher Scientific Inc.).

Cell lines: The NB490 mouse pancreatic cancer cell line was obtained from Nabeel Bardeesy, and Ad-293 cells was purchased from Stratagene Corp. Both cell lines were maintained in

DMEM (Thermo Fisher Scientific Inc.) supplemented with 10% FBS (Sigma Aldrich Co.) and 0.5% gentamycin (Lonza Group LTD). Platinum-E cells were obtained from Cell Biolabs Inc. and maintained in complete DMEM supplemented with 10% FBS, 1 μg/mL puromycin, 10 μg/mL blasticidin, and 0.5% gentamycin (Thermo Fisher Scientific Inc.).

Antibodies: The following antibodies were used in this study:

Antibody	Company	Catalog no.	Host species	Application
AKT1/2/3	Santa Cruz Biotechnology	sc-8312	Rabbit	WB
Anti-RFP	Life Technologies	R10367	Rabbit	IHC
CD3	Abcam	ab5690	Rabbit	IHC
CD45	EMD Millipore	05-1416	Rat	IHC
Total ERK	Cell Signaling Technologies	9102	Rabbit	WB
F4/80	ABD Serotec	MCA497G	Rat	IHC
HSP90	Cell Signaling Technologies	4874	Rabbit	WB
Ly-6B.2	ABD Serotec	MCA771G	Rat	IHC
MEK1	Santa Cruz Biotechnology	SC219	Rabbit	WB
MEK2 (N-term)	Santa Cruz Biotechnology	sc524	Rabbit	WB
p-Akt(T308)	Abcam	ab76297	Rabbit	IHC
pERK (T202/Y204)	Cell Signaling Technologies	4370	Rabbit	WB
Ras	Abcam	1819	Rabbit	WB
Turbo-GFP	Thermo Fisher Scientific	PA5-22688	Rabbit	IHC, WB
β-actin	Santa Cruz Biotechnology	sc-47778	Mouse	WB
Cleaved Caspace 3	Cell Signaling	9664	Rabbit	WB

shRNA retrovirus generation and infection: shRNA plasmid (Mirimus Inc.) was transfected into Platinum-E cells using Lipofectamine 2000 (Life Technologies) prepared in Opti-MEM (Life Technologies) per suppliers instructions and allowed to incubate overnight at 37°C in 5% CO_2. The next day, fresh medium was placed on the cells and allowed to collect virus for 48 hours. Virus conditioned lysate was then harvested and passed through a 0.45μm syringe filter to remove cell debris. NB490 mouse pancreatic cancer cells were plated in 6 well plates and

grown to ~70% confluency. On day of infection, the media in each well was replaced with with fresh complete DMEM + 10µg/µL polybrene (Santa Cruz Biotechnology Inc.) containing either 1mL, 500µL, 250µL, 100µL, 20µL, or no virus conditioned media adjusted to 2mL total media per well. Cells were incubated overnight, then the virus conditioned media was aspirated and the cells were washed with once with DPBS replaced with fresh complete DMEM. Cells were allowed to recover for an additional 24 hours (36 hours post-transduction) then either harvested for flow cytometry to determine transduction efficiency as measured by GFP-expression, or treated with 5µg/mL puromycin for selection. Selection was allowed to proceed for 3-5 days, until no viable cells remained in the uninfected cells.

Protein harvest from cell lines: NB490 cells were plated in 6cm dishes and grown to 70% confluency. The cells were then washed once with ice cold DPBS and then lysed in 500µL of RIPA buffer. The lysate was then cleared by centrifugation at 15000rpm for 10 minutes at 4C, and stored at -80C.

Flow cytometry: To obtain a single cell suspension, cells were washed once with DPBS and treated with Accutase (Innovative Cell Technologies Inc.) at room temperature and triturated occasionally until most of the cells were detached. The resulting cell suspension was then diluted into FACS buffer (1% BSA, 1mM EDTA, 25mM HEPES in HBSS) and analyzed using the 488 laser on a FACS Aria III cell sorter (BD Biosciences).

Harvest of total mouse pancreatic lysate: Mouse pancreas tissue lysate was obtained by quickly removing a piece of the pancreas from mice sacrificed by CO_2 asphyxiation and snap freezing in liquid nitrogen. The frozen tissue was then homogenized in 1.5mL RIPA buffer supplemented with 2X EDTA-free protease inhibitor (Roche) and 1x Phos-STOP phosphatase

inhibitor (Roche Diagnostics) using a Pro 250 Homogenizer (Pro Scientific Inc.). Lysate was then cleared by centrifugation at 15,000 RPM for 10 minutes at 4°C and stored at -80°C.

Western blotting: Lysates were quantified by BCA assay (Thermo Fisher Scientific Inc.) and equal protein amounts were run onto SDS-PAGE gels. Immobilon-FL PVDF membrane was activated with 100% methanol, washed with water, and then equilibrated with transfer buffer. Proteins were transferred from SDS-PAGE gel to Immobilon-FL PVDF membrane in transfer buffer at 4°C overnight at a constant current of 90 mA. Membranes were blocked with 5% milk (Lab Scientific Inc.) in TBST for 1 hour at room temperature then incubated with primary antibodies in 1% BSA in TBST for 2 hours at room temperature. Membranes were then washed 5 times with ddH_2O and equilibrated in TBST for 10 minutes, then incubated in secondary antibody in TBST for 1 hour at room temperature. Membranes were then washed 5x with ddH_2O and equilibrated in TBST for 10 minutes prior to exposure on autoradiography film (Bioexpress) with West Pico ECL (Thermo Fisher Scientific Inc.) or ECL Prime (GE Healthcare) for HRP-linked secondary antibodies, or imaged on an Odyssey CLx infrared scanner (LiCOR Biosciences) for IR-fluorophore conjugated secondary antibodies.

Primary acinar cell isolation: Mice were sacrificed with CO_2, and then washed with 70% ethanol. The outer skin was removed to expose the peritoneum, which was thoroughly treated with providone-iodine. The pancreas was then harvested with sterile tools and placed in HBSS, washed twice with HBSS, and then minced with sterile scissors. The minced pancreas pieces were then centrifuged and re-suspended with 0.2 mg/mL Collagenase P (Roche Diagnostics) in HBSS at 37°C for and allowed to digest for 15 minutes in an orbital incubator. The digested tissue was then washed 3 times in HBSS containing 5% fetal bovine serum to inactivate the collagenase, and then filtered sequentially though through 500-μm and 105-μm polypropylene

mesh (Spectrum Laboratories Inc.). Filtrate was layered on 30% fetal bovine serum in HBSS and centrifuged though the gradient at 300xG for 2 minutes. The pelleted cells were re-suspended in complete Waymouth's MB 752/1 medium (Sigma-Aldrich Co.) 50 μg/mL gentamycin (Life Technologies), 0.4 mg/mL soybean trypsin inhibitor (Life Technologies), and 1 μg/mL dexamethasone (Sigma-Aldrich Co.). The amount of media used to re-suspend the cells was determined empirically by the size of the cell pellet obtained at typical yield of 100,000-400,000 acinar clusters which were re-suspended at ~10,000 cells per mL. The re-suspended cells were then plated in non-tissue culture treated plates and maintained at 37°C in a 5% CO_2 atmosphere.

Protein isolation from primary acinar cell cultures: Primary acinar cell cultures were harvested by pelleting the cells by centrifugation for 2 minutes at 300xG. The pellet was then washed once with ice cold DPBS, then the pellet was lysed in RIPA buffer + 1X protease and phosphatase inhibitors for western blotting or MLB buffer + 1X protease and phosphatase inhibitors for RAS activity assays. Lysate was then cleared by centrifugation at 15000 rpm for 10 minutes at 4C, and then stored at -80C.

RNA isolation and purification from primary acinar cell cultures: Primary acinar cell cultures were harvested by pelleting the cells by centrifugation for 2 minutes at 300xG. The pellet was then washed once with ice cold DPBS, then pellet lysed in RLT+ buffer containing 1% beta-mercaptoethanol, which was then passed through a Qiashredder (Qiagen) column. RNA was then purified using an RNEasy+ kit (Qiagen) using gDNA eliminator columns to remove genomic DNA. RNA was then analyzed on a Nanodrop 2000c (Thermo Fisher Scientific Inc.) spectrophotometer for quantification, and purity was assessed based on the A^{260}/A^{280} ratio. For more stringent downstream application such as Next-Gen sequencing, RNA quality was further

assessed using a total RNA kit on a 2100 Bioanalyzer (Agilent Technologies) the generated RIN number was used to determine quality. Isolated RNA was stored at -80°C.

cDNA synthesis and quantitative PCR: cDNA was synthesized from isolated RNA with an iScript cDNA synthesis kit (Bio-Rad Laboratories) using 1µg of RNA input per 20µL reaction. The resulting cDNA was diluted 1:5 using nuclease free H_2O. Quantitative PCR reactions were carried out at a 20µL scale for a 96 well format, and a 10µL scale for 384 well format. Reactions were made with 2X FastSyber master mix (Life Technologies), a primer concentration of 300nM, and 0.5ng/µL input cDNA. Reactions were then run on a fast cycle on a Viia7 thermocycler (Applied Biosystems). Primer sets used for qPCR are listed below:

Gene	Direction	Primer
Hprt1	5'	TCAGTCAACGGGGGACATAAA
Hprt1	3'	GGGGCTGTACTGCTTAACCAG
Tbp	5'	CCCCACAACTCTTCCATTCT
Tbp	3'	GCAGGAGTGATAGGGGTCAT
Ptf1a	5'	CATCGAGGCACCCGTTCAC
Ptf1a	3'	CAACCCGATGTGAGCTGTCT

Adenoviral production and infection of acinar cell culture: Adeno-GFP, adeno-Cre-GFP, adeno-Notch2ICD-GFP, adeno- $p110\alpha^{H1047R}$, adeno-Myristolated-AKT, adeno-dominant active RAC, and adeno-constitutively active STAT3 adenovirus stocks were prepared from established adenovirus stock by first creating a small scale batch of virus through infection of a 10cm plate of ~70 confluent Ad-293 cells. After the cells in 10cm plate were verified to have undergone cytopathic effect (CPE) as verified by detachment of grapelike clusters of cells into the medium, the cell containing medium was harvested to infect a large scale culture. Three 15cm plate of Ad-293 cells were concurrently grown to ~80-90% confluency and detached using trypsin-EDT.

The trypsinized cells were pelleted, combined with the virus produced in the small scale culture, and then plated out into five 15cm dishes. Cells were cultured until CPE was observed, then the media was harvested and adenovirus was purified using an Adeno-X Maxi purification kit (ClonTech Laboratories Inc.) following manufactures instructions and stored at -20C. The resulting adenovirus titer was determined empirically by transduction of primary acinar cultures using the GFP reporter to monitor infection (typically 1:100). Titers remained stable throughout the lifetime of adenovirus stocks. Infection of primary acinar cells was carried out by adding the adenovirus directly to the primary acinar cell culture in complete medium.

3D acinar cell explant culture: A bovine collagen matrix solution was prepared by mixing bovine collagen (R&D Systems) with 10X (2.5M) NaOH and 10X Waymouth's MB 752/1 medium to a 2X concentration. The 2X collagen matrix mixture was then combined 1:1 with primary acinar cell culture and immediately plated into a 24 well plate, at approximately 3,000 cells in 500µL collagen matrix per well, and placed into a 37°C in a 5% CO_2 atmosphere incubator. The matrix was allowed to set for 30 minutes, and then topped off with 500µL complete Waymouth's MB 752/1 medium. If the experiment required the use of a drug or growth factor the drug, growth factor, or vehicle controls were added to medium at this time. Medium was replenished the next day, and every other day until the end of the experiment adding drugs, growth factors, or vehicle controls when applicable. Trametinib was used at a concentration of 100nM, Erlotonib at 1µM, BMS345541 at 1µM, TGF-α at 50ng/mL, HGF at 20ng/mL, RANTES at 50ng/mL, TNF-α at 50ng/mL, IL-6 at 20ng/mL and HB-EGF at 100ng/mL.

Statistical analysis: Statistics were performed using Graph Pad Prism 6 (Graph Pad Software Inc.) using an unpaired students t test.

Chapter 3: Generation of inducible MEK knockdown mice and characterization in pancreatitis and pancreatic tumorigenesis

Background

Isoform specific contributions of MAPK pathway components in cancer

Downstream of Kras in the MAPK pathway, each protein in the RAF-MEK-ERK cascade has multiple isoforms. As such, in each stage of the pathway, either the isoforms each perform a unique function, or the absence of an individual isoform can be compensated for by the remaining isoforms, which can be seen using development as a model. In the case of the Raf proteins, mice lacking a-Raf are born with no abnormalities into adulthood, however genetic ablation of b-Raf or c-Raf are embryonic lethal[97]. In a mouse model of $Kras^{G12D}$ driven lung cancer, it was determined that c-Raf is the important isoform form for tumor development as ablation lead to 83% increase in survival, however b-Raf is dispensable for oncogenic Kras signaling[98]. In the same system, it was also determined that the MEK and ERK kinase isoforms were able to compensate for the loss of the other, and that the deletion of both isoforms of either kinase was necessary to block lung tumorigenesis.

However in other systems MEK isoforms in particular have been shown to have both overlapping as well as non-redundant roles. Importantly, MEK1 has been shown to be essential for mouse development and growth[99], however MEK2 appears to be dispensable in this context, as MEK2 null mice are viable[100]. An example of similar but different roles is found in intestinal epithelial cells, as induction of MEK1 or MEK2 signaling was shown to be sufficient to cause transformation, however MEK2 was found to be more important for proliferation[101]. In the DMBA/TPA skin cancer model, MEK1 was identified to be required for initiation of

carcinogenesis, however MEK2 was dispensable[102]. Using shRNA mediated RNAi targeting MEK1 or MEK2 in hepatocellular carcinoma cells revealed a dependence for MEK1 but not MEK2 on cell growth, proliferation, and tumorigenesis in mouse xenografts[103]. Interestingly the signaling appeared to be mediated through ERK2, as similar effects were seen when ERK2 but not ERK1 was knocked down, suggesting in this system that the function of both the MEK isoforms and their respective ERK targets were unique. Lastly MEK2 was determined to be the dominant isoform required for the growth and proliferation in a melanoma cancer cell line, while MEK1 had no effect[104].

Limitations of current models of isoform specific MEK interrogation

Previously, two main models have been used to investigate the contribution of individual MEK isoforms, knockout mice or cell lines. The knockout mouse models used are a full body knockout of MEK2[100] and a conditional knockout ($MEK1^{flox/flox}$) mouse[105]. While the conditional $MEK1^{flox/flox}$ can accurately be used in an organ specific fashion *in vivo*, the full body MEK2 knockout affects the entire mouse, not just the organ in question. Crossing these lines together with an epithelial specific Cre can give mice that are null for MEK1 and MEK2 in the epithelium, however it cannot be used as a genuine model for interruption of MEK signaling in cancer due to two intrinsic problems with the model. First, since MEK2 has been deleted in development, a compensatory signaling pathway could be activated embryonically to deal with the loss of MEK2. Second, any phenotypic differences in a model of disease development could be due to inadvertently targeting more than one cell type. For example, pancreatic stellate cells have been shown to require ERK signaling to stimulate the production of COX2[106], which has been shown to be important in RAS induce tumorigenesis[107]. Loss of MEK2 in stellate cells

could be sufficient to interrupt the production of stromal COX2 and lead to a decrease in tumorigenesis entirely unrelated to the epithelial cells, giving misleading results.

Using cell lines to knockdown individual MEK isoforms using RNAi also has limited practical implications in the context of tumorigenesis and pancreatitis. For pancreatitis, no cell line model of immortalized cells can recapitulate the development of an inflammatory disease *in vitro,* and there is currently no model of re-establishing explanted acinar cells back into a mouse, although it has been demonstrated that 3D ductal organoids can re-establish normal ducts when transplanted into mice[108]. Subcutaneous tumor xenograft models cannot recapitulate the natural environment of the organ of origin of the tumor cells, and orthotopic tumor xenograft models necessitate the use of immunocompromised mice. In the development of pancreatic cancer in mutant Kras driven mouse models, immune responses such macrophage infiltration[109,110] and hematopoietic IL-17 signaling[111] have been shown to be an important contributors. In addition, mutant Kras PDA has been shown to generate cytokines such as GM-CSF which brings in immune cells such as myeloid derived tumor suppressor cells[112,113], the lack of which can also lead to misleading results in terms of tumorigenesis and effectiveness of chemotherapy. These important contributions of the immune system are not able to be appreciated in immunocompromised mice.

Given the differences in the roles of different MEK isoforms in other cancers, I set out to define the roles of parenchymal MEK1 and MEK2 in pancreatitis and pancreatic tumorigenesis, by generating a novel shRNA mouse model.

Results

Design of shRNA mice for MEK1, MEK2, and MEK1/2 Knockdown

In order to investigate the isoform-specific contributions of MEK kinases in pancreatitis and pancreatic cancer, I created a mouse model in which I could control the expression of individual MEK isoforms in an inducible fashion. Recently, Lowe and colleagues have engineered mouse embryonic stem cells with a FRT targeting cassette knocked in downstream of the Col1a1 locus, universally expressed in most tissues, which allows efficient recombination with a vector containing a mir-30 based siRNA (sh-Mir) under the control of a tet-operator (Tet-O) coupled to an EGFP reporter[95]. As I am only interested in the effects of MEK knockdown (KD) in the pancreas, I utilized a ROSA26 targeted CAG-LSL-rtTA^{3}-IRES-mKate2 reverse tetracycline transactivator to generate a tissue specific knockdown. The lox-stop-lox (LSL) sequence requires Cre recombination prior to production of rtTA, which can be monitored by the far red fluorophore mKate2 which is translated from the internal ribosome entry site (IRES) downstream of the rtTA. Crossing mice containing the tet-O sh-Mir transgene with ROSA26$^{+/\text{CAG-LSL-rtTA3-IRES-mKate2}}$ mice and Ptf1a$^{+/\text{Cre}}$ mice, I have created triple transgenic mice which allow for pancreas-specific expression of sh-Mir in a doxycycline inducible manner. Using this system, I have generated mice with sh-Mir sequences targeting MEK1 and MEK2 individually. The allelic nature of the sh-Mir transgene allows for the generation of mice containing one allele targeting each MEK isoform allowing us to also target both isoforms of MEK simultaneously. A schematic diagram can be seen in for MEK1 KD, MEK2 KD, and MEK1/2 KD mice in Figure 3 a, b, and c, respectively.

Selection of siRNA sequences

In order to determine the best siRNA sequences to use in the knockdown mice, I screened 14 clones targeting mouse MEK1 and 13 clones targeting mouse MEK2 identified from a validated shRNA "sensor array"[114]. Plasmids containing each siRNA sequence were obtained in a puromycin-selectable mir-30 backbone vector that constitutively expresses the mir-shRNA as well as GFP. Virus particles were made by lipofectamine mediated transfection into the retroviral packaging cell line Platinum-E. A mouse pancreatic cancer cell line, NB490, was then infected at various titers of retrovirus and transduction efficiency was monitored by GFP expression. As the majority of cells will only have a single copy of the shRNA when transduced at a population under 20% as predicted by Poisson's law[115], I puromycin selected populations with a GFP^+ population under 20%, as single copy expression of the shRNA would provide a fair analysis of gene knockdown across clones. After selection was completed, verified by complete loss of viability in uninfected cells and a 100% GFP^+ population in transduced cells, protein was harvested and gene knockdown was quantitated by western blot using isoform specific antibodies. To control for potential off-target effects, I chose the two best knockdown clones for each MEK isoform which can be seen in Figure 4. Map2k1-2268 and Map2k1-2338 were the best two siRNA sequences for MEK1 knockdown, while Map2k2-404 and Map2k2-1229 were the best two siRNA sequences for MEK2 knockdown. I also looked at ERK phosphorylation levels in NB490 cells to see if there was an isoform specific modulation of ERK activation. ERK activation was increased by knockdown of MEK1, which is in agreement with previous data that has shown that loss of MEK1 can lead to a sustained increased in MEK2 activation of ERK[105].

Generation and characterization of shRNA mice

Founder mice were received from Mirimus Inc. which contained either the Map2k1-2338 siRNA sequence or the Map2k2-404 siRNA sequence. The Map2k1-2338 mice were generated in a D34 ES cell line which was homozygous for the ROSA26-CAG-LSL-rtTA3-IRES-mKate2. The Map2k2-404 mice were generated in a KH3 ES cell lines, which was heterozygous for a ROSA26-M2rtTA, which does not allow for tissue specific gene knockdown. To alleviate this problem, the ROSA26-M2rtTA was bred out of these mice and the ROSA26-CAG-LSL-rtTA3-IRES-mKate2 was bred in. I then tested if the fluorophore reporters were working in the correct context; with mKATE2 expression induced after Cre recombination, and GFP expression turned on after doxycycline treatment in only recombined cells. To address this, primary acinar cells were extracted from the pancreas of a mouse containing both the ROSA26-CAG-LSL-rtTA3-IRES-mKate2 and turboGFP-shRNA transgenes. The cells were divided into two groups, one infected with adenoviral Cre (Figure 5b, 5d) and the other as an uninfected control (Figure 5a, 5c). The two groups were further subdivided into two groups, one treated with 1µM doxycycline (Figure 5c, 5d) and the other with vehicle (Figure 5a, 5b). As expected, Cre recombination allowed the expression of mKate2 in the infected cells, which was not seen in the uninfected cells (Figure 5b, 5d). Additionally, TurboGFP expression was only visualized in cells which had been infected with adenoviral Cre and treated with doxycycline (Figure 5d).

To create mice with pancreas-specific shRNA transgene expression, the Map2k1-2338;ROSA26-CAG-LSL-rtTA3-IRES-mKate2 bitransgenic mice were then crossed with Ptf1a$^{+/Cre}$ mice to create Map2k1-2338;ROSA26-CAG-LSL-rtTA3-IRES-mKate2;Ptf1a$^{+/Cre}$ triple transgenic mice (MEK1-KD mice). Similarly Map2k2-404;ROSA26-CAG-LSL-rtTA3-IRES-mKate2 bitransgenic mice were then crossed with Ptf1a$^{+/Cre}$ mice to create Map2k2-

404;ROSA26-CAG-LSL-rtTA3-IRES-mKate2;Ptf1a$^{+/Cre}$ triple transgenic mice (MEK2-KD mice). The MEK1-KD and MEK-2KD mice were further crossed together to create Map2k1-2338;Map2k2-404;ROSA26-CAG-LSL-rtTA3-IRES-mKate2;Ptf1a$^{+/Cre}$ mice (MEK1/2-KD mice).

In order to verify the pancreas-specific expression of the mKATE2-rtTA and the doxycycline inducible expression of the shRNA transgene and turboGFP, I administered doxycycline diet for seven days to either the turboGFP-shRNA;LSL-mKate2-rtTA;Ptf1a$^{+/Cre}$ mice, or mice containing only LSL-mKate2-rtTA;Ptf1a$^{+/Cre}$ as a control. The mice were then sacrificed and the organs were exposed and imaged on an in vivo fluorescence system (Figure 6a). As expected, both mice expressed the mKate2 only in the pancreas, and only the mouse with both the GFP-shRNA and mKate2-rtTA transgenes expressed GFP which was also localized to the pancreas.

Next, to investigate the timeframe required to generate maximum gene knockdown, MEK2-KD mice were placed on doxycycline diet for one, three, or seven days. A turboGFP-Map2k2-404;Ptf1a$^{+/Cre}$ mouse lacking the mKate2-rtTA was used as a control and placed on doxycycline diet for a week. Mice were then sacrificed and total pancreatic protein lysate was harvested and analyzed by western blot for MEK2 protein levels, as well as turboGFP expression (Figure 6b). A partial knockdown was seen by day 3, and a robust knockdown was observed at day 7. TurboGFP expression was seen to increase throughout the time course.

To determine the efficiency and specificity of MEK1-KD and MEK2-KD mice on their respective MEK isoforms a mouse from each genotype, as well as a control mouse containing the rtTA and no shRNA transgene, were placed on doxycycline diet for a week. Mice were then

sacrificed and total pancreatic protein lysate was harvested and analyzed for expression of MEK1, MEK2, and total MEK1/2 (Figure 6c). Both MEK1 and MEK2 were found to be expressed at similar levels in the lysates. MEK1 knockdown was very effective in reduction of MEK1protein levels and had no effect on the levels of MEK2 protein expression. Conversely, MEK2 knockdown was very effective at reducing the protein level of MEK2, with no impact on MEK1 protein expression.

Finally, tissue localization of the expression of the mKate2-rtTA and the GFP-shRNA transgenes were interrogated by immunohistochemistry (Figure 7). The expression of the fluorophores appears to be localized predominantly in the acinar cells, whereas the ducts and islets of Langerhans appeared to be largely GFP and mKate2 negative. This localization was unexpected, given the pan-pancreatic nature of Ptf1a-Cre expression. Importantly, there also appeared to be no morphological effects of expression of the transgenes or knockdown of their respective targets in the pancreas.

MEK1/2-KD, but not MEK1-KD protects against chronic pancreatitis

I next compared MEK1 and MEK1/2 KD mice with wild type mice in the context of chronic pancreatitis by injecting the mice twice daily with 250µg/kg body weight cerulein or sterile saline as a control for two weeks followed by 24 hours of recovery. Unfortunately, I did not have sufficient MEK2-KD mice to include in this experiment. In normal mice pretreated with doxycycline diet for 7 days, this treatment protocol causes massive exocrine tissue damage, acinar-to-ductal metaplasia, immune infiltration, and desmoplastic stromal remodeling (Figure 8a). Tissue damage comparable to the WT mice is seen in chronically treated MEK1-KD mice, however, knockdown of both MEK isoforms almost completely protects from pancreatic damage compared to both WT and MEK1-KD (Figure 8a). Damage induced by chronic pancreatitis also

leads to a loss in pancreas mass as compared to body mass in both WT and MEK1-KD mice, however MEK1/2 KD mice have significantly greater retention of pancreas mass (Figure 8b).

As pancreatitis is an inflammatory disease, I next set out to dissect the immune infiltration in chronic pancreatitis of WT, MEK1-KD, and MEK1/2-KD mice. Immunohistochemical staining for CD-45, an antigen found on all leukocytes, to look at total immune cell infiltration revealed a marked reduction in immune cells present in MEK1/2-KD pancreata as compared to WT and MEK1-KD pancreata (Figure 9). Further dissecting out the type of immune cells present in WT, MEK1-KD, and MEK1/2-KD pancreata after induction of chronic pancreatitis revealed MEK1/2 KD mice had a significant decrease in number of $F4/80^+$ macrophages, $Ly6.B^+$ neutrophils, and $CD3^+$ T-cells as compared to both MEK1-KD and WT mice (Figure 10). MEK1/2 KD pancreata also had much lower levels of ERK phosphorylation, which would be predicted by knocking down MEK, in response to chronic pancreatitis as compared to WT and MEK1-KD mice (Figure 11). However, most of the phospho-ERK staining in the WT and MEK1-KD pancreata was located either in the immune cells in the stroma or in ADM, both of which were drastically reduced in MEK1/2-KD mice.

MEK1/2 and MEK1 KD in Acute Pancreatitis

In order to more accurately compare the cell signaling differences in response to cerulein induced pancreatitis in WT, MEK1-KD, and MEK1/2 KD mice, I turned to an acute pancreatitis model. WT, MEK1-KD, and MEK1/2-KD mice were placed on doxycycline diet for a week, and then were injected once per hour with either 50µg/kg body weight of cerulein or equal volume amounts of sterile saline as a control for seven hours and allowed to recover for one hour prior to harvest. A piece of freshly excised tissue was snap frozen in LN_2 and the rest placed in fixative for normal histology.

Protein lysate was harvested from the frozen tissue and then analyzed via western blot to quantitate the levels of phosphorylated ERK, as well as levels of MEK1 and MEK2 to verify knockdowns, and expression of turboGFP to verify shRNA transgene expression (Figure 12a, 12b). As expected, MEK1-KD mice have marked reduction of MEK1 protein levels, and MEK1/2-KD mice have a loss of both MEK1 and MEK2 proteins levels. Turbo-GFP expression was also only seen in knockdown mice in response to doxycycline treatment. Interestingly, MEK1 expression was also lost in WT mice treated with cerulein, indicating that cerulein treatment alone leads to a loss of MEK1 protein levels. All the cerulein treated groups demonstrated higher levels of ERK phosphorylation as compared to their respective saline controls. Contrary to our prediction of MEK1/2-KD blocking ERK phosphorylation, ERK phosphorylation levels in MEK1/2-KD mice treated with cerulein also were higher than WT mice treated with cerulein. Cerulein treated MEK1-KD mice also demonstrated higher levels of ERK activation compared to WT cerulein treated mice.

Histology of the cerulein treated groups revealed normal characteristics of acute pancreatitis relative to saline treated controls; including edema, necrosis, and immune infiltration (Figure 13). As seen previously by western blot, there were increased levels of ERK phosphorylation in the acinar cells of all the cerulein-treated mice as compared to saline-treated. Cerulein-treated MEK1-KD and MEK1/2 KD mice also had higher levels of activated ERK in the acinar cells than the WT cerulein treated group, which was again consistent with the protein levels seen via western blot.

I next looked into the duration of the cerulein activated ERK phosphorylation event. To address this, mice were placed on doxycycline diet for 1 week, then injected once per hour with 50µg/kg body weight of cerulein for 7 hours and allowed to recover for 1 hour, 2 hours, 4 hours,

or overnight prior to harvest. Again, a piece of freshly excised tissue was snap frozen in LN_2 then homogenized in lysis buffer with protease and phosphatase inhibitors, and ERK phosphorylation levels were analyzed by western blot (Figure 14). At two hours recovery, the ERK activity remained elevated compared to the saline treated control, about the same levels seen in the one hour recovery. After the overnight recovery after cerulein treatment, the ERK levels were on par with untreated mice. As MEK1 protein levels were previously seen to be lost during the cerulein treatment, I also looked at MEK1 levels at the longer recovery time points. At the 2 hour recovery time point, the MEK1 protein levels begin to return and remain lower than untreated mice at 4 hours than untreated mice. After overnight recovery, the MEK1 protein expression returned to similar levels as untreated controls.

Role of MEK isoforms in Kras mediated tumorigenesis

To investigate the role of individual MEK isoforms in tumorigenesis driven by mutant Kras, I crossed $Kras^{+/LSL\text{-}G12D}$ mice with Map2k1-2338;ROSA26-CAG-LSL-rtTA3-IRES-mKate2;$Ptf1a^{+/Cre}$, Map2k2-404;ROSA26-CAG-LSL-rtTA3-IRES-mKate2, and Map2k1-2338;Map2k2-404;ROSA26-CAG-LSL-rtTA3-IRES-mKate2;$Ptf1a^{+/Cre}$. The resulting Map2k1-2338;ROSA26-CAG-LSL-rtTA3-IRES-mKate2;$Ptf1a^{+/Cre}$;$Kras^{+/LSL\text{-}G12D}$, Map2k2-404;ROSA26-CAG-LSL-rtTA3-IRES-mKate2;$Kras^{+/LSL\text{-}G12D}$, and Map2k1-2338;Map2k2-404;ROSA26-CAG-LSL-rtTA3-IRES-mKate2;$Ptf1a^{+/Cre}$;$Kras^{+/LSL\text{-}G12D}$, (MEK1-KC, MEK2-KC, and MEK1/2-KC, respectively) were placed on doxycycline diet for 7 days at four weeks of age, then treated with 250µg/kg body weight cerulein once daily for 5 days. ROSA26-CAG-LSL-rtTA3-IRES-mKate2;$Ptf1a^{+/Cre}$;$Kras^{+/LSL\text{-}G12D}$ (rtTA-KC mice) were used as controls. 4 week old control mice were placed on doxycycline chow for a week and then underwent the same cerulein treatment, or

were injected with an equal volume of sterile saline to serve as an untreated control. After 7 days recovery, mice were sacrificed and tissues were weighed and processed for histology.

In cerulein treated rtTA-KC, MEK1-KC, and MEK2-KC mice there was a nearly complete replacement of acinar cells with fibrotic stroma, immune infiltration, ADM, and PanIN lesions as compared to saline treated mice (Figure 15a). MEK1/2 KC mice have markedly increased acinar cell retention; however there was still abundant stromal replacement, ADM, and PanIN lesions present. Pancreatic mass in relation to body weight was also increased in cerulein treated rtTA-KC, MEK1-KC, and MEK2-KC mice, however cerulein treated MEK1/2 KD mice significantly display smaller pancreas to body weight ratio than rtTA-KC mice (Figure 15b).

Next I attempted to address the dependence of MEK signaling in pre-established tumors. I treated 5-week old MEK1/2-KC mice and treated with 250µg/kg body weight of cerulein daily for five days. The mice were allowed to recover for a week, which is sufficient for a nearly complete conversion to tumor, when a group of mice was placed on doxycycline diet for a week, and the rest remained on normal chow for ten days. The mice were then sacrificed and tissue harvested for histology (Figure 16). Unfortunately, tumor weights were unable to be compared due to the presence of large fluid filled cysts on several of the pancreata in both the experimental and control groups. Comparison of the tissue morphology showed a slight increase in the amount of acinar cells present in the doxycycline treated cohort, but there was not a significant difference between the two groups. However, phosphorylated ERK levels were drastically decreased in the doxycycline treated group as compared to the mice on control chow, demonstrating that the MEK-ERK pathway has been inhibited.

Discussion

The role of MEK kinases in ADM, pancreatitis, and tumorigenesis has been demonstrated in previous studies with the use of MEK inhibitors[72,79]. However, the use of MEK inhibitors does not allow for the role of the individual MEK isoforms, MEK1 and MEK2, to be determined. The use of an inhibitor also does not allow for compartmentalization of inhibition in an organ. To address this, I have identified shRNA sequences targeting MEK1 or MEK2 specifically and used these sequences to create a transgenic mouse model to express MEK shRNA in the pancreas epithelium in response to doxycycline treatment. Using fluorescent reporters to track both the localization of the rtTA used to drive the expression of the shRNA and the shRNA expression itself, I confirmed that shRNA is expressed predominantly in the acinar cells of the pancreas and only in response to doxycycline treatment.

Pancreatitis is the most commonly diagnosed digestive inflammatory condition which results in hospitalization[14], however there are no approved treatment options beyond pain management and supportive treatment[116]. To determine if interruption of the MEK-ERK pathway in the pancreas parenchyma is important in pancreatitis, I examined the impact of MEK1 or both MEK1 and MEK2 gene knockdown in the pancreas in response to cerulein induced pancreatitis. MEK1 knockdown was insufficient to prevent the induction of pancreatitis, however combined knockdown of MEK1 and MEK2 was able to block damage to the pancreas by chronic cerulein treatment. Additionally, concurrent MEK1 and MEK2 knockdown resulted in significantly reduced total immune cell infiltration as well as reduced numbers of macrophages, T-cells, and neutrophils. These data suggest that MEK inhibition is a powerful way to prevent the onset of pancreatitis, and the acinar cells in particular are resistant to cerulein induced pancreatitis without intact MEK signaling. However it remains to be seen if MEK

inhibition or gene knockdown will be effective in amelioration of pancreatitis once it is already established.

In order to look at an "apples to apples" comparison when dissecting the signaling pathways responsible for the MEK1/2 knockdown protection against pancreatitis, I utilized an acute cerulein treatment protocol. Surprisingly genetic knockdown of MEK1/2 protein levels was not able to block the activation of the ERK pathway in 2 out of 3 MEK1/2-KD mice treated acutely with cerulein. While unexpected, activation of ERK in a MEK independent fashion has been previously reported[117]. Additionally, ERK activity is also controlled by dual-specificity phosphatase (DUSP) family proteins responsible for maintenance of a phosphorylation/de-phosphorylation equilibrium of ERK signaling in normal cells[118]. The loss of a DUSP protein in response to cerulein induced stress could also result in the increase in the levels of active ERK seen in MEK1/2 KD mice. Further elucidation of this mechanism will be necessary.

To test ability of MEK1, MEK2, and MEK1/2 gene knockdown to block tumorigenesis, I generated KC mice harboring the shMEK1, shMEK2, and both shMEK1 and shMEK2 transgenes. I then treated mice after a week of doxycycline administration to test if knockdown of the respective MEK isoforms was sufficient to prevent tumorigenesis. Contrary to studies using MEK inhibitors[72,79], tumor formation was observed in MEK1/2-KC mice, although the mice did retain a large number of intact acinar cells as well. This could be a result of incomplete MEK inhibition by gene knockdown, or it could be a result of non-epithelial MEK signaling which is inhibited by treatment with pharmacological inhibitors. There was also a subpopulation of the MEK1/2-KC mice which displayed large cysts not seen in the MEK1, MEK2, or rtTA-KC mice. Chronic MEK inhibition has also been shown to lead to AKT activation[74], which could

potentially lead to the formation of these large cysts. Further investigation will be required to explain this observation.

In order to validate if MEK inhibition in the epithelium is able to inhibit the growth of tumors after they have already formed, mimicking the clinical setting of a patient presenting with a tumor, I generated tumors in MEK1/2-KC mice by cerulein induced pancreatitis and administered doxycycline to a cohort of the treated mice. In the time examined, there was not a complete regression of tumors in the doxycycline treated group, however there was a drastic reduction in the amount of ERK phosphorylation. Further investigation into longer time periods of MEK1/2 gene knockdown after the formation of tumors will be necessary to determine the effectiveness of this strategy, although the ability to drastically reduce the level of Erk signaling is a good indication that longer doxycycline treatment could lead to complete tumor regression. Long term doxycycline treatment of MEK1/2 mice will also be useful to determine what, if any, escape mechanisms that Kras induced tumors will have to MEK inhibition.

Future Directions

I have successfully demonstrated that a genetic knockdown model of MEK1, MEK2, and concurrent knockdown of MEK1 and MEK2 in the mouse pancreas can impact the development of pancreatitis, as well as impair tumorigenesis. However, much work is still needed to finish this project. First, only one clone of MEK1 and one clone of MEK2 have been validated *in vivo*. Technical problems in the generation of the second MEK2 clone have forced us to switch to a different clone which is currently in the process of recombination into mouse ES cells for founder generation. The second MEK1 clone is currently in the process of crossing in Ptf1a-Cre to allow validation and subsequent experimentation. The observation of our phenotypes in only the combination of the two MEK isoforms indicates that nonspecific shRNA effects are likely

not a problem in our model, however it will still be useful to show two clones of each isoform to strengthen that argument.

To more properly control our shRNA experiments, I have obtained a mouse containing a shRNA sequence targeting Renilla luciferase[95] (shRen713) to use as a non-target shRNA control. This mouse was generated in the same KH3 ES cell line as the MEK2-404 mouse, so I am currently in the process of breeding out the whole body rtTA and breeding in the LSL-rtTA used in the rest of the study to allow for pancreas specific shRNA expression. The shRen13 mice will then be bred to the KD and KC genotypes to use for the pancreatitis and tumorigenesis experiments, respectively.

For pancreatitis experiments, MEK2-KD mice will be subjected to chronic pancreatitis and acute pancreatitis and analyzed in the same fashion as MEK1-KD and MEK1/2-KD mice. The ability of the MEK1-KD, MEK2-KD, and MEK1/2-KD mice to respond to acute cerulein treatment will also be verified by serum amylase levels, which are again waiting for MEK2-KD mice in order to allow comparison across all the genotypes. As all the genotypes tested respond to cerulein treatment by activation of ERK, it would be surprising not to see serum amylase levels elevated in response to cerulein treatment as well. Work will also be done to focus on the mechanism of MEK1/2-KC resistance to chronic pancreatitis. The first experiment toward this end will be a time course of MEK1/2-KD recovery from acute cerulein treatment to determine if the ERK activation is sustained with the same kinetics of WT acinar cells treated acutely with cerulein.

I am also planning to test if MEK inhibition has any effect in reducing the symptoms of pancreatitis both pharmacologically and genetically. I first plan to treat WT mice for 1 week

with twice daily injections of cerulein, then continue the cerulein regiment for 2 more weeks with the addition of trametinib treatment, or vehicle control. When I have MEK1/2-KD mice available, I plan to do a similar experiment treating the mice for 7 days with twice daily cerulein injections, then putting the mice either on doxycycline chow or leaving them on control diet for 2 more weeks while continuing the cerulein treatments to determine if inhibition of ERK signaling in the pancreas parenchyma has the same result as pharmacological inhibition of the entire mouse.

In order to try and solve the cyst formation problem seen in MEK1/2-KC mice, I am currently in the process of switching the Cre recombinase from the Ptf1a-Cre, which is activated in all pancreas progenitor cells, to the tamoxifen inducible Ptf1a-Cre^{ERT2}. This Cre recombinase will allow specific recombination of the LSL-Kras^{G12D} as well as the LSL-rtTA3-IRES-mKATE2 in adult acinar cells. Conversely, I am also considering obtaining a Sox9-Cre^{ERT2} mouse, which would allow for recombination in the ductal and centroacinar compartments of the adult pancreas, to determine if the cysts are potentially derived from ductal cells.

I am also planning to cross the mutant p53^{R172H} allele into MEK1-KC, MEK2-KC, and MEK1/2-KC mice, which rapidly accelerates the development of PDA, to assess the effect of MEK knockdown on overall survival. The tumors formed in KC mice with the p53^{R172H} mutation can also be made into cell lines, which will be used to test the dependence of MEK isoforms in cell line based assays for growth, anchorage-independent survival, migration, and invasion. The cell lines can then also be used for orthotopic xenograft tumor modeling as well. This can be of particular interest, as chronic MEK inhibition is known to lead to activation of compensatory pathways, such ask PI3K-AKT signaling, which can be more easily modeled with a chronic genetic knockdown.

Figures for Chapter 3: Generation of inducible MEK knockdown mice and characterization in pancreatitis and pancreatic tumorigenesis

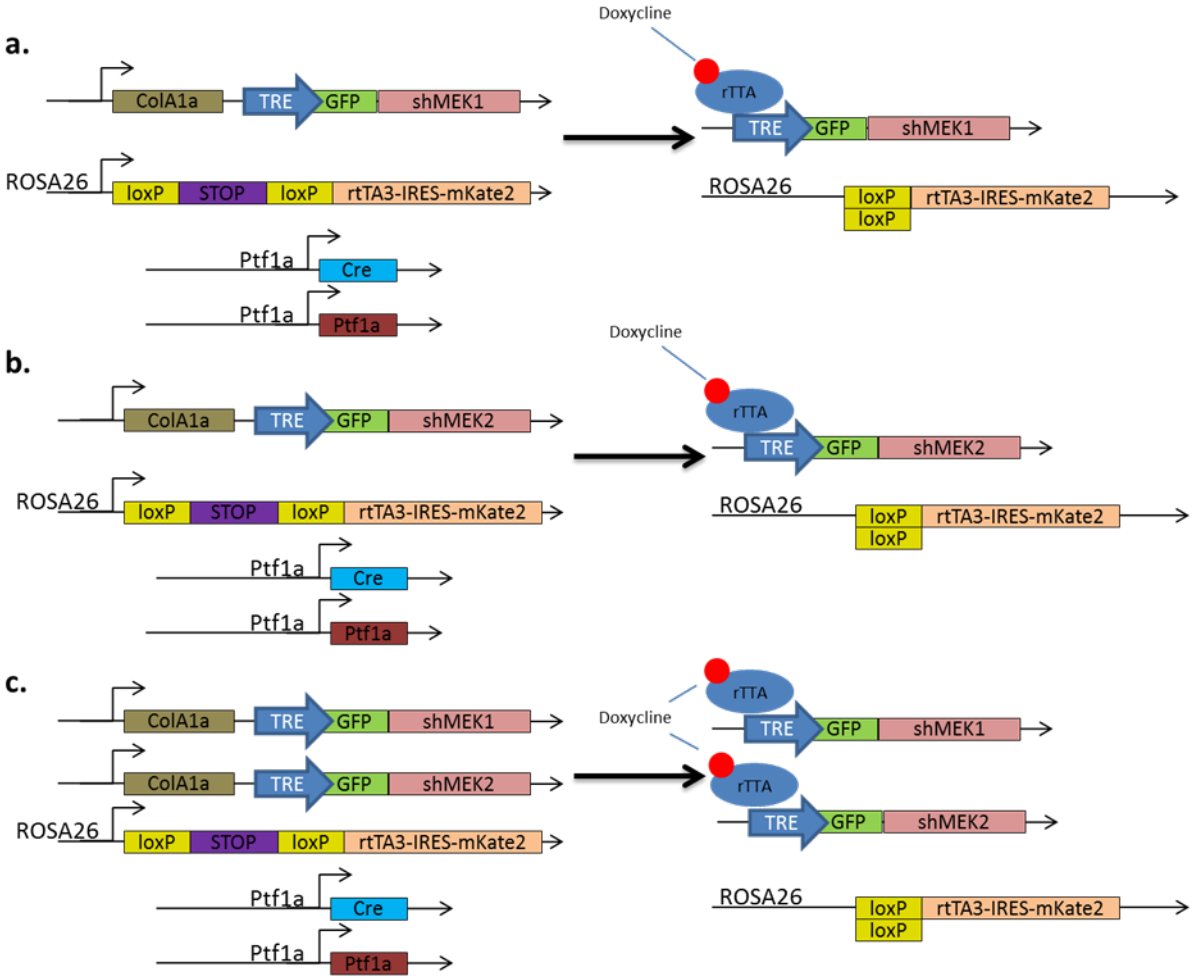
a.
ColA1a
TRE
GFP
shMEK1
ROSA26
loxP
STOP
loxP
rtTA3-IRES-mKate2
Ptf1a
Cre
Ptf1a
Ptf1a
Doxycline
rTTA
TRE
GFP
shMEK1
ROSA26
loxP
loxP
rtTA3-IRES-mKate2
b.
ColA1a
TRE
GFP
shMEK2
ROSA26
loxP
STOP
loxP
rtTA3-IRES-mKate2
Ptf1a
Cre
Ptf1a
Ptf1a
Doxycline
rTTA
TRE
GFP
shMEK2
ROSA26
loxP
loxP
rtTA3-IRES-mKate2
c.
ColA1a
TRE
GFP
shMEK1
ColA1a
TRE
GFP
shMEK2
ROSA26
loxP
STOP
loxP
rtTA3-IRES-mKate2
Ptf1a
Cre
Ptf1a
Ptf1a
Doxycline
rTTA
TRE
GFP
shMEK1
rTTA
TRE
GFP
shMEK2
ROSA26
loxP
loxP
rtTA3-IRES-mKate2

Figure 3: Genetic shRNA mouse model. Schematic of proposed mouse model to create a pancreas specific expression of a short hairpin RNA targeting MEK1, MEK2, MEK1/2 (**a**, **b**, and **c**, respectively). A ROSA26 locus LSL-rtTA-IRES-mKATE2 is recombined in pancreas progenitor cells by Cre recombinase driven from the endogenous Ptf1a promoter. Once recombined, the rtTA will drive transcription of the GFP-shRNA in the Col1a1 locus only in the presence of doxycycline.

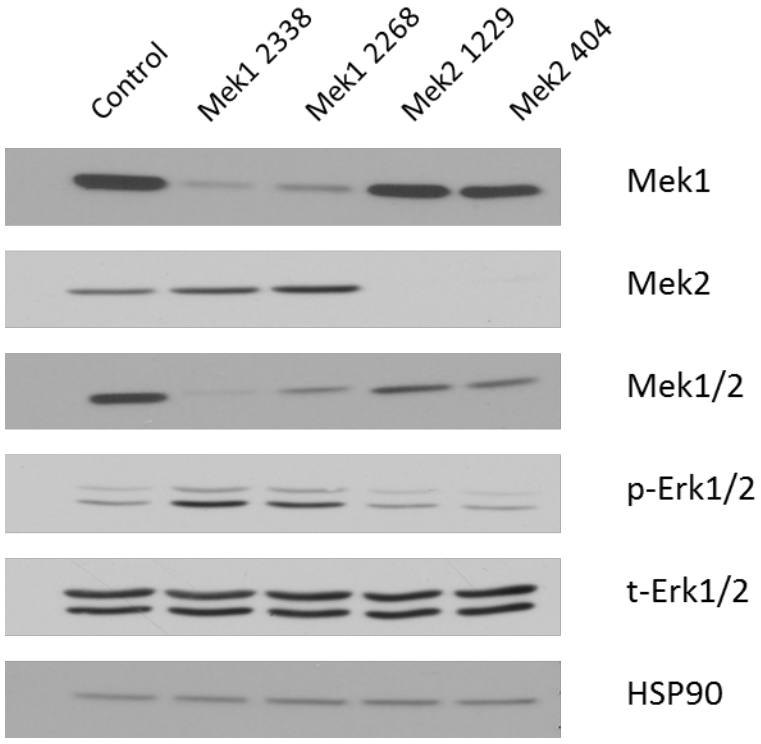
Control
Mek1 2338
Mek1 2268
Mek2 1229
Mek2 404
Mek1
Mek2
Mek1/2
p-Erk1/2
t-Erk1/2
HSP90

Figure 4: shRNA clone selection. NB490 mouse pancreatic cancer cells infected at a low MOI with retroviruses containing short hairpin RNAs targeted for MEK1 or MEK2 were analyzed by western blot. The two knockdowns from each MEK isoform shown were chosen to move forward into mice, and demonstrate potent knockdown of their target isoform while having no effect on the expression of the other MEK isoform. Knockdown of MEK1 also leads to an increase in the level of p-Erk compared to MEK2 knockdown or control in NB490 cells.

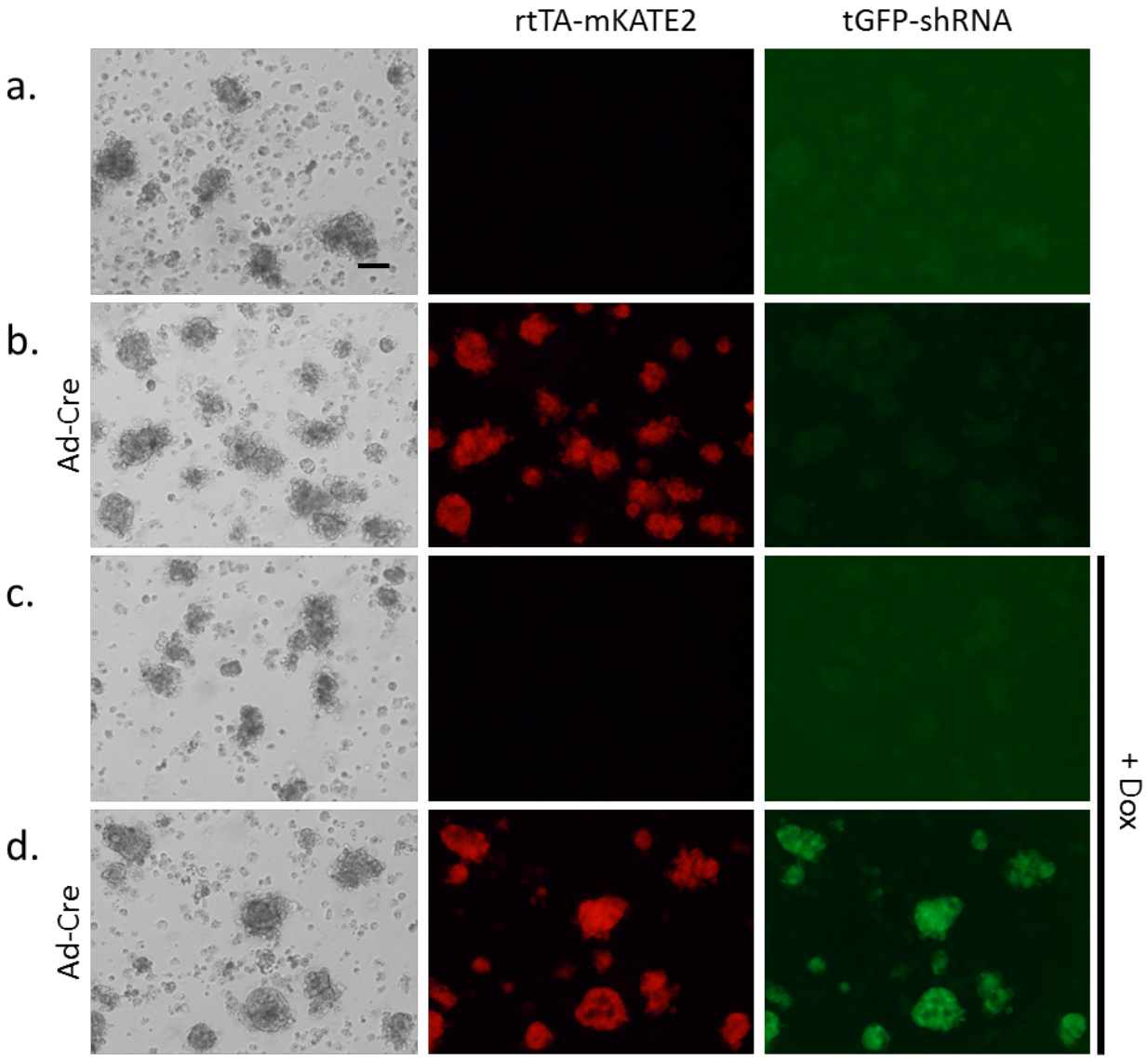
rtTA-mKATE2
tGFP-shRNA
a.
b.
Ad-Cre
c.
d.
Ad-Cre
+ Dox

Figure 5: Validation of fluorescent reporters. Infection of primary acinar cells from a LSL-rtTA-IRES-mKATE2;tet-O-turbo-GFPshRNA mouse with adenoviral Cre (**b**, **d**) led to the expression the red fluorophore mKATE2. Treatment of infected (**d**) or uninfected (**c**) acinar cells with 1μM doxycline for 24 hours led to the production of turbo-GFP only in the acinar cells which had been infected with adenoviral Cre. Scale bar = 100μm.

a.

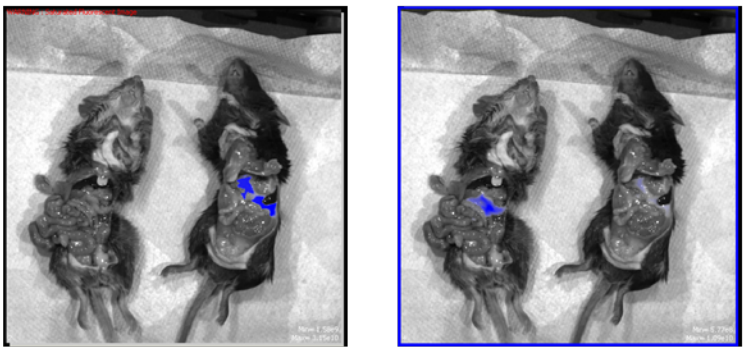

+ rttA - shRNA | + rttA + shRNA | + rttA - shRNA | + rttA + shRNA

b.

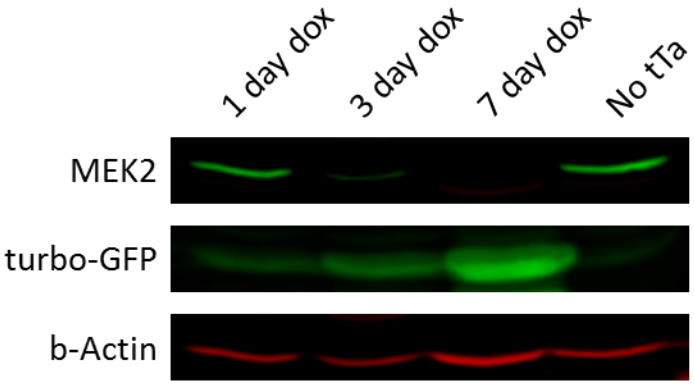

c.

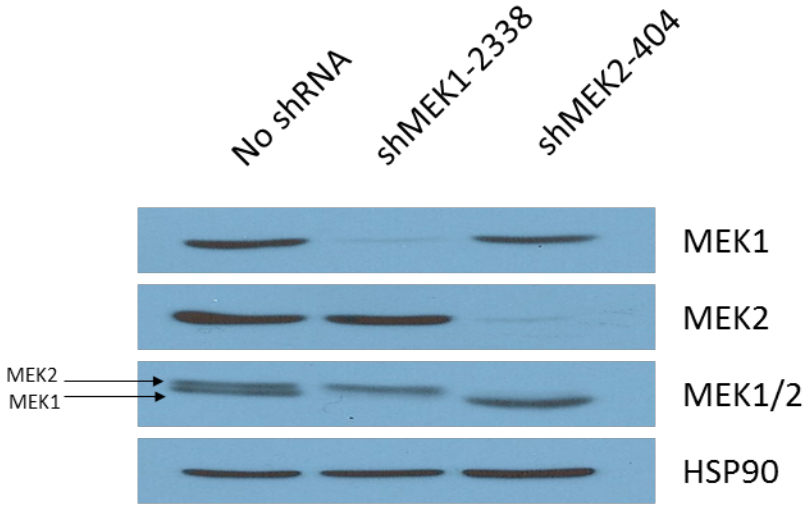

Figure 6: In vivo validation of shRNA organ specificity, kinetics, and efficiency. a. The abdominal cavities of Ptf1a$^{+/Cre}$;CAG-LSL-rtTA-IRES-mKATE2 and a tGFP-shRNA; Ptf1a$^{+/Cre}$;CAG-LSL-rtTA-IRES-mKATE2 mouse on doxycycline chow for 1 week prior to euthanization were exposed and imaged on an IVIS Spectrum scanner for both GFP and RFP fluorescence. Both mice exhibit RFP fluorescence, however GFP fluorescence is only observed in the mouse containing all three transgenes. **b**. Assessment of the kinetics of gene knockdown and GFP expression was performed by western blot of whole pancreas lysates from shMEK2 mice put on doxycycline chow for 1,3, or 7 days. GFP expression is seen within 24 hours of administration of doxycycline, however MEK2 protein levels are first affected at 72 hours after doxycycline administration. The loss of MEK2 expression as well as the induction of GFP expression was maximized after seven days. **c.** Whole pancreas extract of a control, shMEK1, and shMEK2 mice were analyzed by western blot to determine specificity of the knockdown to each MEK isoform, as well as the level of knockdown. Both shMEK1 and shMEK2 were specific to their targets, and generated efficient gene knockdown.

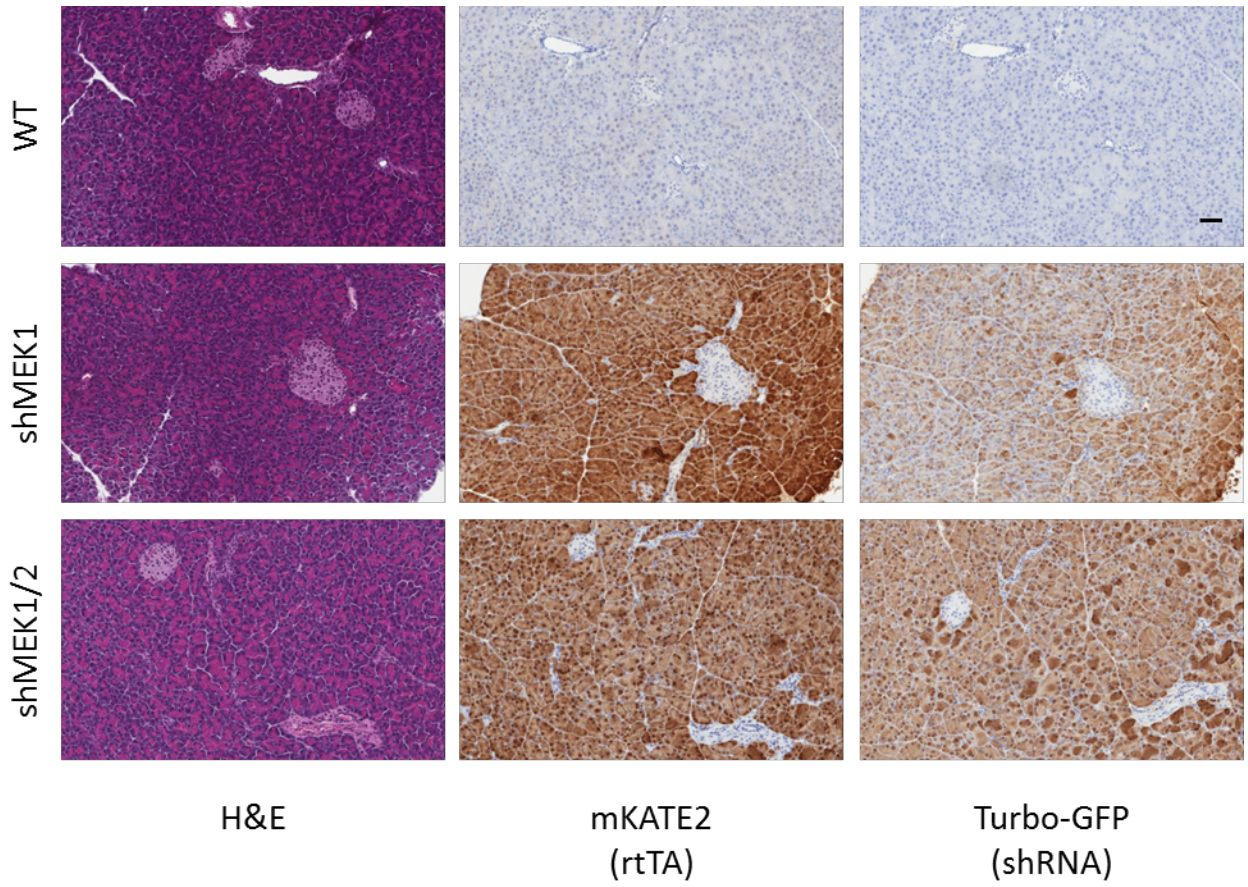
WT
shMEK1
shMEK1/2
H&E
mKATE2
(rtTA)
Turbo-GFP
(shRNA)

Figure 7: Histology of reporter fluorophores in pancreatic tissue. Expression of the rtTA and shRNA transgenes examined in tissue of mice placed on doxycycline water for 1 week by immunohistochemistry for mKATE2 or GFP expression, respectively, revealed that the expression of both reporters were co-localized in the tissue. The reporters appeared to be expressed only in acinar cells, not duct cells or islets. Scale bar = 100μm

a.

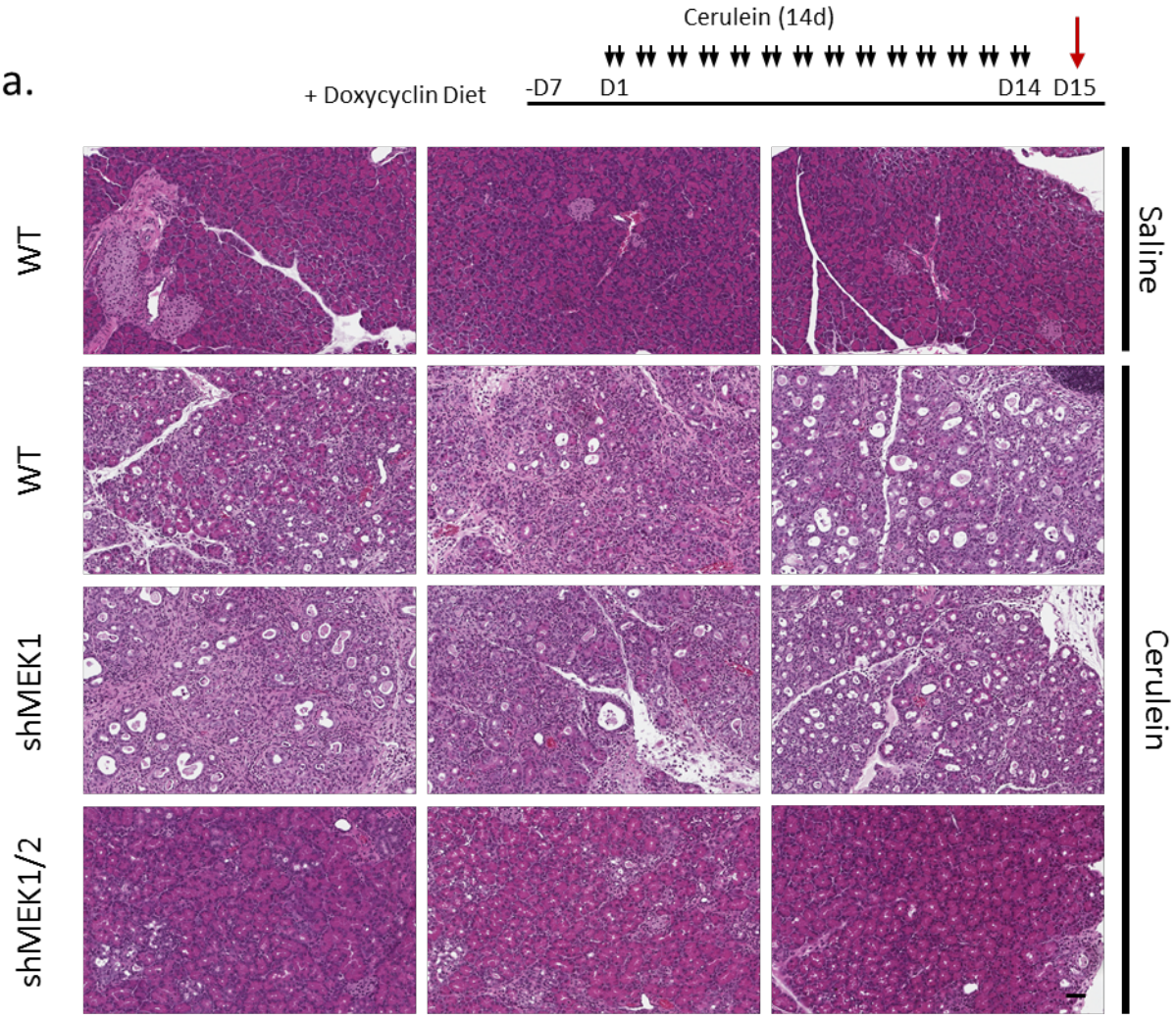
Cerulein (14d)
+ Doxycyclin Diet
-D7
D1
D14
D15
WT
WT
shMEK1
shMEK1/2
Saline
Cerulein

b.

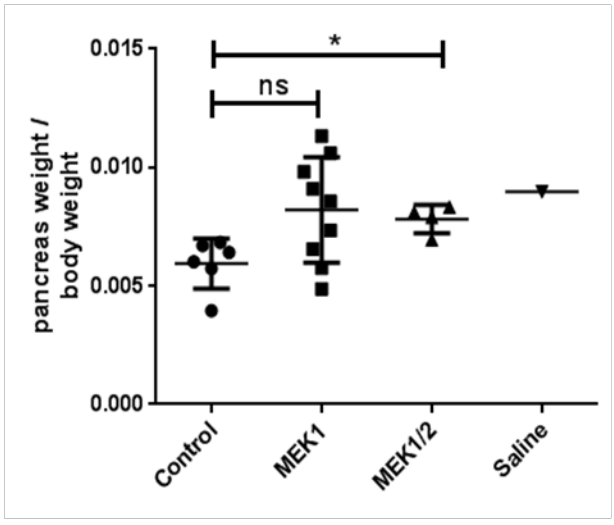
pancreas weight / body weight
0.015
0.010
0.005
0.000
*
ns
Control
MEK1
MEK1/2
Saline

n=6 n=9 n=4 n=1

Figure 8: Histology of chronic pancreatitis in WT and shRNA mice. a. Tissue of WT, shMEK1, and shMEK1/2 mice treated chronically with cerulein twice per day for 2 weeks then sacrificed 24 hours after the last injection were stained with hematoxylin and eosin. Each image represents an individual mouse. WT and shMEK1 mice demonstrated heavy loss of acinar cells and subsequent replacement by desmoplastic stroma. shMEK1/2 mice retained the majority of the acinar structure with small pockets of damaged cells throughout the tissue. **b.** Chronic treatment of WT and shMEK1 mice lead to a reduction in pancreas to bodyweight ratio, however shMEK1/2 pancreata retained significantly more mass than WT chronic cerulein treated pancreata. Scale bar = 100μm. Statistics were done using an unpaired student's T test, with significance annotated at $p<0.05$.

a.

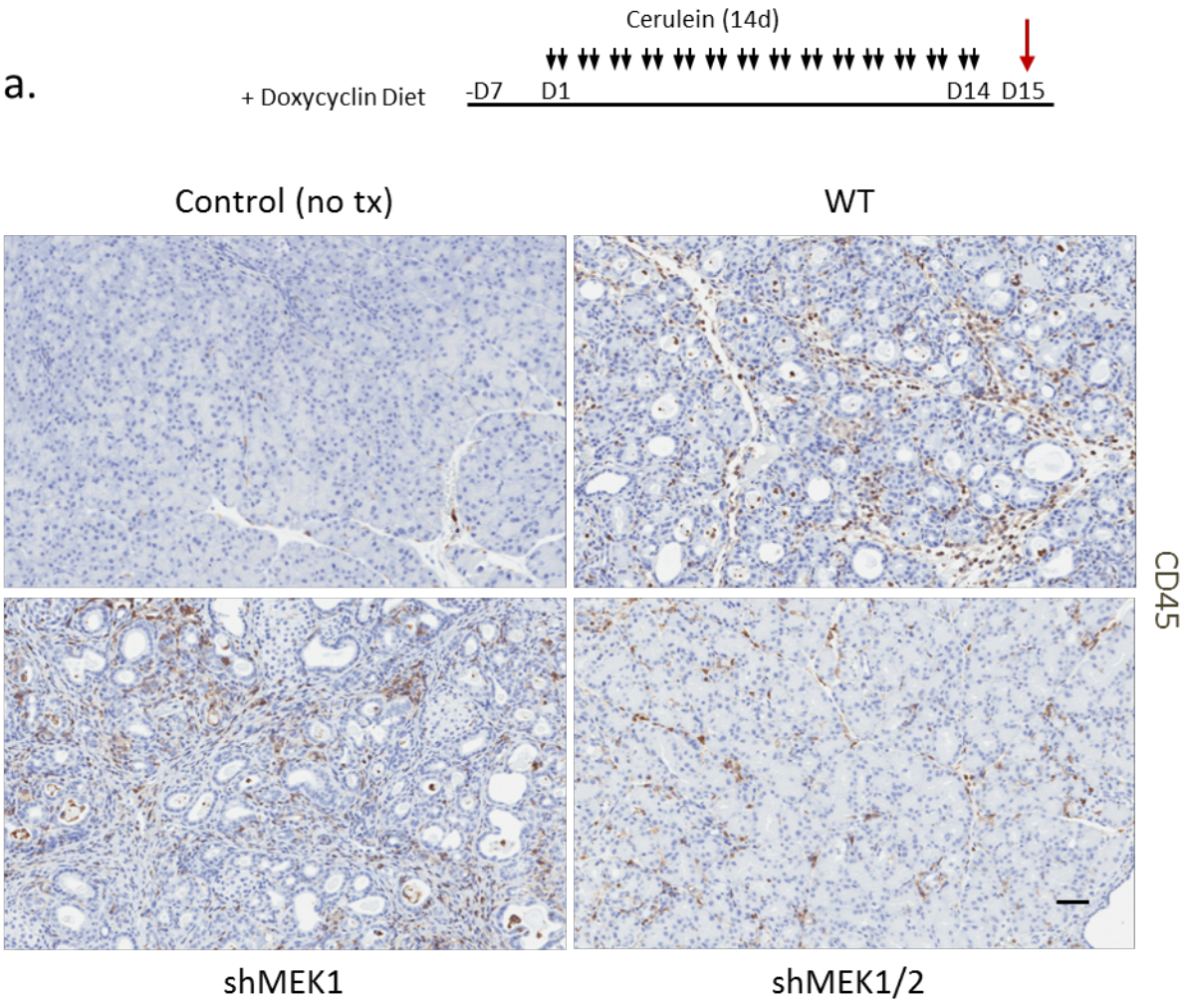
Cerulein (14d)
+ Doxycyclin Diet
-D7
D1
D14
D15
Control (no tx)
WT
CD45
shMEK1
shMEK1/2

b.

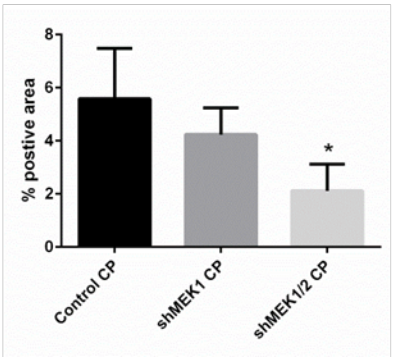
% postive area
8
6
4
2
0
*
Control CP
shMEK1 CP
shMEK1/2 CP

Figure 9: shMEK1/2 mice have less immune cell infiltration. a. Tissues from WT, shMEK1, and shMEK1/2 mice treated chronically with cerulein twice per day for 2 weeks then sacrificed 24 hours after the last injection were stained with CD45 antibody to look at total immune cell infiltration in response to cerulein treatment. CD45 positive cells were prevalent throughout WT and shMEK1 tissues, and shMEK1/2 tissue to a lesser extent. **b.** Quantitation of CD45 positive pixels demonstrated that shMEK1/2 mice had significantly less CD45 positive staining than either shMEK1 or WT treated animals. n= 3 from all samples. Scale bar = 100μm. Statistics were done using an unpaired student's T test, with significance annotated at $p<0.05$.

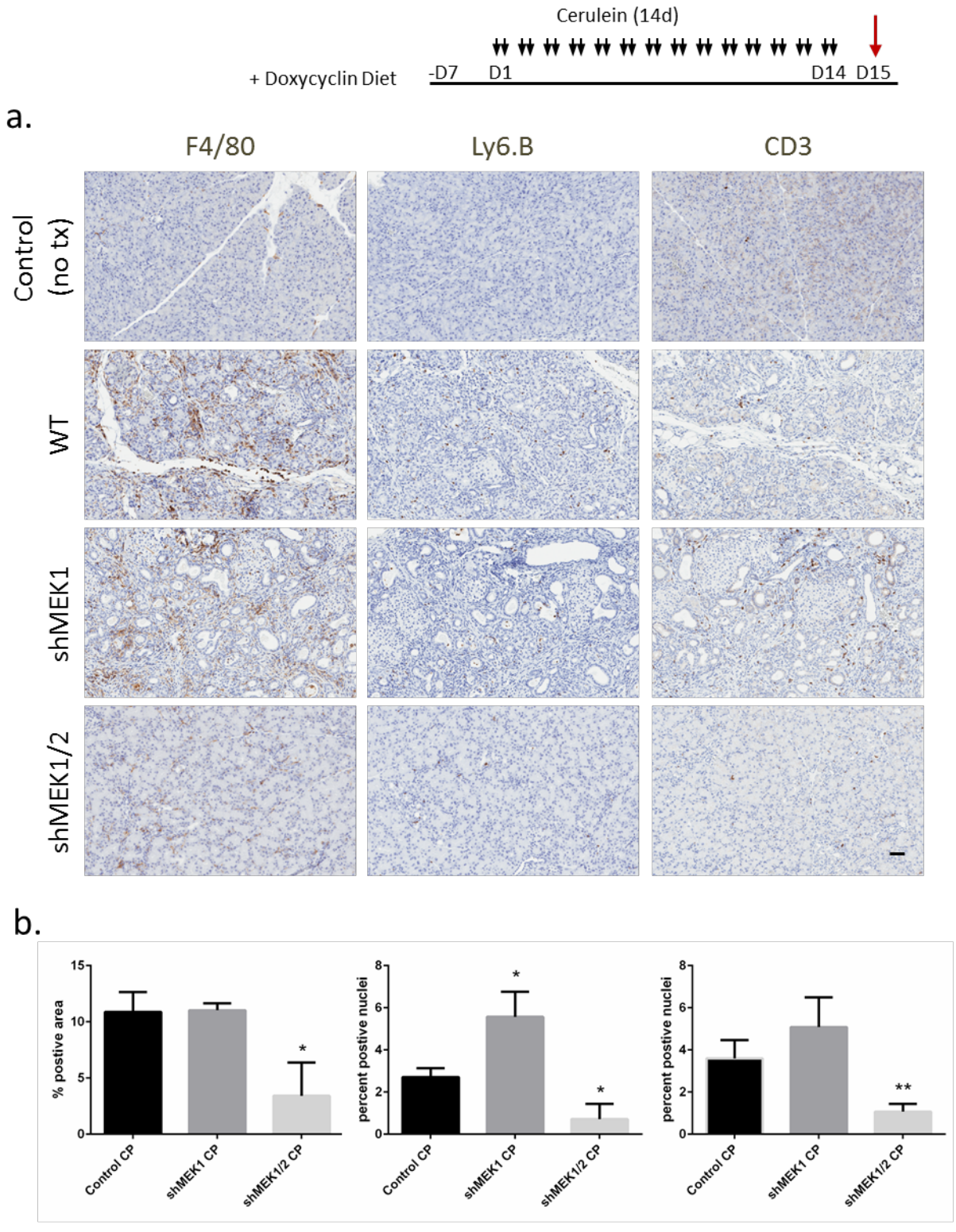
Cerulein (14d)
+ Doxycyclin Diet
-D7
D1
D14
D15
a.
F4/80
Ly6.B
CD3
Control (no tx)
WT
shMEK1
shMEK1/2
b.
% postive area
percent postive nuclei
percent postive nuclei
Control CP
shMEK1 CP
shMEK1/2 CP
Total Macrophages
Total Neutrophils
Total T-Cells

Figure 10: shMEK1/2 mice demonstrate reduced numbers of macrophages, neutrophils and T-cells. a. WT, shMEK1, and shMEK1/2 mice were treated chronically with cerulein twice per day for 2 weeks then sacrificed 24 hours after the last injection and tissues were then stained for F4/80, Ly6.B, or CD3 to look at populations of macrophages, neutrophils, and T-cells, respectively. All three immune populations were mostly absent in untreated pancreata, which contrasted with cerulein treated tissues. **b.** Quantitation of the F4/80, Ly6.B, or CD3 staining revealed significantly lower numbers of all immune cell populations in the shMEK1/2 mice as compared to both the cerulein treated WT and shMEK1 mice. Cerulein treated shMEK1 mice also demonstrated a significantly increased number of neutrophils over WT treated mice. n= 3 from all samples. Scale bar = 100μm. Statistics were done using an unpaired student's T test, with significance annotated at $p<0.05$.

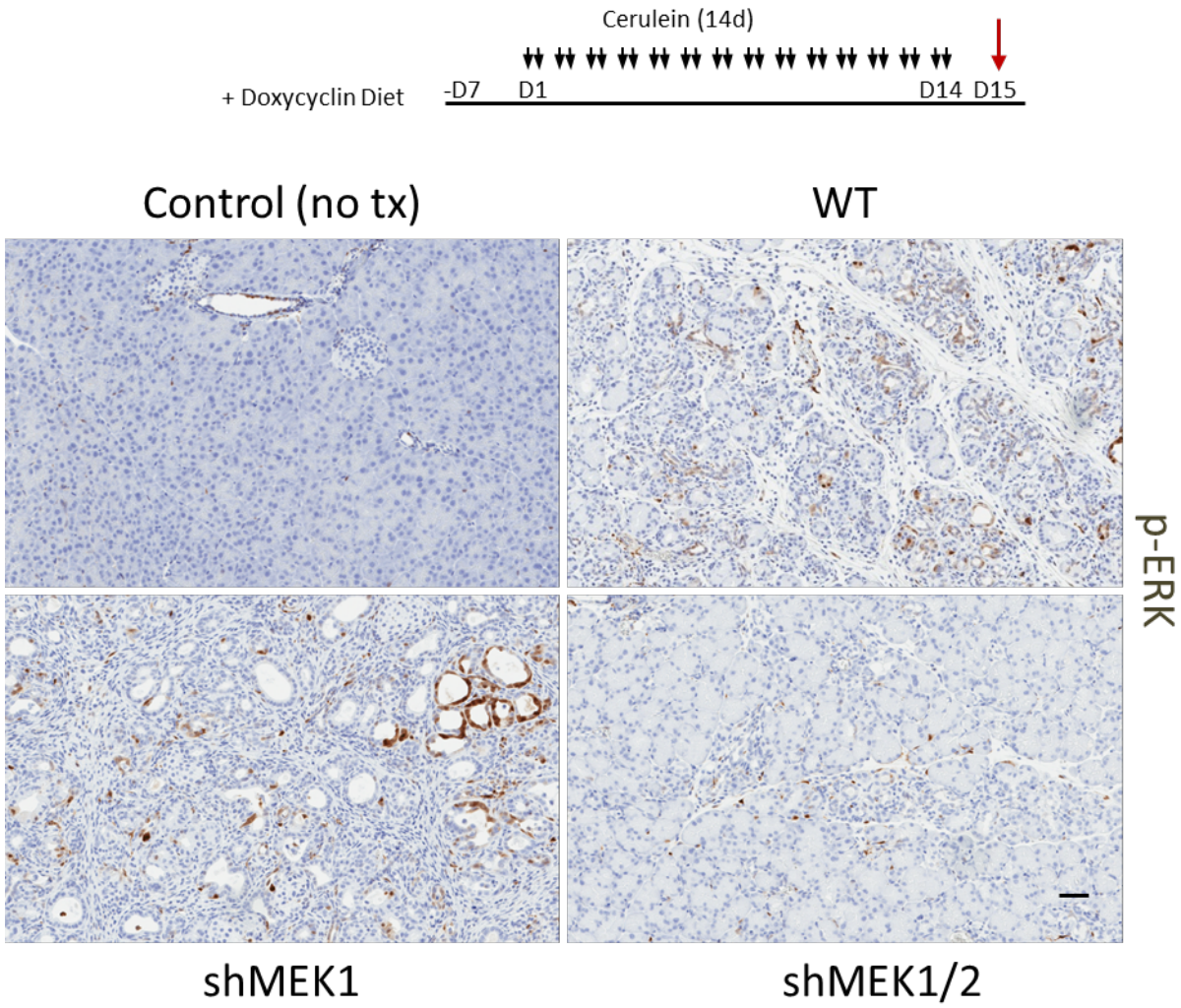
Cerulein (14d)
+ Doxycyclin Diet
-D7
D1
D14
D15
Control (no tx)
WT
p-ERK
shMEK1
shMEK1/2

Figure 11: Chronic cerulein activation of ERK is reduced in shMEK1/2 mice. Assessment of the levels of ERK phosphorylation by IHC in chronically cerulein treated WT, shMEK1, and shMEK1/2 mice and a nontreated WT control revealed that WT and shMEK1 mice had high levels of activated ERK as compared to untreated or shMEK1/2 mice. The p-ERK stain was located predominantly in ADM, as well as in the stroma. shMEK1/2 mice demonstrated an overall lower level of staining which was all located in the stroma, however the lack of ADM in shMEK1/2 mice makes a direct comparison impossible to the other cerulein treated genotypes. Scale bar = 100μm.

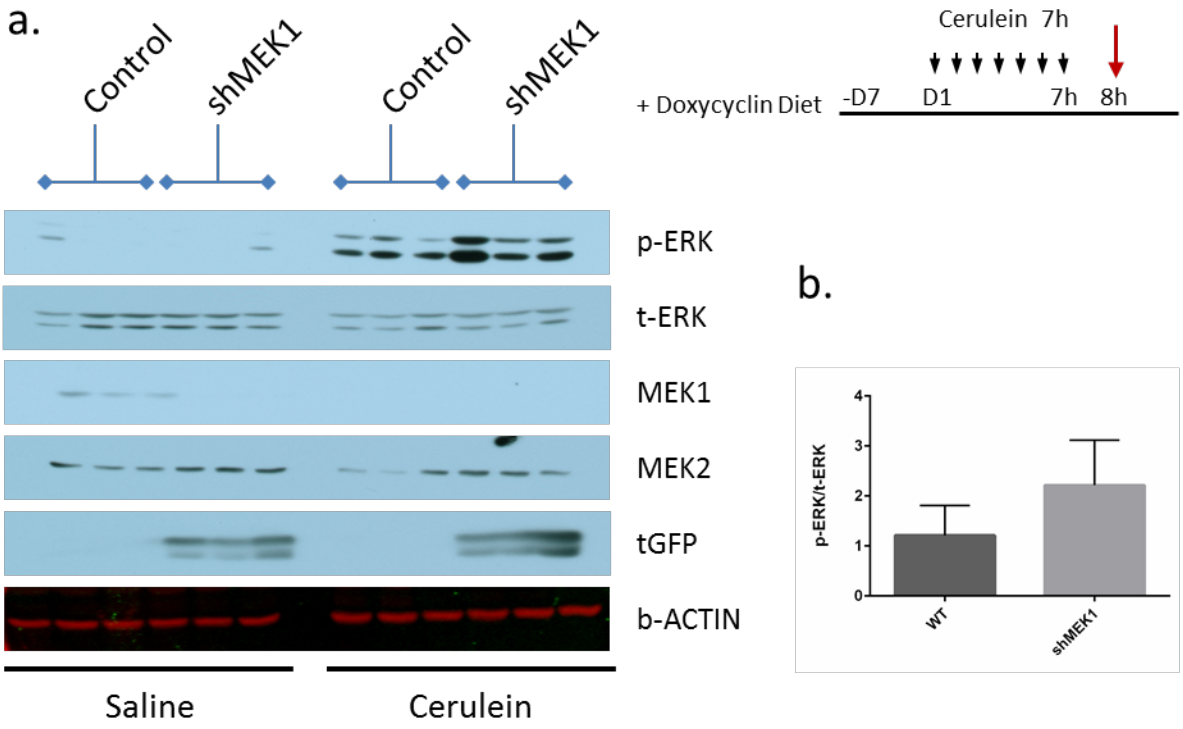
a.
Control
shMEK1
Control
shMEK1
Cerulein 7h
+ Doxycyclin Diet
-D7
D1
7h
8h
p-ERK
t-ERK
MEK1
MEK2
tGFP
b-ACTIN
Saline
Cerulein
b.
p-ERK/t-ERK
WT
shMEK1

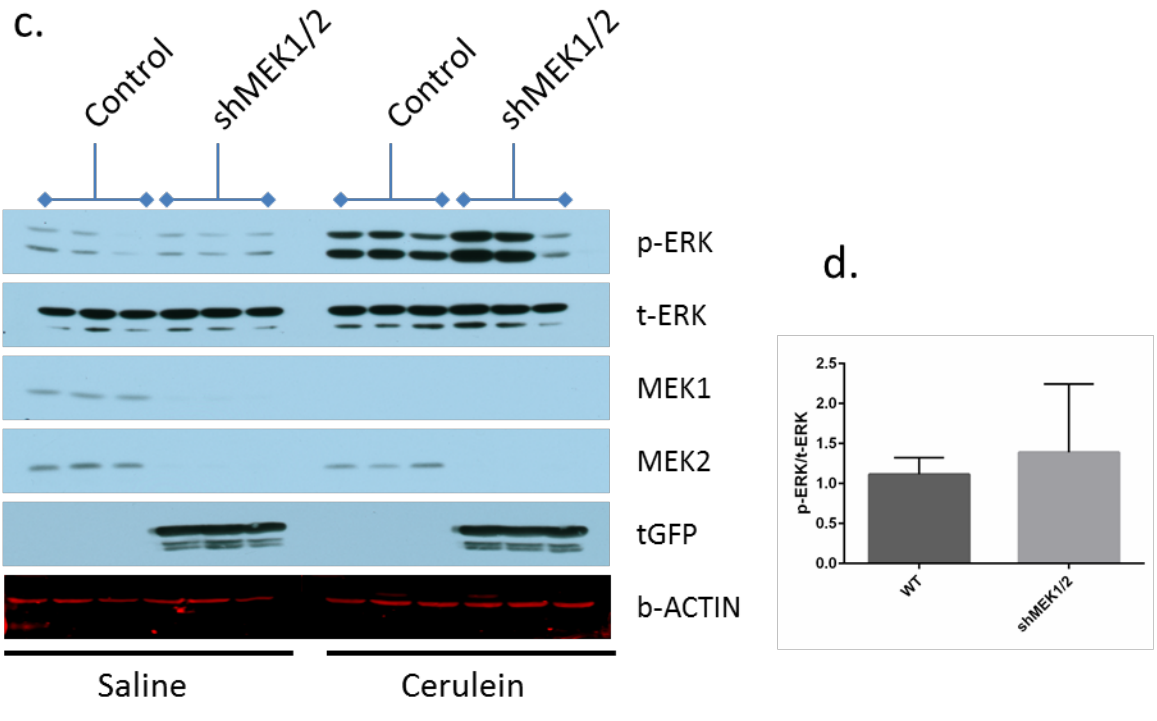
c.
Control
shMEK1/2
Control
shMEK1/2
p-ERK
t-ERK
MEK1
MEK2
tGFP
b-ACTIN
Saline
Cerulein
d.
p-ERK/t-ERK
WT
shMEK1/2

Figure 12: ERK is activated in shMEK1/2 mice treated acutely with cerulein. a. Comparison of ERK phosphorylation WT or shMEK1 mice on doxycline diet for one week treated with cerulein or saline by western blot of total pancreas lysate revealed an increased level of activation of ERK in response to cerulein treatment in both WT and shMEK1 mice as compared to saline treated controls. shMEK1 mice treated with cerulein also appeared to have a higher level of ERK activation in response to cerulein compared to WT mice (**b**). Levels of MEK1 protein successfully was reduced in shMEK1 mice compared to controls, which was accompanied by the acquisition of turboGFP expression. WT mice treated with cerulein also demonstrated a loss of MEK1 protein levels compared to untreated controls. **c.** Comparison of WT and shMEK1/2 mice on doxycline diet for one week then treated with cerulein or saline revealed an increase in the levels of ERK phosphorylation in response to cerulein treatment in both WT and shMEK1/2 mice. shMEK1/2 mice treated with cerulein had an increased amount of ERK activation as compared to cerulein treated WT mice (**d**). Both MEK1 and MEK2 protein levels were reduced in shMEK1/2 mice compared to WT, which corresponded to expression of turboGFP.

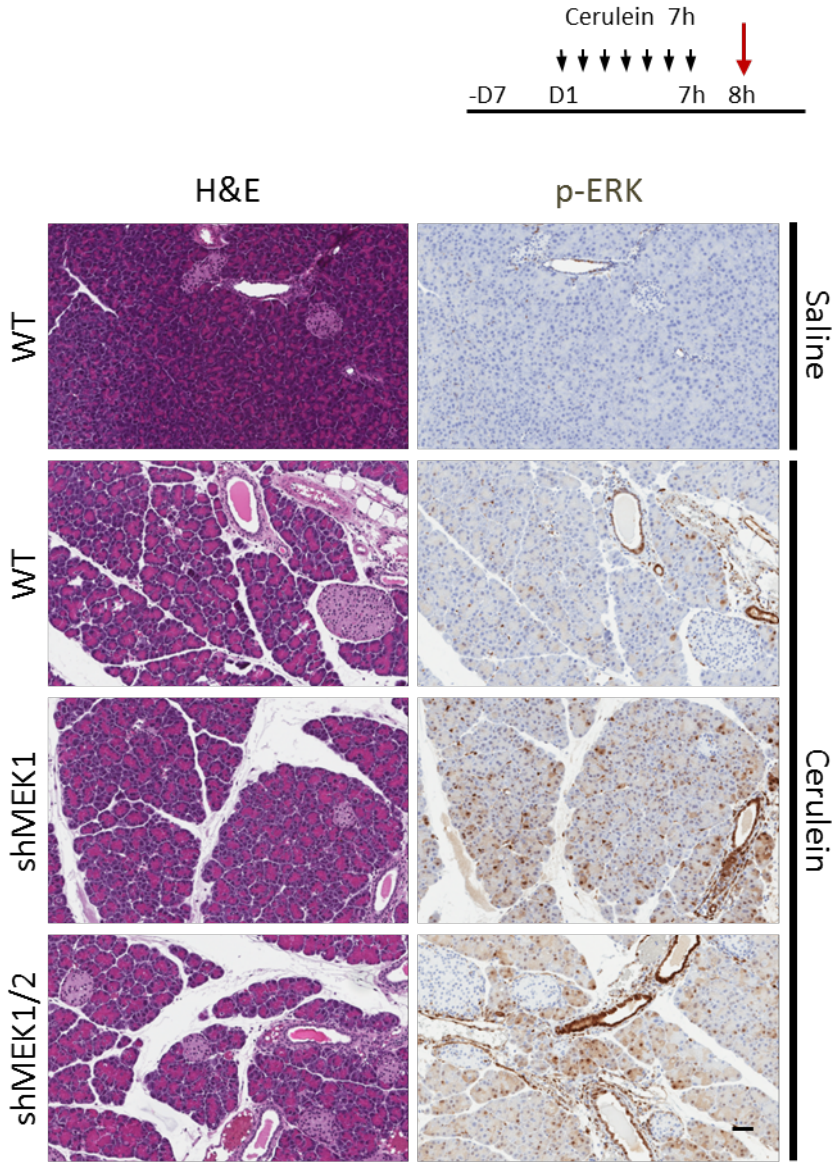
Cerulein 7h
-D7
D1
7h
8h
H&E
p-ERK
WT
WT
shMEK1
shMEK1/2
Saline
Cerulein

Figure 13: shMEK1/2 mice have acinar cell activation of ERK in response to acute cerulein treatment. Immunohistochemistry of WT, shMEK1, and shMEK1/2 mice treated acutely with cerulein compared to a saline treated WT revealed an increase in ERK phosphorylation levels in acinar cells as well as in duct cells. Cerulein treated shMEK1 and shMEK1/2 also had more frequent staining of phospho-ERK in acinar cells compared to cerulein treated WT mice. Scale bar = 100μm.

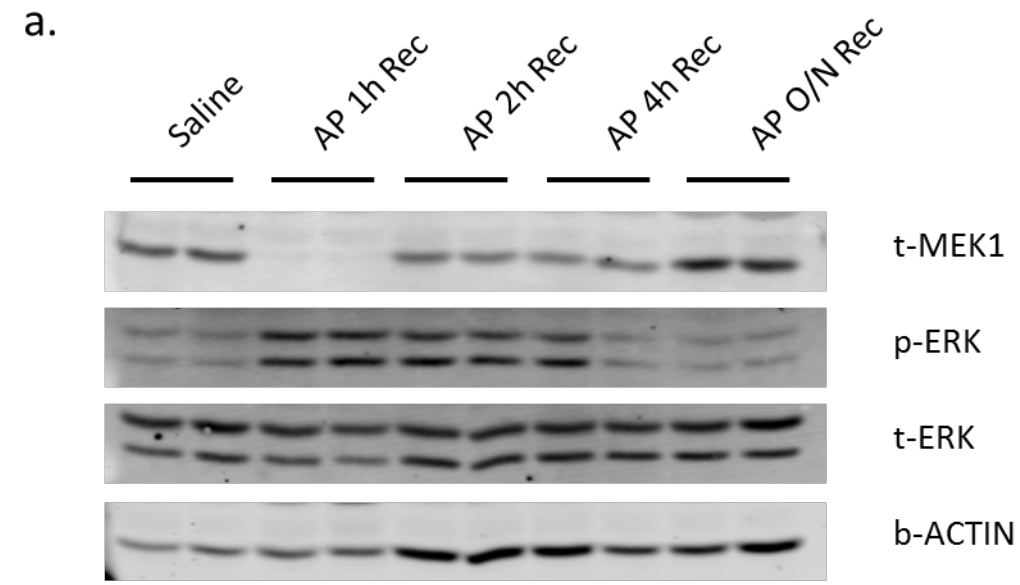
a.
Saline
AP 1h Rec
AP 2h Rec
AP 4h Rec
AP O/N Rec
t-MEK1
p-ERK
t-ERK
b-ACTIN

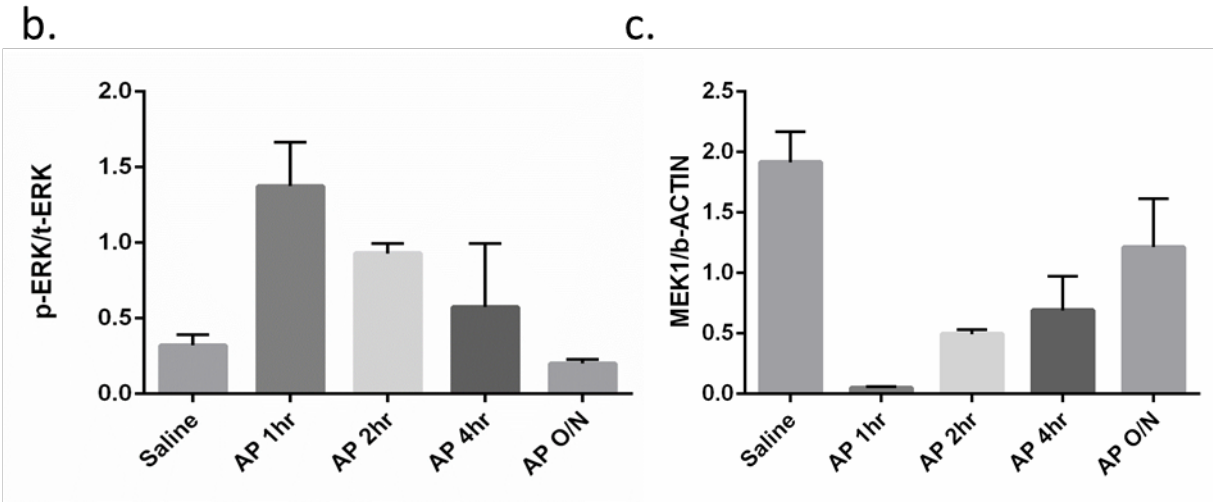
b.
p-ERK/t-ERK
2.0
1.5
1.0
0.5
0.0
Saline
AP 1hr
AP 2hr
AP 4hr
AP O/N
c.
MEK1/b-ACTIN
2.5
2.0
1.5
1.0
0.5
0.0
Saline
AP 1hr
AP 2hr
AP 4hr
AP O/N

Figure 14: Kinetics of ERK activation and MEK1 protein equilibrium in WT mice. a. WT mice treated acutely with cerulein were harvested at specific recovery time points and compared to WT mice treated with saline as controls. At 1 hour recovery from cerulein treatment, WT mice had increased levels of ERK phosphorylation (**b)** as well as decreased MEK1 protein levels (**c**). By 2 hours post treatment, the phospho-ERK levels remained elevated, and MEK1 protein levels began to return. By 4 hours recovery after cerulein treatment, phospho-ERK levels began to decline, and after an overnight recovery had returned to a level comparable with saline treated mice. MEK1 protein levels in cerulein treated mice were also found to be restored to the levels of saline treated mice after overnight recovery.

a.

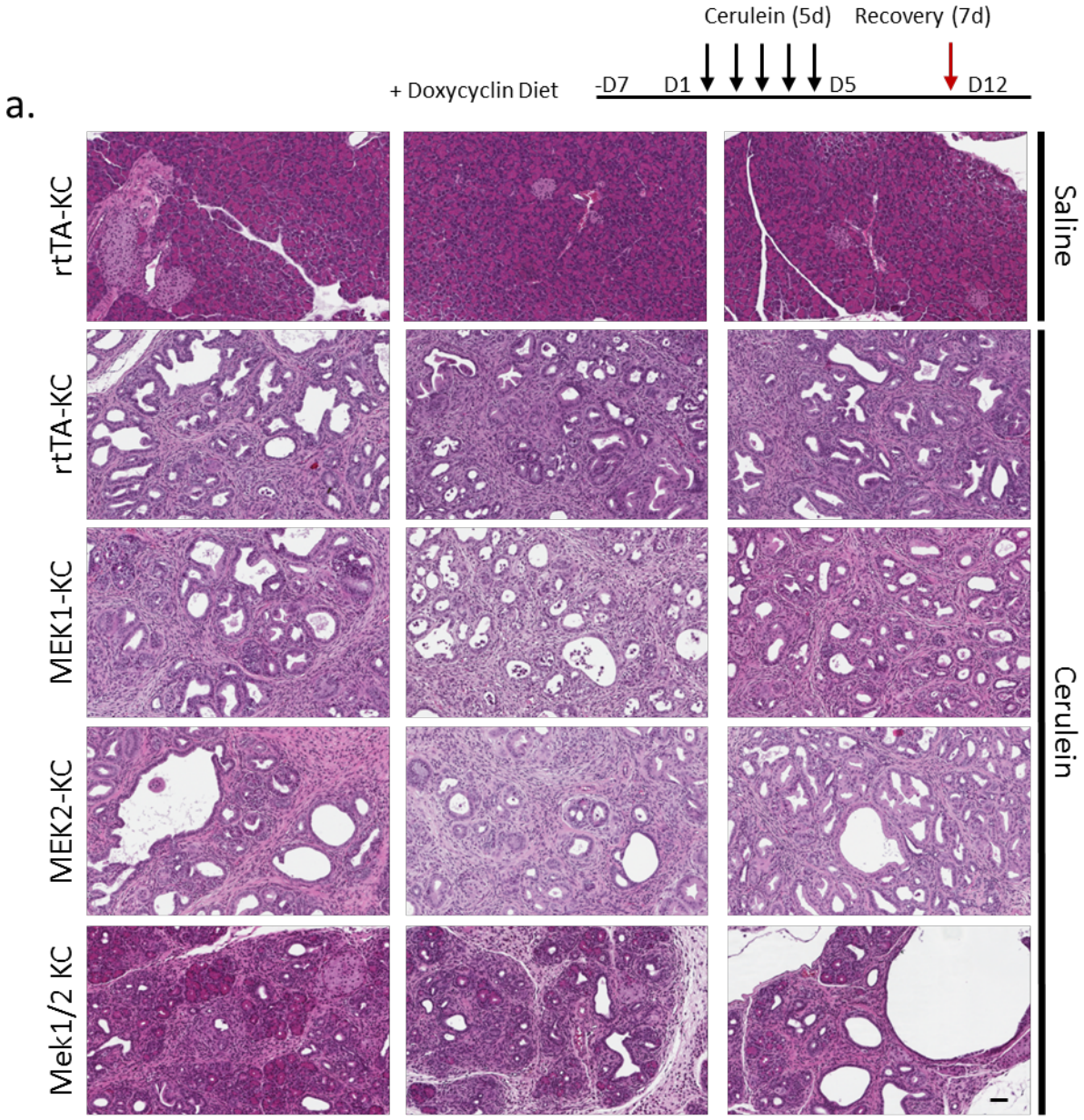
Cerulein (5d)
Recovery (7d)
+ Doxycyclin Diet
-D7
D1
D5
D12
rtTA-KC
rtTA-KC
MEK1-KC
MEK2-KC
Mek1/2 KC
Saline
Cerulein

b.

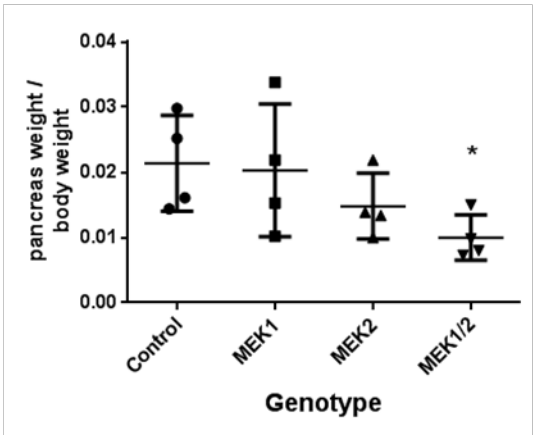
pancreas weight / body weight
0.04
0.03
0.02
0.01
0.00
*
Control
MEK1
MEK2
MEK1/2
Genotype

Figure 15: shMEK1/2 KC mice retain acinar cells and have smaller pancreata in response to cerulein challenge. a. Histology of WT KC, MEK1 KC, MEK2 KC, and MEK1/2 KC mice placed on doxycycline chow for a week prior to a 5 day cerulein or saline treatment protocol followed by a 7 day recovery demonstrates that all the genotypes had acinar cell mass replaced with tumors in response to cerulein treatment. Tumor formation is absent in WT KC mice treated with saline. There was also abundant formation of desmoplastic stroma in all the cerulein treated animals, however shMEK1/2 mice treated with cerulein retained a greater amount of normal epithelial areas compared to WT, shMEK1 and shMEK2 mice. Scale bar = 100μm. **b.** shMEK1/2 mice had a significantly lower pancreas to bodyweight ratio compared to cerulein treated WT KC mice. n= 3 from all samples. Statistics were done using an unpaired student's T test, with significance annotated at $p<0.05$

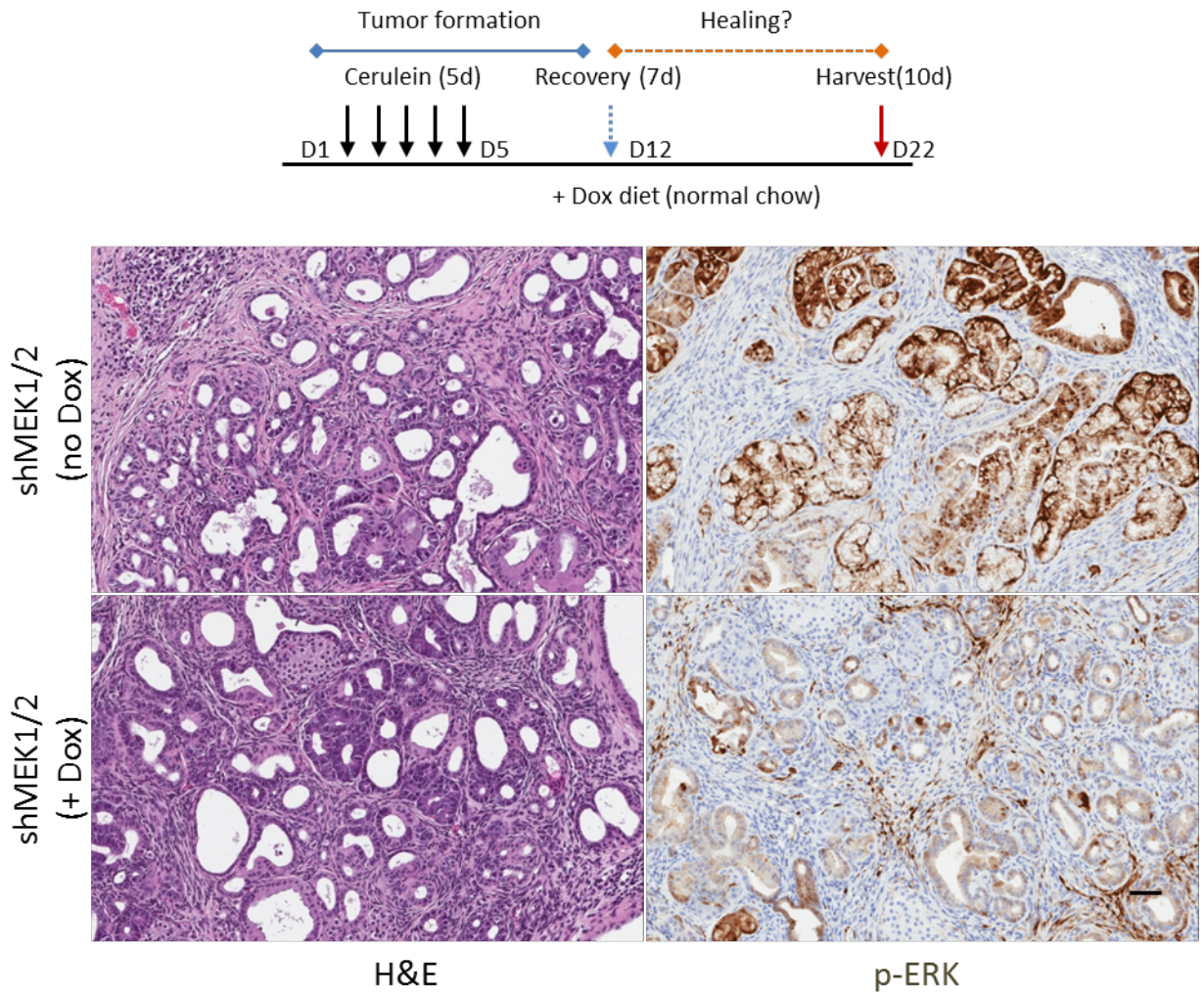
Tumor formation
Healing?
Cerulein (5d)
Recovery (7d)
Harvest(10d)
D1
D5
D12
D22
+ Dox diet (normal chow)
shMEK1/2 (no Dox)
shMEK1/2 (+ Dox)
H&E
p-ERK

Figure 16: MEK1/2 knockdown in established tumors leads to loss of ERK activation. Histology of shMEK1/2 mice treated with cerulein for 5 days followed by a 7 day recovery then administered either doxycycline chow or normal for 10 days prior to harvest showed that both cohorts had acinar cell mass largely replaced by tumors and desmoplastic stromal. Immunohistochemistry analysis of ERK phosphorylation levels revealed that the doxycycline treated group had a dramatic reduction in the amount of phospho-ERK in PanIN lesions. Scale bar = 100μm.

Chapter 4: EGFR activation of ERK is required for Notch induced ADM

Background

Notch pathway in ADM

EGFR signaling has been identified long ago as a contributor to ADM, as ectopic expression of an EGFR ligand by transgenic expression under a generic zinc-inducible metallothionein or acinar cell-specific elastase promoter caused wild spread ADM in the pancreas[58]. This observation was harnessed to create an *in vitro* ADM transdifferentiation assay by treating collagen embedded acinar cell explants with recombinant TGF-α[119]. In the transdifferentiation assay, collagen embedded acinar cells treated with TGF-α undergo ADM in 5 days as demonstrated by a loss of acinar markers and a gain of ductal markers by immunostaining. There is also a striking change in morphology from a cluster of acinar cells to a hollow cyst, or "tube structure", which we now recognize as ADM.

Investigation into the signaling pathways that are active in ADM of the transgenic TGF-α overexpression mice revealed an activation of Notch1 and the expression of the Notch pathway target Hes1 in ADM[60]. Treatment of collagen embedded acinar cells with TGF-α was seen to increase the transcription levels of several Notch targets and the Notch receptors after transdifferentiation into ductal cysts as compared to normal acinar cells. Inhibition of either EGFR or gamma-secretase was sufficient to block ADM driven by TGF-α treatment. Expression of an adenoviral Notch1-ICD (N1ICD), which would override the need for Notch receptor activation, is sufficient for induction of ADM even in the presence of gamma-secretase

inhibition. Finally, while treatment with an EGFR inhibitor is able to block TGF-α induced ADM, N1ICD driven ADM is not completely blocked by EGFR inhibition. This result suggested that Notch signaling is activated downstream of the EGFR pathway as and is required for acinar to ductal metaplasia without additional need of EGFR signaling.

Notch has also been shown to be important for ADM in several contexts not specifically related to EGFR activation, although none have demonstrated that this role of Notch in ADM is independent of EGFR activation. TGF-α treated acinar cells from MMP7 null mice are incapable of undergoing ADM in collagen cultures due to a lack of Notch activation[120]. The MMP7 dependent block in ADM could be rescued by expression of either N1ICD or Notch2-ICD (N2ICD). Additionally, recombinant MMP7 itself is capable of inducing ADM by the activation of Notch signaling, which could be blocked with either gamma-secretase inhibition or the expression of a dominant-negative RBP-Jκ protein to inhibit Notch signaling.

PKD1 has also been suggested to activate Notch during ADM, as inhibition of PKD1 blocks ADM as well as lowers the expression of the Notch target genes Hes1 and Hey1[121]. ADM is also blocked in acinar cells expressing $Kras^{G12D}$ by inhibition of PKD1 or inhibition of gamma-secretase inhibitors, which led the authors to the conclusion that PKD1 was signaling downstream of Kras. Expression of an active form of the PKD1 protein was also shown to be sufficient to drive ADM in a manner which could be blocked by gamma secretase inhibition, or knockdown of Notch1 protein by shRNA[121]. The Notch1 dependence of active PKD1 induced ADM is surprising, as acinar cells from Notch1 knockout mice have no defect in ADM formation induced by either TGF-α or $Kras^{G12D}$ expression[122].

EGFR pathway activation is required for ADM and tumorigenesis

Recently, we and others have shown that EGFR is required for pancreatic tumorigenesis by crossing $EGFR^{flox/flox}$ mice with $Kras^{+/G12D}$;$Ptfa1^{+/Cre}$ mice (KC mice) to generate $EGFR^{flox/flox}$;$Kras^{+/G12D}$;$Ptfa1^{+/Cre}$ mice (EKC mice)[72,73]. EKC mice rarely developed PanINs as they aged, and the lesions that did develop were found to be EGFR positive by immunohistochemical staining. Treatment of EKC mice with cerulein also did not result in pancreatitis induced ADM or PanIN formation as seen in normal mice. Furthermore, KC acinar cells underwent spontaneous ADM by day 3 in collagen, whereas EKC acinar cell explants failed to transdifferentiate in that timeframe. Importantly, EKC mice with a conditional loss of the p53 tumor suppressor protein developed PanINs and PDA, with EGFR ablation generating relatively no benefit in survival.

We also determined that acinar cells harvested from mice with a pan-pancreatic EGFR deletion, $EGFR^{flox/flox}$;$Ptfa1^{+/Cre}$ mice (E-KO mice), embedded in collagen were resistant to ADM by cerulein treatment as compared to cells with functional EGFR, and E-KO mice demonstrated resistance to cerulein induced chronic pancreatitis. Lastly, blockade of MEK-kinase by pharmacological inhibition in KC mice treated with cerulein was sufficient to block induction of tumorigenesis, and treatment of KC acinar cultures with a MEK inhibitor was able to block ADM.

Taken together, these data suggest that EGFR signaling, in the presence of WT p53, is necessary for ADM and subsequent tumorigenesis by activation of ERK signaling. Given the previous work suggesting that Notch activation is sufficient to drive ADM and tumorigenesis as downstream targets of EGFR[60], MMP7[120], and PKD1[121], I set out to determine if Notch

activation was sufficient to bypass the blockade of ADM in E-KO and EKC mice using *ex vivo* acinar cell explants.

Results

EGFR signaling is necessary for Notch induced ADM

To validate that N2ICD expression can cause ADM in acinar cells, I harvested and infected acinar cells from WT mice with either adenoviral GFP (ad-GFP) or adenoviral Notch2ICD-GFP (ad-N2ICD). After a brief incubation, the acinar cells and viral media were embedded in collagen and topped with media (Figure 17a). After 3 days, the ad-N2ICD infected acinar cells underwent ADM whereas the ad-GFP infected acinar cells did not. To determine if EGFR ablation would block N2ICD induced ADM, I harvested acinar cells from E-KO mice and infected with ad-N2ICD or ad-GFP prior to embedding in collagen (Figure 17b). Surprisingly, after 3 days in culture there was no ADM seen in either the ad-GFP infected acinar cells or the ad-N2ICD infected acinar cells. I next tested if pharmacological inhibition of EGFR was also sufficient to block N2ICD promoted ADM by treating WT acinar cells infected with ad-N2ICD with the EGFR inhibitor erlotinib or DMSO as a control (Figure 17c). As with genetic ablation of EGFR, erlotinib treatment was able to block ADM of ad-N2ICD infected cells compared to DMSO controls.

I then verified if EKC acinar cells are incapable of spontaneous ADM as seen with EGFR WT KC acinar cells. I harvested acinar cells from KC and EKC mice and embedded them in collagen, and observed that only KC acinar cells underwent ADM by day 3 in culture (Figure 18a). To test if acinar cells were even capable of undergoing transdifferentiation in the absence of EGFR, I then harvested acinar cells from an E-KO and EKC mice and embedded in Matrigel,

which contains an array of different growth factors (Figure 18b). By day 3 in Matrigel culture, both E-KO and EKC acinar cells had undergone a morphological change to hollow cysts. These results demonstrated that EGFR was not necessary for an acinar cell to have the ability to undergo transdifferentiation. EKC cells were also able to form much larger cysts by day 3 in Matrigel culture as opposed to E-KO acinar cells, indicating that the expression of $Kras^{G12D}$ in the absence of EGFR still granted acinar cells an advantage in transdifferentiation.

I next set out to determine if $Kras^{G12D}$ expression would be sufficient to rescue the block in ad-N2ICD ADM seen in E-KO acinar cells. To this end, I harvested EKC acinar cells and infected with either ad-GFP or ad-N2ICD prior to embedding in collagen (Figure 18c). The EKC acinar cells infected with ad-N2ICD readily underwent ADM by day 3, which was not observed in ad-GFP infected control EKC acinar cells. To determine if the EKC rescue was a product of RAS activation of ERK signaling, I treated EKC acinar cell cultures infected with ad-N2ICD or ad-GFP with either the MEK inhibitor trametinib or DMSO (Figure 19a). Trametinib treatment effectively blocked N2ICD induced transdifferentiation as compared to DMSO controls. I next tested if the trametinib inhibition of MEK was also sufficient to block N2ICD induced ADM in EGFR WT acinar cells. To address this, I infected WT acinar cells with either ad-GFP or ad-N2ICD and treated with trametinib or DMSO (Figure 19b). Again, trametinib treatment was sufficient to block N2ICD induced ADM as compared to DMSO controls. Taken together, these results demonstrate that genetic ablation or pharmacological inhibition of EGFR can block ADM driven by Notch pathway activation. $Kras^{G12D}$ expression requires EGFR to initiate ADM by day 3 in collagen culture, however $Kras^{G12D}$ expression can cooperate with Notch pathway activation to promote ADM in the absence of EGFR. Finally, ADM driven by

N2ICD expression requires MEK-ERK signaling in both WT and EKC acinar cells, suggesting a central role of ERK activation in ADM.

To determine if the inability of Notch to promote ADM in the absence of EGFR or MEK-ERK signaling was a result of the loss of viability of the acinar cells, I used the GFP reporter expression as a viability marker for infected acinar cells. GFP fluorescence in ad-N2ICD infected E-KO acinar cells was mostly lost by day 3 of the transdifferentiation assay, which was not seen in ad-GFP infected controls (Figure 20a). The same observation was made in both EKC and WT acinar cells infected with N2ICD and treated with trametinib (Figure 20b and 20c, respectively). In order to explore the cell death induced by ad-N2ICD, E-KO and WT acinar cells were harvested and plated in a non-tissue culture treated petri dish and infected with ad-GFP or ad-N2ICD. The WT acinar cells were then treated with erlotinib, trametinib, or DMSO. After 48 hours the acinar cells were harvested for protein lysate, and assessed for level of cleaved caspase-3, an apoptotic marker, by western blot (Figure 21). I also examined levels of total and phosphorylated ERK to determine the effectiveness of the inhibitors on the pathway, or contributions to the MAPK pathway by N2ICD signaling. Blockade of either EGFR by genetic ablation or pharmacological inhibition in cells expressing N2ICD both resulted in an increase in the levels of cleaved caspase 3, as well as a loss of ERK phosphorylation. Inhibition of MEK kinase also resulted in an increase in cleaved caspase 3 levels and a loss of ERK phosphorylation as opposed to DMSO control. Importantly cleaved caspase 3 levels were increased in all instances where ERK activation was inhibited and Notch signaling was activated, indicating that Notch activation in the absence of ERK activation can lead to acinar cell death.

PI3K activation can cooperate with Notch in EGFR KO acinar cells

Besides the MAPK pathway EGFR can also activate the PI3K pathway, therefore it was possible that PI3K pathway activation would be sufficient to rescue ADM in ad-N2ICD infected EKO acinar cells. In order to first assess the phenotype of PI3K activation on collagen embedded acinar cells, I infected WT acinar cells with a constitutively active $p110\alpha^{H1047R}$ adenovirus (ad-p110α) or ad-GFP. Ad-p110α infected acinar cells were seen to be much larger than ad-GFP acinar cells and by day 5 there were several acinar clusters which had undergone ADM (Figure 22a). I then harvested EKO acinar cells and co-infected with a combination of adCA-p110α and ad-N2ICD, or infected with adCA-p110α alone, ad-N2ICD alone, or ad-GFP as controls (Figure 22b). The ad-p110α and ad-N2ICD co-infection provided a rescue from N2ICD induced death in EKO acinar cells and resulted in ADM. EKO acinar cells infected with ad-p110α alone appeared to be larger, but there was not readily observed ADM. These results demonstrated that PI3K activation allows N2ICD driven ADM in the absence of EGFR signaling.

PI3K has many known downstream effectors. To determine if ad-p110α rescue of cell death in ad-N2ICD infected EKO acinar cells was due to activation of the PI3K downstream target AKT, which has been previously implicated as a the mechanism of $p110\alpha^{H1047R}$ driven ADM[81], I used an adenovirus containing an AKT kinase in which the PH domain has been replaced with a Src myristoylation signal domain. The subsequent addition of a myristoyl group at the myristoylation site drives the trafficking of AKT to the plasma membrane where it remains in a constitutively active state[123]. Unexpectedly, infection of adenoviral myristoylated AKT (ad-MyrAKT) did not result in ADM in WT acinar cell cultures (Figure 23a). Consistent with this, E-KO acinar cells co-infected with both ad-N2ICD and ad-MyrAKT failed to undergo ADM

(Figure 23b), implying that the p110α^{H1047R} rescue mechanism was not completely due to AKT activation.

Rac1 activation by PI3K is another important step in the formation of stable metaplasia[85]. To determine if Rac1 activation is sufficient to drive ADM, I obtained an adenovirus which encodes a dominant active Rac1 (ad-Rac). To determine if infection of acinar cells with ad-p110α was activating AKT, Rac1, or both AKT and RAC1 together, I co-infected WT acinar cells with ad-Rac and ad-MyrAKT, or either ad-Rac or ad-MyrAKT alone, prior to embedding in collagen (Figure 24). The combination of Rac and AKT signaling also did not appear to be sufficient to cause ADM to occur in WT acinar cells.

Activation of Notch signaling can result in RAS activation in the absence of EGFR

The inability of EKC acinar cells to undergo ADM in collagen cultures has been linked to the lower levels of RAS and ERK activity[72]. Since initiation of Notch signaling in either EKC or WT acinar cells is able to initiate ADM, it could be a result of an increase in the levels of RAS and ERK activity. To address this question, acinar cells were harvested from a Ptf1a$^{+/Cre}$ mouse, a KC mouse, an E-KO mouse, or an EKC mouse and then infected with either ad-GFP or ad-N2ICD and plated in a non-tissue culture treated plate. After 48 hours, protein lysate was harvested from the acinar cells and active RAS levels were assessed by RBD-GST pulldown followed by western blotting (Figure 25). As expected, ad-GFP KC acinar cells had elevated levels of RAS activity as opposed to ad-GFP EKC acinar cells, and Ptf1a$^{+/cre}$ and E-KO acinar cells did not have detectable levels of RAS-GTP. ad-N2ICD infection led to an increase in the levels of RAS-GTP in EKC acinar cells, but not in KC acinar cells. I also examined levels of ERK and AKT phosphorylation in the same lysates to determine if ad-N2ICD infection stimulated either the MAPK or the PI3K pathways, respectively (Figure 25). KC and EKC

acinar cells had higher levels of phospho-ERK then either EKO or Ptf1a$^{+/Cre}$ acinar cells. The level of phosphorylated ERK was also elevated by N2ICD expression in EKC and KC acinar cells, but not in Ptf1a$^{+/Cre}$ or EKO acinar cells. KC acinar cells expressed higher levels of phospho-AKT than EKC or WT acinar cells, while EKO acinar cells expressed much lower levels than the rest of the genotypes. N2ICD expression led to elevation of phospho-AKT levels in acinar cells lacking EGFR as compared to GFP controls. Ptf1a$^{+/Cre}$ acinar cells infected with ad-N2ICD had less phospho-AKT than ad-GFP infected acinar cells, while the levels of phospho-AKT in KC acinar cells remained unchanged by N2ICD expression. Taken together, these data show that RAS activity is increased by activation of the Notch pathway only in EKC acinar cells, which results in upregulation of ERK activity near the levels seen in Ptf1a$^{+/Cre}$ acinar cells. Ptf1a$^{+/Cre}$ and EKC acinar cells, which are capable of undergoing ADM with ad-N2ICD infection, demonstrate much higher levels of both AKT and ERK activity than E-KO acinar cells which are incapable of ADM by activation of Notch pathway alone.

STAT3 is upregulated in ADM, but STAT3 activation is insufficient to cause ADM

A link between MMP7 and Notch activity levels in pancreatic acinar cells has been previously demonstrated[120], as has a relationship between signal transducer and activator of transcription 3 (STAT3) activity and MMP7 expression[124]. Given these observations, I decided to investigate a potential link between the STAT3 and Notch pathways. To this end I compared the levels of STAT3 expression and the level of phosphorylated STAT3 in protein lysates from Ptf1a$^{+/Cre}$, KC, E-KO, and EKC acinar cells harvested 48 hours after infection with either ad-GFP or ad-N2ICD (Figure 26). Ptf1a$^{+/Cre}$ ad-N2ICD infected acinar cells showed a marked up regulation of both total and phosphorylated STAT3 as compared to ad-GFP controls. KC acinar cells expressed a high level of total and phosphorylated STAT3 regardless of N2ICD expression.

E-KO acinar cells appeared to up regulate the level of STAT3 protein in response to N2ICD expression, however STAT3 activation was not seen in either ad-N2ICD or ad-GFP infected E-KO acinar cells. EKC acinar cells expressed a high level of STAT3 protein as compared to E-KO acinar cells, and ad-N2ICD expression resulted in an increase in STAT3 phosphorylation levels compared to ad-GFP controls. Importantly, in Ptf1a$^{+/Cre}$ and EKC acinar cells infected with ad-N2ICD which undergo ADM, the levels of active STAT3 were increased over their respective ad-GFP infected controls which are incapable of transdifferentiation. In KC acinar cells the levels of active STAT3 are already high in ad-GFP infected acinar cells compared to the other three genotypes, and are unchanged in the ad-N2ICD infected acinar cells. Since KC acinar cells transdifferentiate in the absence of N2ICD, this lack of increase of STAT3 activity is not surprising. Lastly, in EKO acinar cells which do not undergo ADM by expression of N2ICD, the levels of phosphorylated STAT3 are unchanged from ad-GFP infection levels and remain markedly lower than the other genotypes.

It is possible that the lack of STAT3 activation in EKO acinar cells could be the missing signal to allow N2ICD induced ADM to proceed in the absence of EGFR. In order to determine if STAT3 activation was sufficient to rescue the loss of ad-N2ICD induced ADM in EKO cells, I tried two different methods of STAT3 pathway activation. First, I treated ad-N2ICD infected E-KO acinar cells with recombinant Interleukin 6 (IL-6), which can activate the STAT3 pathway downstream through its receptor IL-6R (Figure 27a). Secondly, I obtained an adenoviral construct containing a constitutively active STAT3 (adCA-STAT3) and co-infected E-KO acinar cells with ad-N2ICD and adCA-STAT3 (Figure 27b). However both avenues of STAT3 pathway activation proved to be insufficient to promote ADM with concurrent ad-N2ICD expression in EGFR null acinar cells.

Macrophage conditioned media and HGF can initiate ADM without EGFR

Macrophages and macrophage secreted growth factors and cytokines have been demonstrated to be important in ADM and tumorigenesis[109,110,125]. Using bone marrow-derived macrophages (BMM) I have found that M2 polarized macrophage conditioned media (M2-CM) treatment readily induces ADM in WT acinar cells (Dr. Hui-Ju Wen, unpublished). To determine if M2-CM is capable of initiating ADM in acinar cells in the absence of EGFR or potentiate Notch induced ADM in the absence of EGFR; E-KO acinar cells were infected with either ad-GFP or ad-N2ICD and embedded in collagen. The cells were then cultured in Waymouth's media which had been conditioned for 24 hours by M2 polarized macrophages or normal Waymouth's media as a control (Figure 28a). Ad-GFP infected E-KO acinar cells failed to undergo ADM with M2-CM treatment, however M2-CM treatment was able to facilitate ADM in ad-N2ICD infected E-KO acinar cells. I then took collagen embedded EKC acinar cells and treated them with M2-CM media or normal media as a control to determine if there was a soluble factor in the media capable of inducing ADM without N2ICD expression in the absence of EGFR (Figure 28b). EKC acinar cells readily underwent ADM in response to M2-CM treatment as opposed to control media.

Several growth factors and cytokines produced by macrophages have been reported to initiate ADM in collagen embedded acinar cells including heparin-binding epidermal growth factor-like growth factor (HB-EGF)[125], tumor necrosis factor-α (TNF-α)[109], regulated on activation, normal T cell expressed and secreted (RANTES)[109], and hepatocyte growth factor (HGF)[61]. I first tested the ability of TNF-α or RANTES initiate ADM in WT acinar cells (Figure 29a), however neither TNF-α nor RANTES treatment is sufficient to induce ADM. I next attempted to rescue N2ICD promoted ADM in EKO acinar cells by treatment with either TNF-

alpha or RANTES (Figure 29b). I also tried a treatment with a combination of TNF-alpha and RANTES, as they have both been shown to have a similar mechanism of action, activating the nuclear factor kappa-light-chain-enhancer of activated B cells (NF-kB) signaling pathway[109] (Figure 29b). However TNF-alpha, RANTES, or the combination of RANTES and TNF-α was insufficient rescue N2ICD driven ADM in E-KO acinar cells. To test if Notch induced ADM required NF-kB signaling, I used a NF-kB inhibitor reported to block TGF-α induced ADM[109], BMS345541, to treat WT acinar cells infected with ad-N2ICD (Figure 27c). BMS345541 treatment resulted in smaller ductal cyst formation, but was not able to block N2ICD induced ADM.

While HB-EGF readily induces ADM in WT acinar cells (Dr. Hui-Ju Wen, unpublished) as an EGFR ligand, EKO acinar cells or EKO acinar cells infected with ad-N2ICD were unable to undergo ADM (Figure 30), implying that there is no cross activation of ErbB3 or other ErbB family members by HB-EGF. Last, I found that HGF treatment of WT acinar cells was not sufficient to cause ADM by day 5 in cultures, however EKO acinar cells treated with HGF readily underwent ADM by day 5 (Figure 31). Treatment of ad-N2ICD infected EKO acinar cells with HGF also resulted in widespread ADM by day 3 (Figure 31), demonstrating a synergistic effect of the Notch and HGF pathways in the absence of EGFR.

$p53^{R172H}$ mutation allows for EGFR independent N2ICD driven ADM

It has previously been observed that EKC mice with an ablation of the tumor suppressor protein p53 were able to undergo tumorigenesis, whereas EKC mice which expressed normal p53 did not[72,73]. To determine if normal p53 function was required to block N2ICD induced ADM in E-KO acinar cells, I utilized a mouse model with a $p53^{R172H}$ mutation, which is an oncogenic gain of function mutation[94]. I crossed $EGFR^{flox/flox}$;$Ptf1a^{+/Cre}$ mice with $p53^{+/R172H}$

mice to obtain $EGFR^{flox/flox}$;$Ptf1a^{+/Cre}$; $p53^{+/R172H}$ mice (E-KO-p53*). I harvested acinar cells from an E-KO-p53* mouse and infected with either ad-N2ICD or ad-GFP and embedded them in collagen (Figure 32). Widespread ADM was observed in the E-KO-p53* acinar infected with ad-N2ICD by day 3, which was not seen in E-KO-p53* acinar cells infected GFP. These results suggest that the expression of $p53^{+/R172H}$ is indeed able to override the EGFR dependent block in N2ICD induced ADM.

As ADM driven by expression of N2ICD is dependent on MEK kinase activity in either WT or EKC acinar cells, I set out to determine if ADM in E-KO-p53* acinar cells could proceed with ADM despite MEK inhibition. To address this, I harvested acinar cells from an E-KO-p53* mouse and infected with ad-GFP or ad-N2ICD prior to embedding in collagen then treated with either DMSO or trametinib. Trametinib treatment was sufficient to block ADM in ad-N2ICD infected E-KO-p53* acinar cells, however the ad-N2ICD infected acinar cells treated with trametinib still expressed a high level of GFP, indicating survival not seen in trametinib treated WT or EKC acinar cells expressing N2ICD.

Notch and MAPK activation cooperate to repress Ptf1a expression

Notch pathway activation has been previously shown to drive the maintenance of an undifferentiated state in development[11] due at least in part to the suppression of exocrine differentiation[13]. It has also been suggested that Notch activity also relies on the Erk activity for NICD activation[126]. To determine if there is cooperation between the MAPK pathway and Notch pathway in acinar cell de-differentiation I utilized an *in vitro* model to activate or regulate MAPK and Notch pathway components. Using MAPK activation by either TGF-α treatment to activate of EGFR-MAPK signaling or $Kras^{G12D}$ expression, both of which are able to drive loss of acinar differentiation, I then used inhibitors or protein expression to determine the individual

contributions of Notch and MAPK to acinar de-differentiation. To negatively regulate the MAPK pathway, I used the MEK1/2 inhibitor trametinib to block ERK activation downstream of either EGFR or KRAS. To modulate Notch pathway signaling components I used either the gamma-secretase inhibitor DAPT to block Notch activation, or infected acinar cells with ad-N2ICD to activate the Notch pathway.

First, I harvested WT acinar cells and plated in a non-tissue culture treated petri dish and treated with TGF-α. After 24 hours, I added fresh TGF-α combined with DMSO, trametinib, DAPT, trametinib and DAPT, ad-N2ICD, ad-N2ICD and DAPT, or ad-N2ICD and trametinib. I also left one dish untreated with TGF-α as a control. I then harvested the acinar cells and isolated RNA and looked at the transcript levels of Ptf1a by qPCR as a readout of acinar differentiation (Figure 33a). TGF-α stimulation resulted in a decrease in Ptf1a levels as compared to acinar cells which were unstimulated. Treatment with TGF-α and either DAPT or trametinib alone resulted in increased levels of Ptf1a expression, indicating retention of acinar differentiation, although the level of upregulation of Ptf1a by trametinib treatment was much more pronounced than DAPT treatment. Treatment with TGF-α and a combination of DAPT with trametinib resulted in levels of Ptf1a expression similar to trametinib and TGF-α alone. Infection of TGF-α treated acinar cells with ad-N2ICD dramatically reduced the level of Ptf1a expression. Infection of TGF-α treated acinar cells with ad-N2ICD and concurrent trametinib inhibition of MEK lead to a loss of the N2ICD mediated reduction of Ptf1a expression levels, however the Ptf1a levels were not elevated to the levels seen in the trametinib treatment alone. Concurrent inhibition of gamma-secretase and infection with ad-N2ICD of TGF-α treated acinar cells resulted in a decreased level of Ptf1a expression similar to ad-N2ICD infection alone.

Next, I isolated acinar cells from KC mice and plated in non-tissue culture treated petri dishes and treated immediately with DMSO, trametinib, DAPT, trametinib and DAPT, ad-N2ICD, ad-N2ICD and trametinib, or ad-N2ICD and trametinib and DAPT. After 24 hours of incubation, I harvested RNA from the acinar cultures and looked at Ptf1a transcript levels by qPCR (Figure 33b). In contrast to the TGF-α treated WT acinar cells, inhibition of gamma-secretase with DAPT did not have any impact on the level of Ptf1a expression in KC acinar cells as compared to DMSO treatment. However infection of KC acinar cells with ad-N2ICD was able to significantly lower the levels of Ptf1a expression over DMSO controls. Conversely, trametinib treatment of KC acinar cells resulted in significantly elevated levels of Ptf1a expression compared to controls. Combination of ad-N2ICD infection and trametinib treatment of KC acinar cells resulted in no net change over the untreated cells, as the levels of Ptf1a expression were on par with the DMSO only treatment. Taken together, these results indicate that MEK-ERK signaling and Notch pathway activation are both important contributors to the process of de-differentiation, however in the context of $Kras^{G12D}$ signaling, gamma-secretase inhibition has no effect.

Discussion

In mouse models of transgenic TGF-α overexpression, acinar-to-ductal metaplasia is readily observed, as well as Notch pathway activation[60]. $Kras^{G12D}$ expression in the pancreas also leads to the development of ADM, and the concurrent activation of Notch with $Kras^{G12D}$ expression rapidly accelerates ADM and tumorigenesis[55]. However the relationship between the EGFR-Kras-MAPK pathway and Notch signaling pathway remains cloudy. In *ex vivo* primary acinar explants embedded in collagen, TGF-α activation of EGFR results in ADM which can be blocked by gamma-secretase inhibition, suggesting Notch activation downstream of EGFR

activation[60]. This idea was further enhanced with the observation that NICD expression can also result in ADM of primary acinar cell explants, which was not completely blocked by the EGFR inhibitor AG-1478[60]. However, by genetically ablating EGFR, I was able to show a complete block in ADM induced by N2ICD expression. Furthermore using the EGFR inhibitor Erlotinib, I was also able to block N2ICD driven ADM in WT acinar cells. There are several possible explanations for the differences in these observations. Erlotinib is an ATP competitive inhibitor of EGFR[127], whereas AG1478 is a tyrosine kinase inhibitor[128], so it is possible that the mechanism of action of Erlotinib may make it a more effective inhibitor. However, the more likely explanation is that the composition of the medium used in other experiments contained 1% FBS, which I found to be unnecessary in N2ICD induced ADM, therefore all of my experiments were carried out serum free. The presence of growth factors in Matrigel are able to drive ADM in the absence of E-KO acinar cells, and growth factor and cytokine containing M2-CM is able to rescue N2ICD induced ADM in E-KO acinar cells, therefore it is entirely possible that the growth factors present in FBS can override the requirement of EGFR signaling in ADM driven by Notch as well.

Previous studies have already demonstrated that $Kras^{G12D}$ induced ADM and tumorigenesis requires MEK activity[72,79]. This observation is also true of Notch induced ADM, as no transdifferentiation of ad-N2ICD infected WT acinar cells is seen when MEK signaling is inhibited using trametinib. Acinar cells lacking EGFR, which are incapable of Notch induced ADM can undergo transdifferentiation when N2ICD expression is combined with $Kras^{G12D}$ expression. In the absence of EGFR, ERK activity is almost undetectable in acinar cells as compared to $Ptf1a^{+/Cre}$ acinar cells, however expression of $Kras^{G12D}$ in acinar cells lacking EGFR is able to restore the level of phospho-ERK back to levels comparable with $Ptf1a^{+/Cre}$ acinar cells.

Finally, inhibition of MEK-ERK signaling in EKC acinar cells expressing N2ICD with trametinib treatment is also able to block ADM, illustrating the central role that MEK-ERK signaling plays in ADM driven by Notch pathway activation.

The ability of PI3K activation to rescue N2ICD driven ADM in E-KO acinar cells was not surprising as transgenic expression of $p110\alpha^{H1047R}$ *in vivo* was shown to be capable of tumorigenesis in mice[81]. However, the inability of constitutively activated AKT to either promote ADM in WT acinar cells or rescue N2ICD induced ADM in E-KO cells was unexpected, as expression of constitutively activated AKT *in vivo* was shown to result in ADM[82]. However, it is important to note that this model activated the expression of the constitutively activated AKT transgene in acinar progenitor cells during development, and it has been shown that adult acinar cells are more resistant to transdifferentiation than acinar cells in development[53].

Investigation into RAS activation levels provided some insight into the separation of the Notch and EGFR-RAS-ERK pathways, as consistent N2ICD activation of RAS signaling would have provided a direct link between the two pathways. Furthermore, the ability of $Ptf1a^{+/Cre}$ acinar cells infected with N2ICD to undergo ADM without RAS activation lends strength to the idea that the primary purpose of Notch activation in ADM is to suppress acinar differentiation. When acinar differentiation is suppressed by Notch, the basal level of ERK activity in $Ptf1a^{+/Cre}$ acinar cells may then be sufficient to drive ADM.

STAT3 activity levels also provided a strong correlation between ADM and STAT3 activation. In $Ptf1a^{+/Cre}$ and EKC acinar cells, which transdifferentiated only with Notch pathway activation, N2ICD expression increased the levels of active STAT3. KC acinar cells displayed high levels of STAT3 activation without the need for further stimulus, which again

correlates to their inherent ability to undergo ADM. STAT3 has also been shown to be important in pancreatic tumorigenesis[124,129], and that IL-6 trans-signaling is an important component of STAT3 activation in PanIN progression, and abberant STAT3 activation by Socs3 deletion accelerates tumor development[130]. However the failure of STAT3 activation by IL-6 treatment or expression of a constitutively active STAT3 protein to rescue ADM in N2ICD infected E-KO acinar cells indicates that STAT3 is activated as a byproduct of transdifferentiation, and is not a driver of ADM.

Macrophages are an important component of the immune response in the pancreas to both cerulein and Kras induced pancreatitis. Depletion of macrophages has been shown to impair ADM and tumorigenesis in mice[109,110], and well inhibit the ability of pancreatic tissue to regenerate in response to damage[131]. Conditioned media from M2 macrophages is able to rescue N2ICD driven ADM in E-KO acinar cells, however the exact mechanism of this is unknown at this time. HGF is a viable candidate growth factor, as it is known to be secreted by macrophages (Dr. Hui-Ju Wen, unpublished) and is capable of inducing ADM in acinar cells lacking EGFR both by itself and in cooperation with Notch activation. However, additional experiments will be necessary to determine if there is a shared mechanism between HGF and M2-CM treatment of E-KO acinar cells.

Previous data has suggested, though not shown, that acinar cells lacking EGFR are still capable of Kras driven transdifferentiation by genetic ablation of p53[72,73]. Similarly, I have shown that Notch activation in the absence of EGFR can still lead to ADM in the context of altered p53 function, although it still requires MEK activity in order to initiate transdifferentiation. Importantly, although trametinib treatment blocks ADM ad-N2ICD infected in E-KO-p53* acinar cells, there is still strong GFP fluorescence produced in these cells,

indicating that they are still viable, which is not seen in any other acinar cells expressing N2ICD and treated with trametinib. This survival mechanism granted by $p53^{R172H}$ mutation warrants further investigation.

Finally, the Notch and EGFR signaling pathways do not appear to have a linear relationship in their ability to modulate de-differentiation of acinar cells. TGF-α treatment and $Kras^{G12D}$ expression both demonstrated the ability to downregulate the expression of acinar cell transcription factor Ptf1a, which in both systems was entirely dependent on MEK signaling. N2ICD expression was capable of further suppressing the expression of Ptf1a when combined with either TGF-α treatment or $Kras^{G12D}$ expression, however, N2ICD suppression of Ptf1a expression was also dependent on MEK signaling. Importantly, the ability of gamma-secretase inhibition to block TGF-α downregulation of Ptf1a expression was not seen in acinar cells expressing $Kras^{G12D}$, which can underline a difference between ADM driven TGF-α treatment and $Kras^{G12D}$ expression. There are some discrepancies in the literature about ADM that are in line with this observation as ADM initiated by TGF-α treatment in collagen embedded acinar explants was found to be non-proliferative[61], however ADM formed by $Kras^{G12D}$ acinar cells in collagen was found to be highly proliferative[65]. *In vivo* ADM expressing $Kras^{G12D}$ can go to form PanIN lesions, while normal ADM is capable of re-differentiation. I believe that with more investigation into the role that the Notch and EGFR-Ras-MEK pathways play in the formation and stabilization of ADM, we may gain further insights into what allows mutant Ras to hijack ADM programing into a path to tumorigenesis.

Future Directions

I have currently demonstrated a requirement for EGFR and MEK signaling to permit the Notch pathway to promote acinar-to-ductal metaplasia in acinar cell explant cultures embedded

in collagen. However there are many questions that need to be addressed. EGFR ablation, as well as blockade of MEK kinase, are effective in preventing N2ICD driven ADM to proceed. There are several different mechanisms I have found which allow for N2ICD induced ADM to proceed despite genetic ablation of EGFR; $Kras^{G12D}$ expression, $p110\alpha^{H1047R}$ expression, treatment with M2 macrophage conditioned media or HGF, or $p53^{R172H}$ mutation. $Kras^{G12D}$ expression is seen to increase the level of ERK activity in EGFR null acinar cells, so it is possible that $p110\alpha^{H1047R}$ expression, treatment with M2 macrophage conditioned media or HGF, and $p53^{R172H}$ mutation also restore ERK signaling lost from EGFR ablation. In order to test this, I need to take acinar cells from E-KO mice and treat with each of the mentioned conditions and harvest protein lysates to look at ERK activation. It is my hope that this will shed some light on the requirement of ERK activity for ADM.

Another important experiment that I plan to do is to verify that my results using Notch2 intercellular domain and my method of Notch activation is also comparable with previous studies which used Notch1 intercellular domain as the method of Notch activation. To this end I have a N1ICD adenovirus with a V5 tag which I can use to try and replicate my ad-N2ICD results. This particular construct will be useful to address another important question raised by my results, in what way is ERK signaling affecting Notch signaling. One obvious answer could be trafficking of the Notch-ICD to the nucleus, for which the V5 tag can be used to track by subcellular fractionation of acinar cells infected with N1ICD and treated with either trametinib or control. If there is no change in the trafficking of Notch-ICD, there is also a question of activation, as it has previously been suggested using pancreatic cancer cell lines that Notch-ICD needs to be phosphorylated by MEK[126]. As this can potentially be difficult to show, it is also suggested that the lack of MEK-ERK signaling can lead to less interaction of Notch-ICD with the binding

partners such as MAML, which could be addressed by co-immunoprecipitation for MAML and blotting back for V5, or vice versa.

Another point that needs to be clarified in my data concerns HGF and M2 macrophage conditioned media rescue of N2ICD driven ADM in E-KO acinar cells. To determine if HGF is indeed the component of M2-CM which is allowing E-KO acinar cells to undergo ADM, I plan to treat E-KO acinar cells with M2-CM in the presence of a HGF-R inhibitor. If this is unable to block ADM, then there is likely another growth factor or cytokine in M2-CM responsible which needs to be parsed out.

To determine if acinar differentiation, or just Ptf1a levels are being regulated by MAPK and Notch, I am also planning to look at the same sets of cDNA for a second acinar marker, Mist. If Mist1 expression is independent of this process, then it is possible that Ptf1a is a direct target of either pathway. In terms of markers of acinar and ductal differentiation, I have also had a bit of trouble finding reliable markers to quantitate acinar clusters in collagen as "acinar" or "ductal". Previously, our lab has used CK19 and amylase as acinar and ductal markers, respectively, however in my hands these have not proven to mark distinct populations in whole mount collagen disk staining. I am in the process of trying a variety of methods to solve this problem. I have formalin fixed and paraffin embedded (FFPE) several collagen disks to attempt to use immunohistochemistry as opposed to immunofluorescence to stain these markers. I am also in the process of assessing a protocol involving quick fixation of collagen disks, then freezing in optimal cutting temperature compound and sectioning via cryostat to stain frozen sections of collagen disks as opposed to whole mount immunofluorescence. Lastly, I am going to try to use other established ductal markers, such as claudin-18 or carbonic anhydrase-II to see if they mark a more distinct population than CK-19.

Figures for Chapter 4: EGFR activation of ERK is required for Notch induced ADM

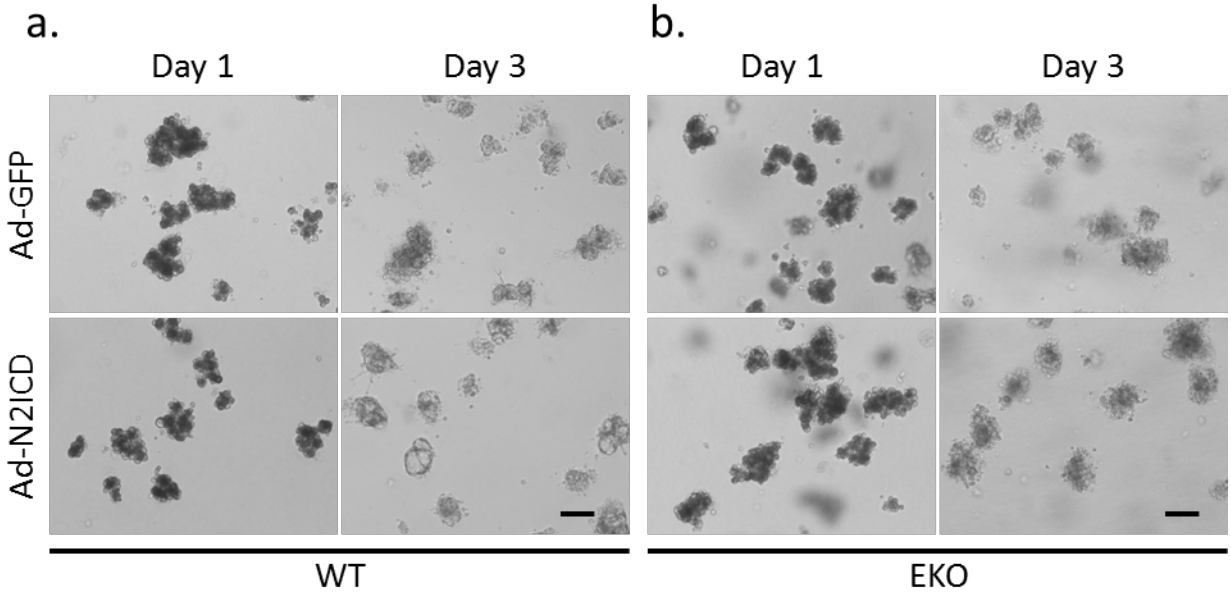
a.
Day 1
Day 3
Ad-GFP
Ad-N2ICD
WT
b.
Day 1
Day 3
EKO

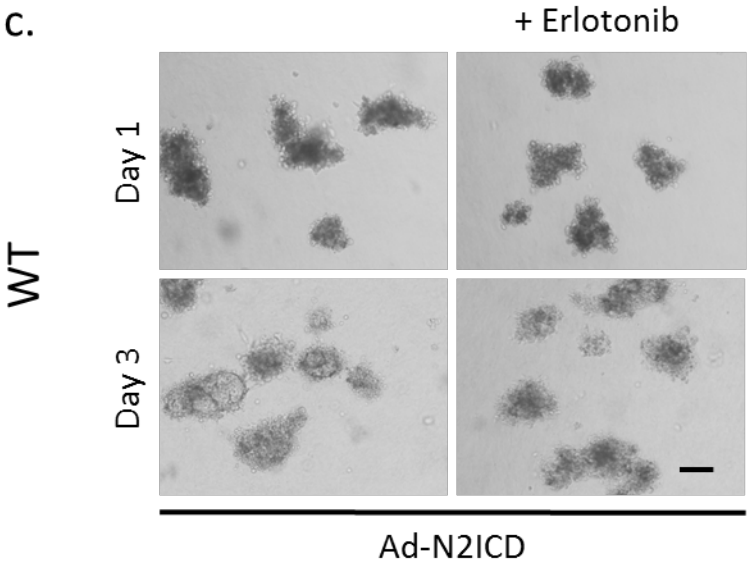
c.
+ Erlotonib
WT
Day 1
Day 3
Ad-N2ICD

Figure 17: EGFR signaling is required for Notch induced ADM. a. Adenoviral Notch2ICD drives ADM in WT acinar cells embedded in collagen after 3 days in culture, which is not seen in adenoviral GFP infected control. **b.** Acinar cells harvested from E-KO mice and infected with ad-N2ICD do not initiate an ADM program, and are comparable to ad-GFP infected controls at day 3 in culture. **C.** WT acinar cells infected with ad-N2ICD and treated with the EGFR inhibitor erlotinib at a concentration of 1uM do not undergo ADM as seen in vehicle treated controls. Scale bar = 100μm.

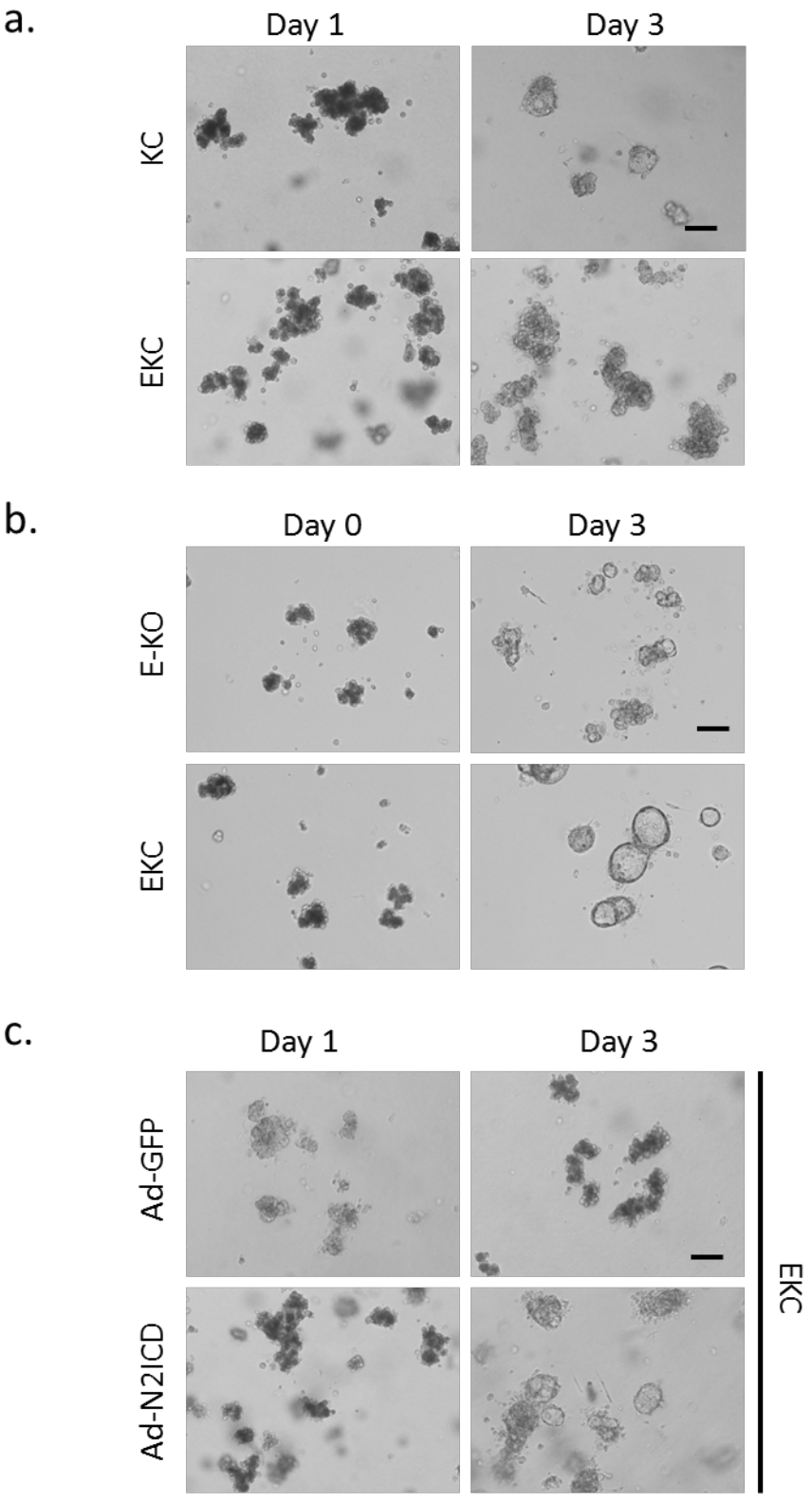
a.
Day 1
Day 3
KC
EKC
b.
Day 0
Day 3
E-KO
EKC
c.
Day 1
Day 3
Ad-GFP
Ad-N2ICD
EKC

Figure 18: EGFR is not required for ADM; Notch-Kras cooperation can initiate ADM in absence of EGFR. a. Acinar cells from EGFR WT KC mice embedded in collagen undergo spontaneous transdifferentiation by day 3 in culture, whereas acinar cells harvested from EKC mice do not. **b.** Acinar cells harvested from E-KO and EKC mice and embedded in matrigel are both capable of undergoing transdifferentiation by day 3 in culture. EKC cysts in matrigel culture form dramatically larger cysts in the same timeframe as E-KO acinar cells. **C.** EKC acinar cells infected with ad-N2ICD and embedded in collagen are capable of undergoing ADM, which was not observed in EKC acinar cells infected with ad-GFP. Scale bars = 100μm.

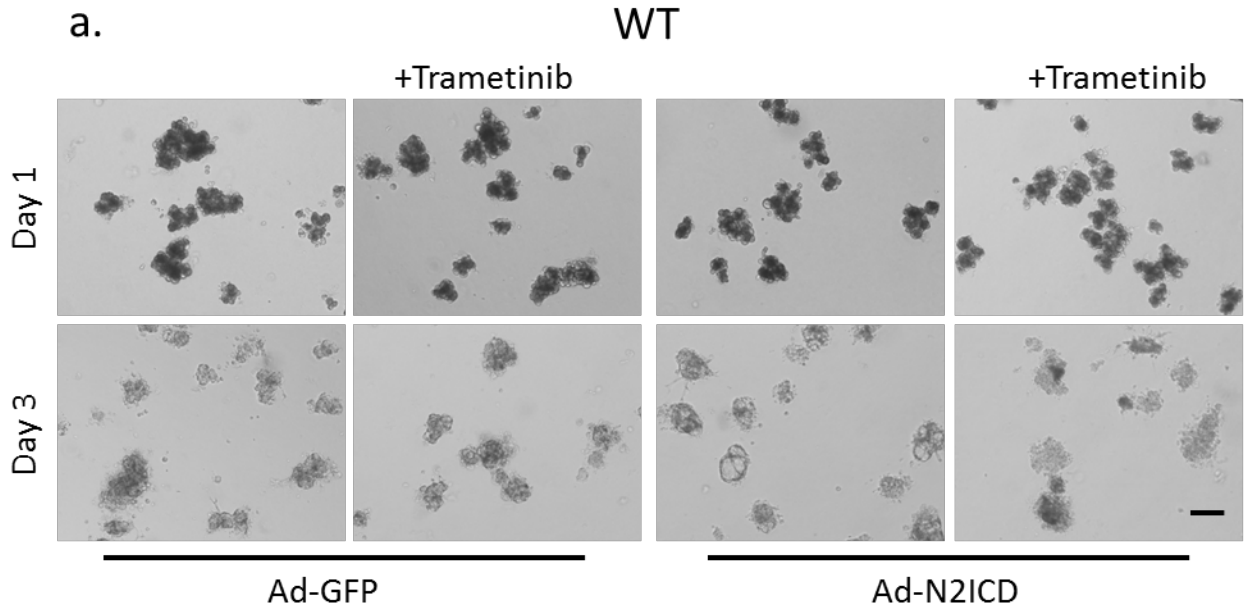
a.
WT
+Trametinib
+Trametinib
Day 1
Day 3
Ad-GFP
Ad-N2ICD

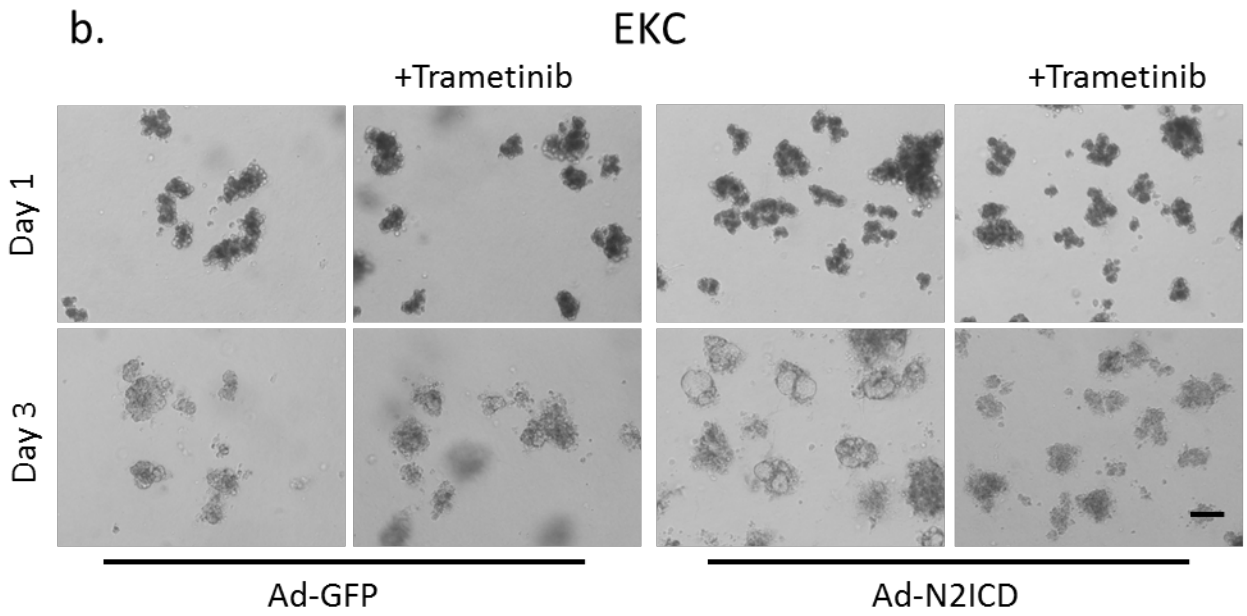
b.
EKC
+Trametinib
+Trametinib
Day 1
Day 3
Ad-GFP
Ad-N2ICD

Figure 19: MEK-ERK signaling is required for Notch induced ADM. Treatment with the MEK inhibitor trametinib at a concentration of 100nM is capable of blocking ad-N2ICD driven ADM in acinar cells harvested from WT (**a**) and EKC (**b**) acinar cells as compared to vehicle treated, or ad-GFP infected controls. Scale bars = 100μm.

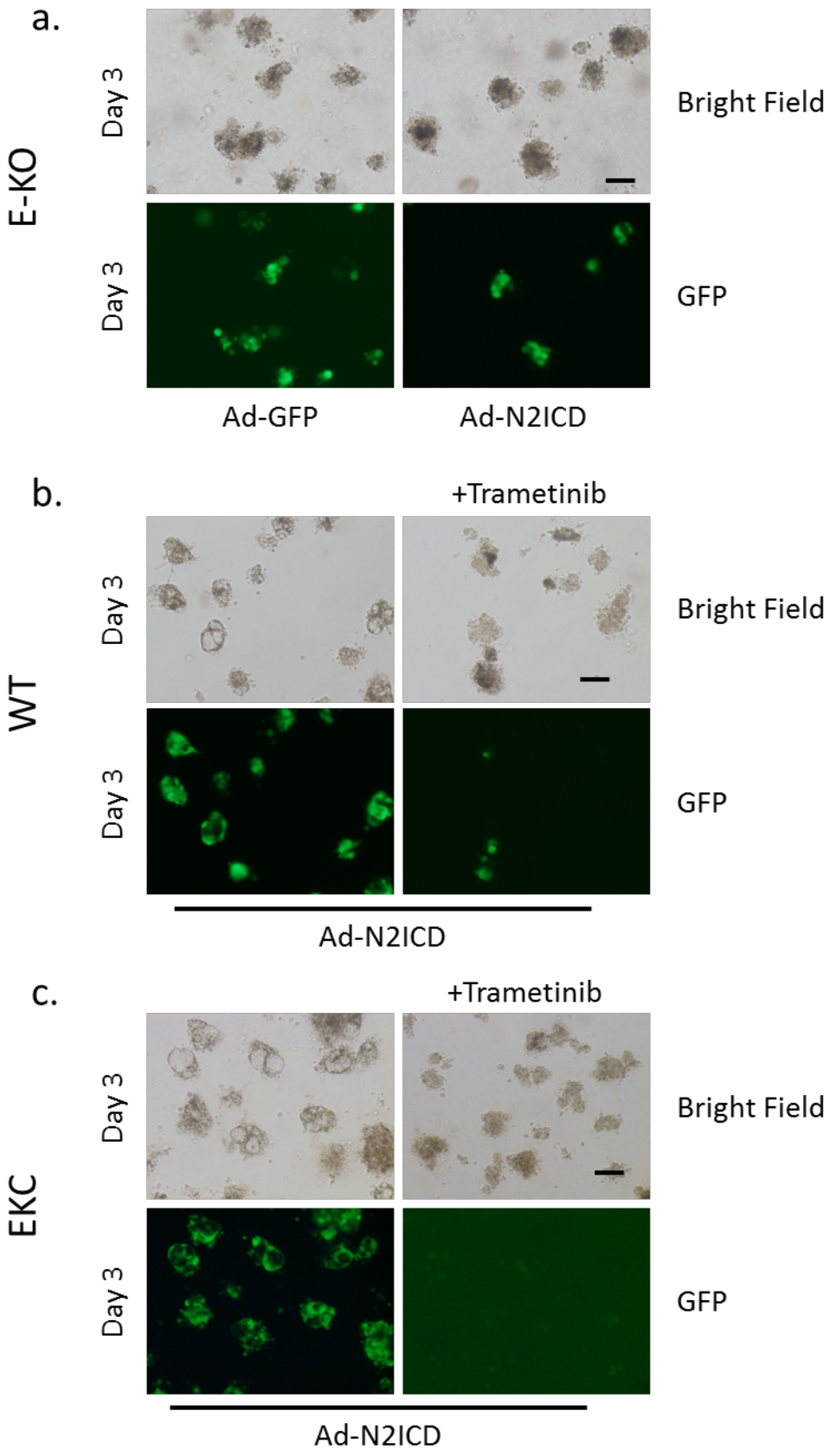
a.
E-KO
Day 3
Day 3
Bright Field
GFP
Ad-GFP
Ad-N2ICD
b.
+Trametinib
WT
Day 3
Day 3
Bright Field
GFP
Ad-N2ICD
c.
+Trametinib
EKC
Day 3
Day 3
Bright Field
GFP
Ad-N2ICD

Figure 20: Loss of EGFR or MEK-ERK signaling results in loss of viability of acinar cells expressing N2ICD. a. E-KO acinar cells embedded in collagen and infected with ad-N2ICD lost the expression of the GFP reporter by day 3 in culture which is not seen in ad-GFP infected E-KO acinar cells. Collagen embedded WT (**b**) and E-KO (**C**) acinar cells infected with ad-N2ICD both show a loss of GFP reporter expression by day 3 in culture when treated with 100nm trametinib which was not seen in their respective vehicle treated controls. Scale bar = 100μm.

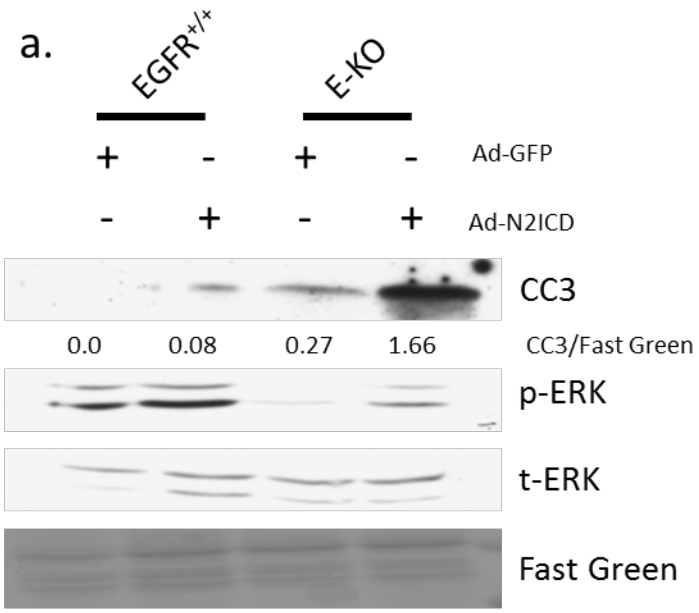
a.
EGFR+/+
E-KO
+ - + - Ad-GFP
- + - + Ad-N2ICD
CC3
0.0 0.08 0.27 1.66 CC3/Fast Green
p-ERK
t-ERK
Fast Green

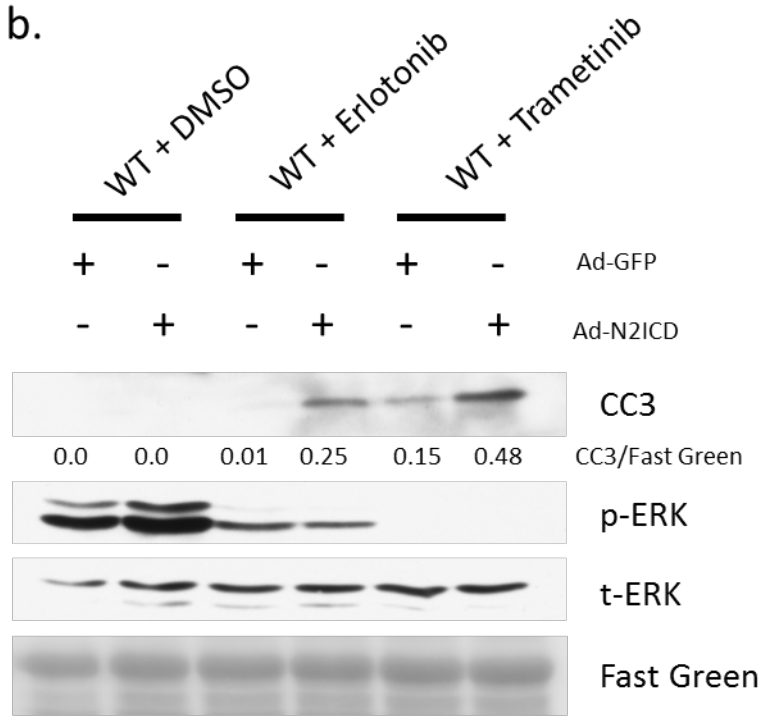
b.
WT + DMSO
WT + Erlotonib
WT + Trametinib
+ - + - + - Ad-GFP
- + - + - + Ad-N2ICD
CC3
0.0 0.0 0.01 0.25 0.15 0.48 CC3/Fast Green
p-ERK
t-ERK
Fast Green

Figure 21: Loss of EGFR and MEK-ERK signaling results in increased apoptosis in acinar cells expressing N2ICD. a. Acinar cells from E-KO mice infected with ad-N2ICD showed a dramatic increase in caspase 3 cleavage as compared to ad-GFP infected controls. EGFR WT acinar cells also had an increase in caspase 3 cleavage with N2ICD expression compared to GFP infection, however the levels of caspase 3 cleavage in EGFR WT acinar cells were lower than E-KO acinar cells. **b.** WT acinar cells infected with ad-N2ICD and treated with 1μM erlotinib or 100nm trametinib had a dramatic increase in caspase 3 cleavage levels over ad-GFP infected acinar cells. In vehicle treated WT acinar cells, there was no difference in the levels of caspase 3 cleavage between ad-N2ICD or ad-GFP infection.

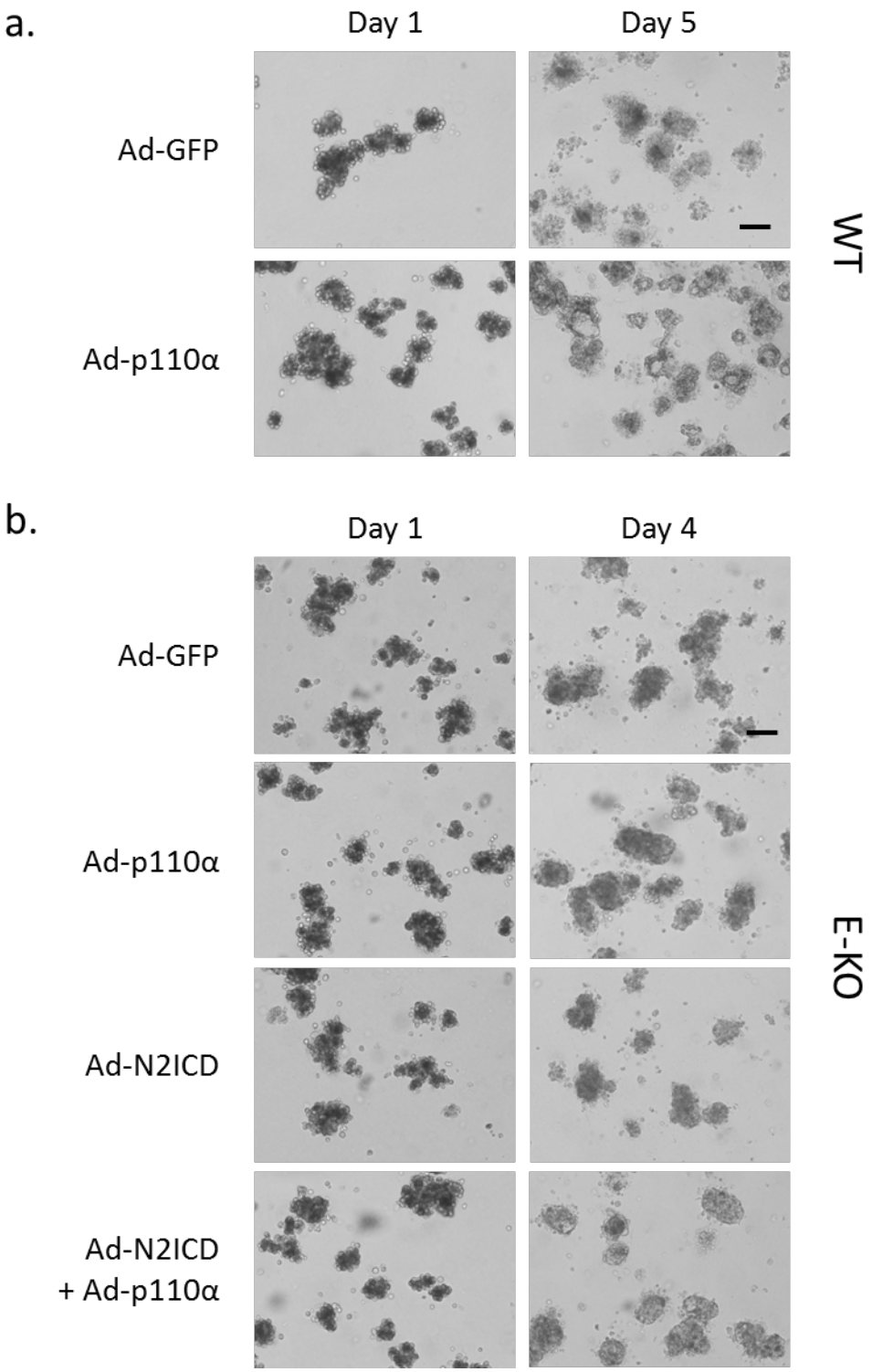
a.
Day 1
Day 5
Ad-GFP
Ad-p110α
WT
b.
Day 1
Day 4
Ad-GFP
Ad-p110α
Ad-N2ICD
Ad-N2ICD
+ Ad-p110α
E-KO

Figure 22: Activation of PI3K can drive ADM and rescue N2ICD induced ADM in E-KO acinar cells. a. Wild type acinar cells infected with ad-p110α embedded in collagen undergo ADM by day 4 in culture. **b.** E-KO acinar cells co-infected with ad-N2ICD and ad-p110α undergo ADM by day 4 in culture, whereas infection of E-KO cells with ad-N2ICD or ad-p110α alone is insufficient. E-KO acinar cells infected with ad-p110α are also noticeably larger than ad-GFP infected E-KO cells at day 4. Scale bars = 100μm.

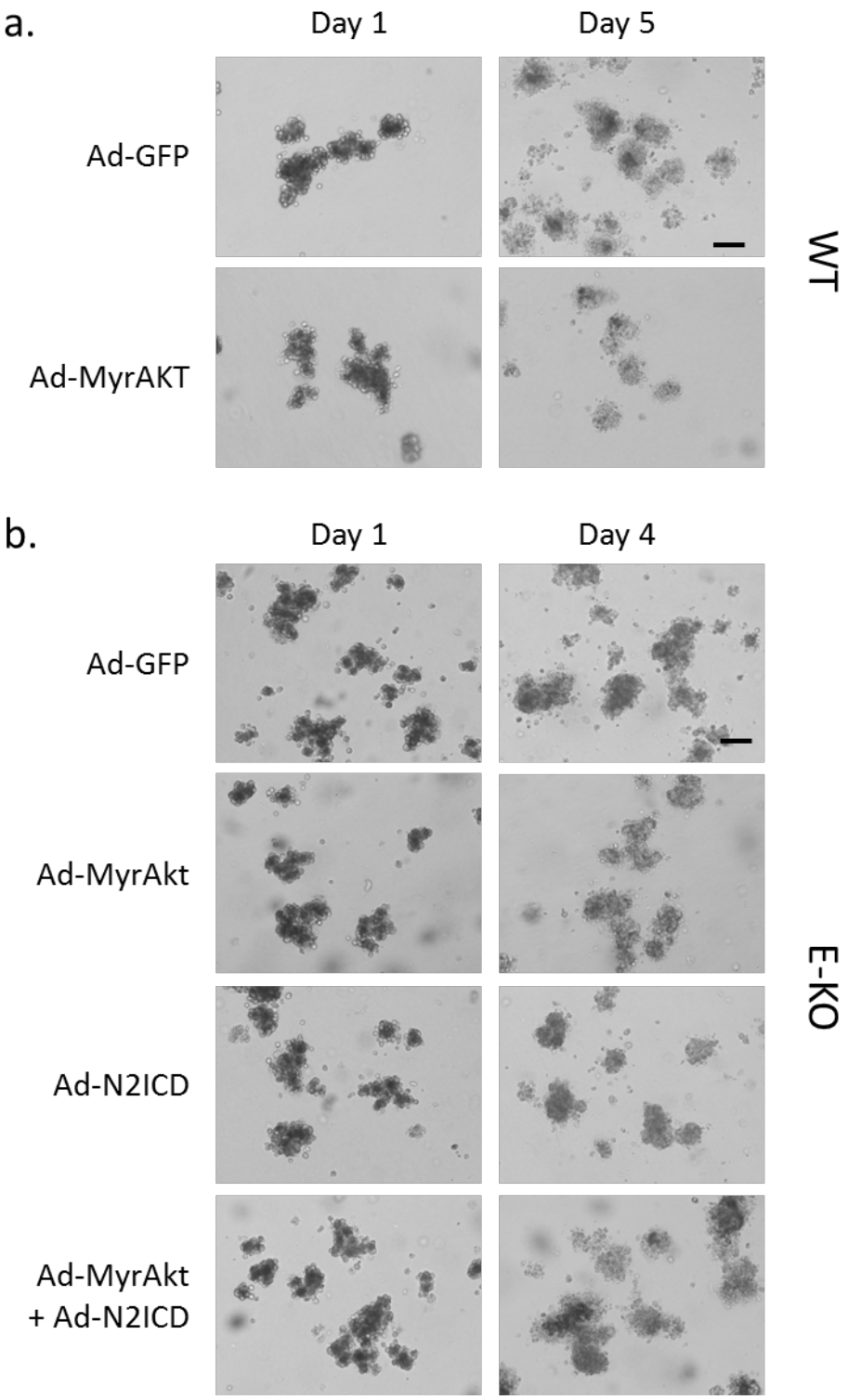
a.
Day 1
Day 5
Ad-GFP
Ad-MyrAKT
WT
b.
Day 1
Day 4
Ad-GFP
Ad-MyrAkt
Ad-N2ICD
Ad-MyrAkt
+ Ad-N2ICD
E-KO

Figure 23: AKT activation is insufficient to cause ADM or rescue N2ICD driven ADM without EGFR. **a.** WT acinar cells infected with ad-MryAKT and embedded in collagen do not undergo ADM, even after 5 days in culture. **b.** E-KO cells infected with ad-MryAKT, ad-N2ICD, or co-infected with both ad-MyrAKT and ad-N2ICD are not able to undergo ADM. Scale bars = 100μm.

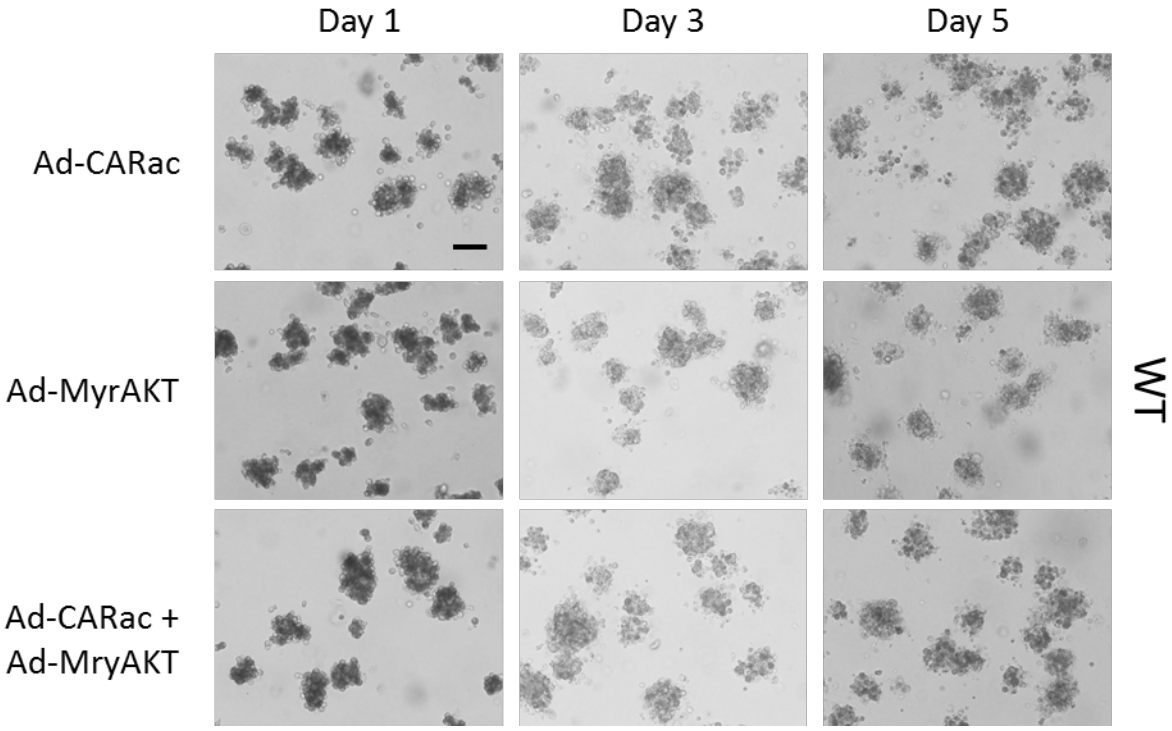
Day 1
Day 3
Day 5
Ad-CARac
Ad-MyrAKT
Ad-CARac +
Ad-MryAKT
WT

Figure 24: Activation of RAC, or combined activation of RAC and AKT cannot phenocopy ad-p110a expression. WT acinar cells infected with ad-RAC, ad-MryAKT, or co-infected with ad-RAC and ad-MryAKT embedded in collagen are unable to undergo ADM. Scale bar = 100μm.

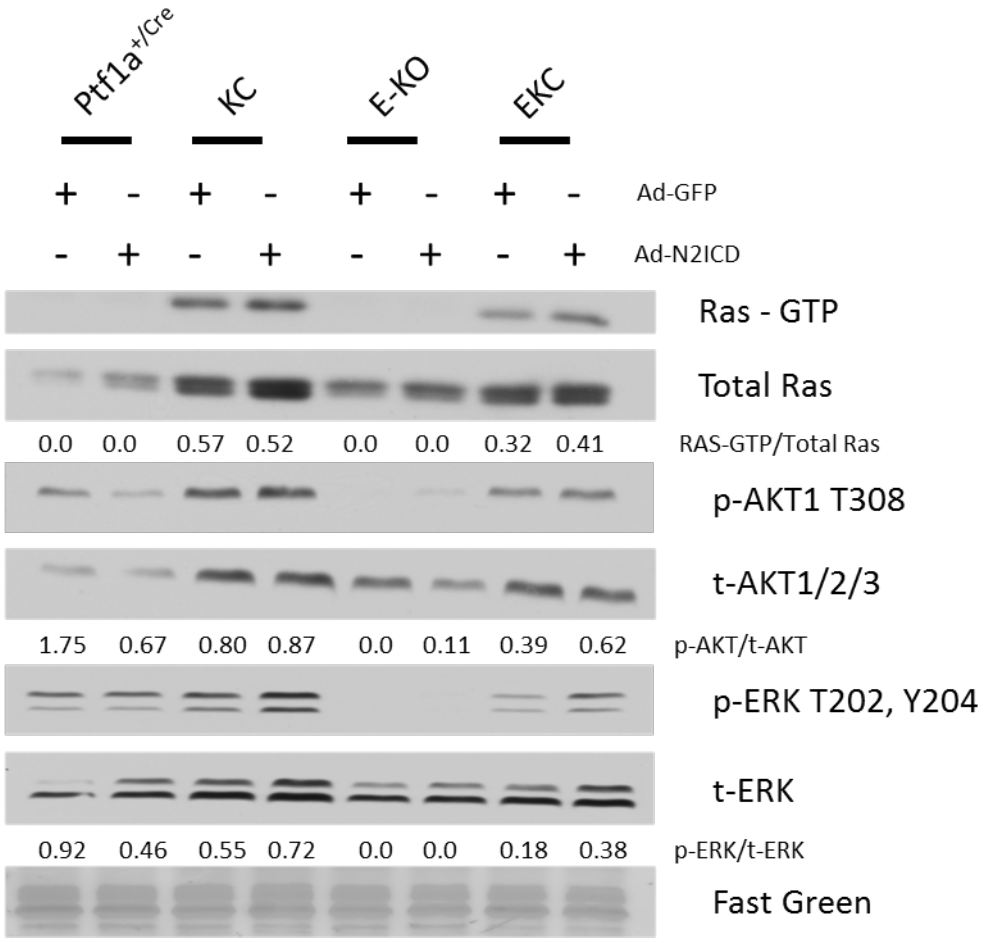
Ptf1a+/Cre
KC
E-KO
EKC
+ - + - + - + - Ad-GFP
- + - + - + - + Ad-N2ICD
Ras - GTP
Total Ras
0.0 0.0 0.57 0.52 0.0 0.0 0.32 0.41 RAS-GTP/Total Ras
p-AKT1 T308
t-AKT1/2/3
1.75 0.67 0.80 0.87 0.0 0.11 0.39 0.62 p-AKT/t-AKT
p-ERK T202, Y204
t-ERK
0.92 0.46 0.55 0.72 0.0 0.0 0.18 0.38 p-ERK/t-ERK
Fast Green

Figure 25: Notch pathway activation can increase RAS activity. GTP bound RAS levels in EKC acinar cells increase with N2ICD expression. N2ICD expression in EKC cells also results in an increase in ERK phosphylation as compared to GFP-controls. The levels of RAS and ERK activation in Ptf1a$^{+/Cre}$ acinar cells are unchanged with ad-N2ICD infection as compared to ad-GFP controls. The levels of AKT and ERK phosphorylation in E-KO acinar cells is much lower than in the other genotypes, which could be indicative of the inability of these cells to undergo ADM.

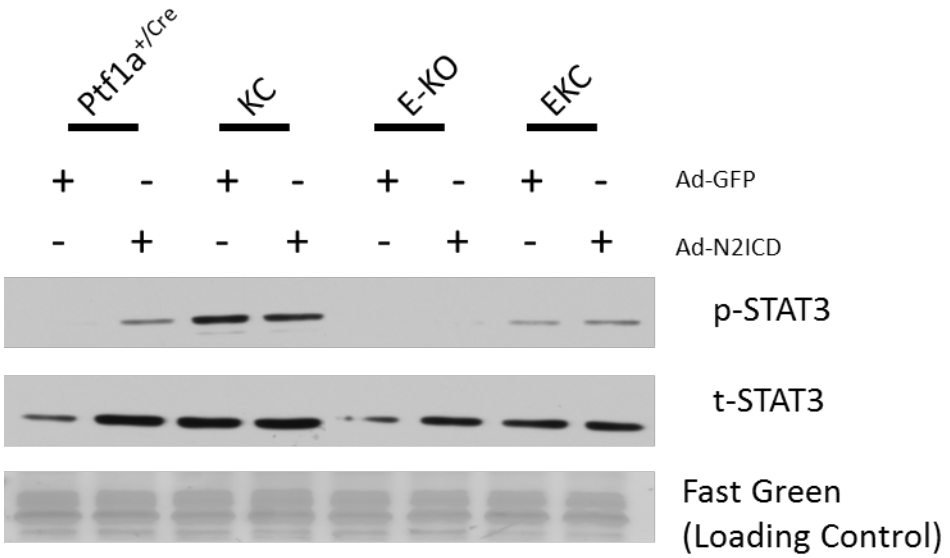
Ptf1a+/Cre
KC
E-KO
EKC
+ - + - + - + -
Ad-GFP
- + - + - + - +
Ad-N2ICD
p-STAT3
t-STAT3
Fast Green
(Loading Control)

Figure 26: STAT3 signaling is activated in acinar cells which undergo ADM. Western blot of protein lysates from both ad-GFP and ad-N2ICD infected acinar cells from Ptf1a$^{+/Cre}$, KC, E-KO, and EKC mice revealed increased STAT3 phosphorylation in response to N2ICD expression in Ptf1a$^{+/Cre}$ and EKC mice as opposed to ad-GFP infected controls.

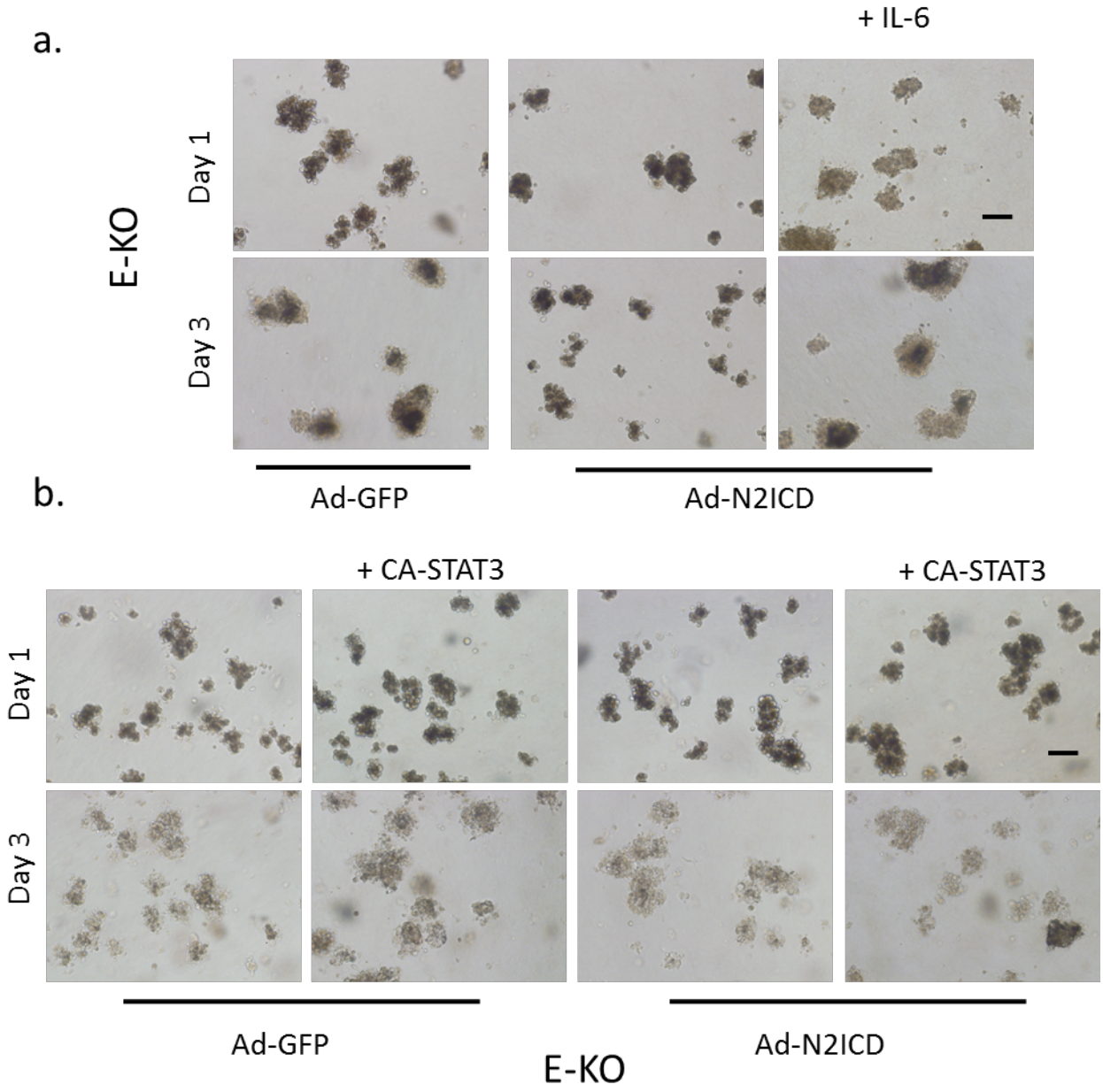
a.
+ IL-6
E-KO
Day 1
Day 3
Ad-GFP
Ad-N2ICD
b.
+ CA-STAT3
+ CA-STAT3
Day 1
Day 3
Ad-GFP
Ad-N2ICD
E-KO

Figure 27: Activation of Stat3 is not sufficient to rescue N2ICD driven ADM in the absence of EGFR. a. Treatment of E-KO acinar cells infected with ad-N2ICD with IL-6 to activate STAT3 signaling is not able to drive ADM. **b.** Co-infection of ad-GFP and adCA-STAT3 or ad-N2ICD and adCA-STAT3 or infection of ad-GFP or ad-N2ICD alone in E-KO acinar cell did not result in ADM. Scale bars = 100μm.

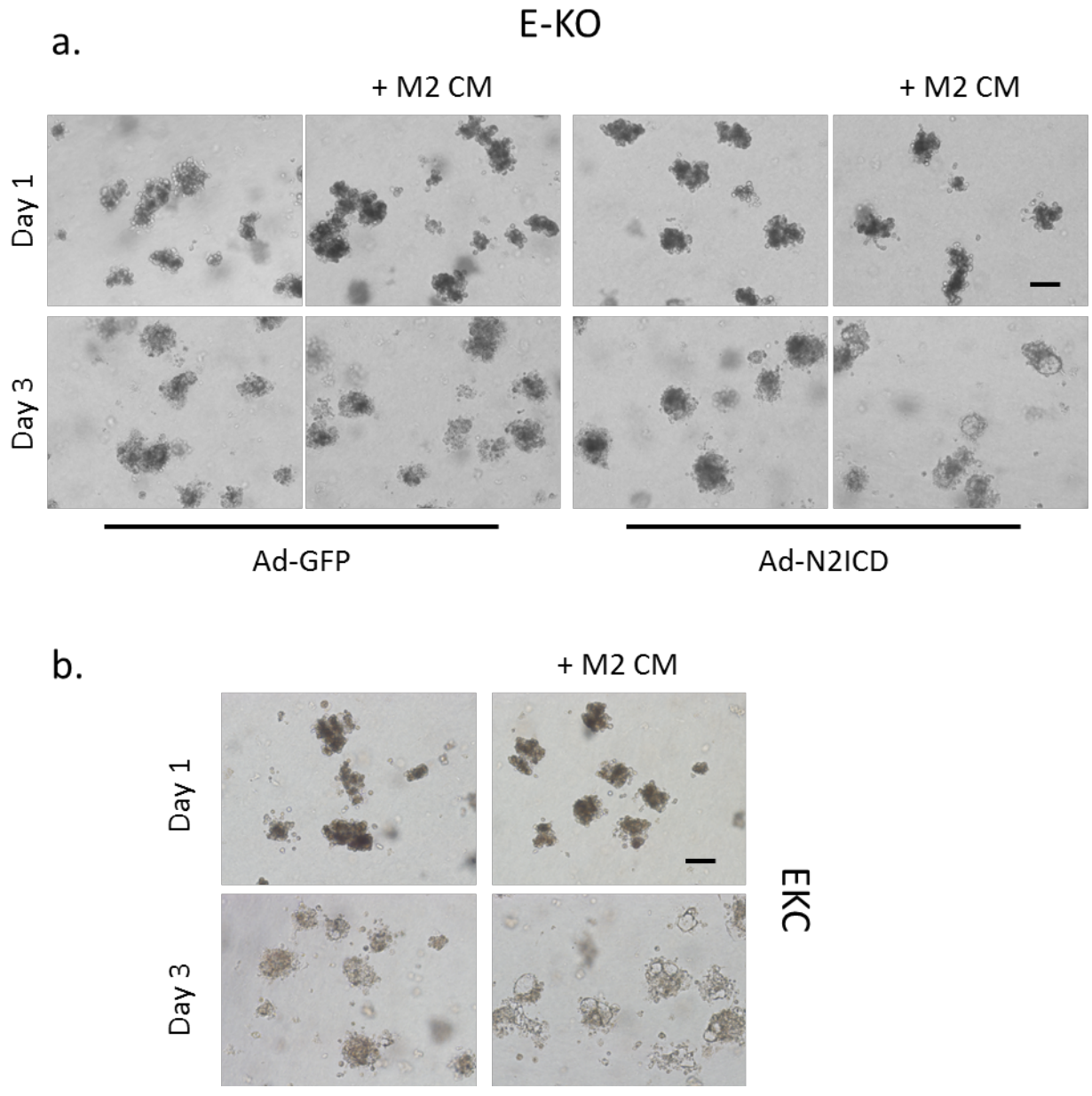
a.
E-KO
+ M2 CM
+ M2 CM
Day 1
Day 3
Ad-GFP
Ad-N2ICD
b.
+ M2 CM
Day 1
Day 3
EKC

Figure 28: M2 macrophage conditioned media can rescue N2ICD and Kras induced ADM in the absence of EGFR. a. Acinar cells harvested from E-KO mice and infected with ad-N2ICD and treated with M2 macrophage conditioned media in collagen are able to transdifferentiate by day 3 in culture. ADM was not seen in E-KO acinar cells infected with ad-N2ICD and treated with control media, nor in E-KO acinar cells infected with ad-GFP and treated with either M2 macrophage conditioned media or control media. **b.** EKC acinar cells embedded in collagen treated with M2 macrophage conditioned media readily underwent ADM by day 3 in culture, which was not seen in EKC acinar cells treated with control media. Scale bars = 100μm.

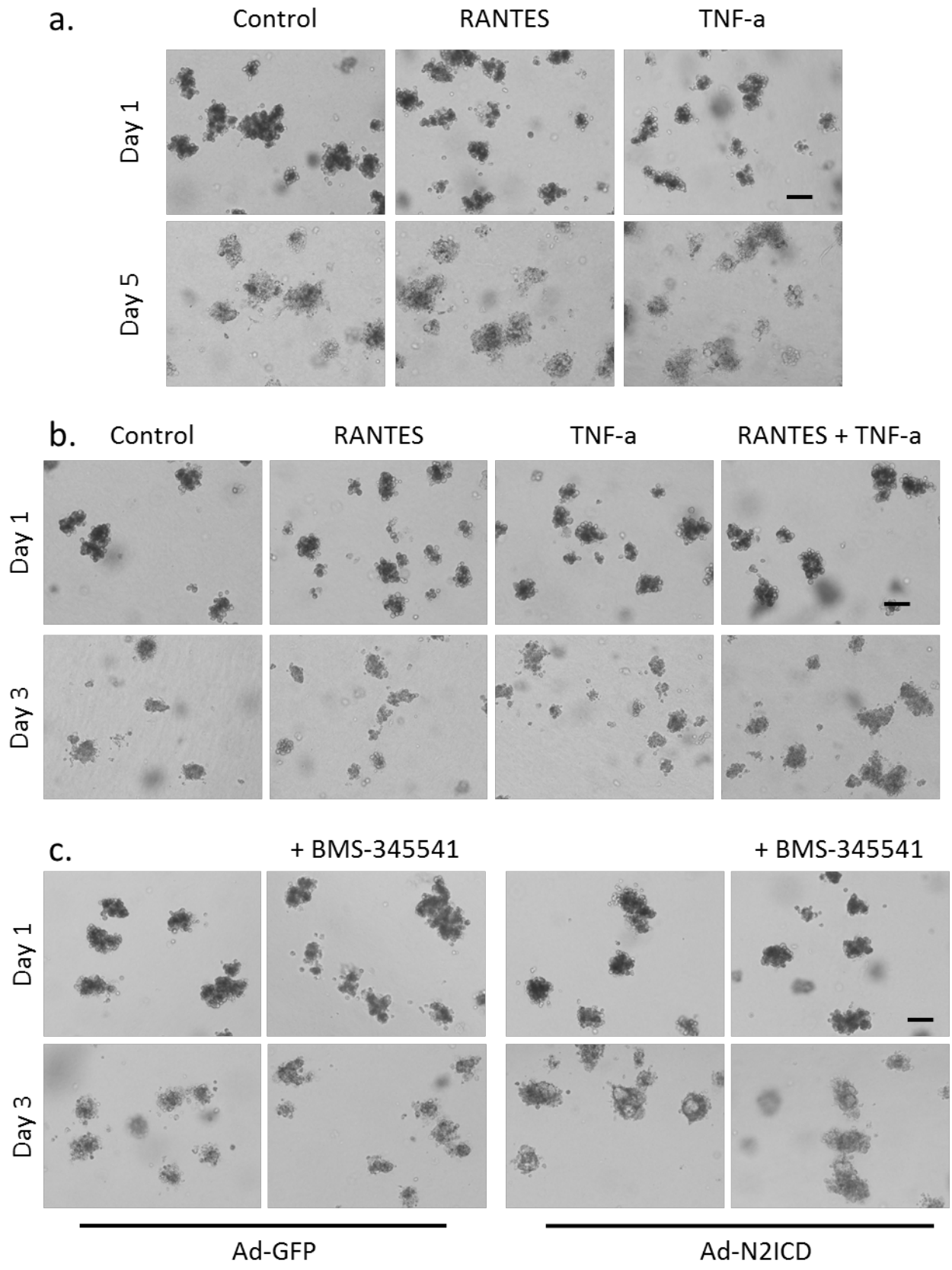
a.
Control
RANTES
TNF-a
Day 1
Day 5
b.
Control
RANTES
TNF-a
RANTES + TNF-a
Day 1
Day 3
c.
+ BMS-345541
+ BMS-345541
Day 1
Day 3
Ad-GFP
Ad-N2ICD

Figure 29: TNF-alpha and RANTES treatment did not cause ADM in the presence or absence of EGFR; Notch driven ADM is not NF-KB dependent. a. Treatment of WT acinar cells with RANTES or TNF-α was insufficient to cause ADM. **b.** E-KO cells infected with ad-N2ICD are not able to undergo ADM by treatment with RANTES, TNF-α, or a combination of both. **C.** N2ICD driven ADM is not blocked by treatment with the NF-KB inhibitor BMS-345541 at 1μM, although the cyst size is reduced.

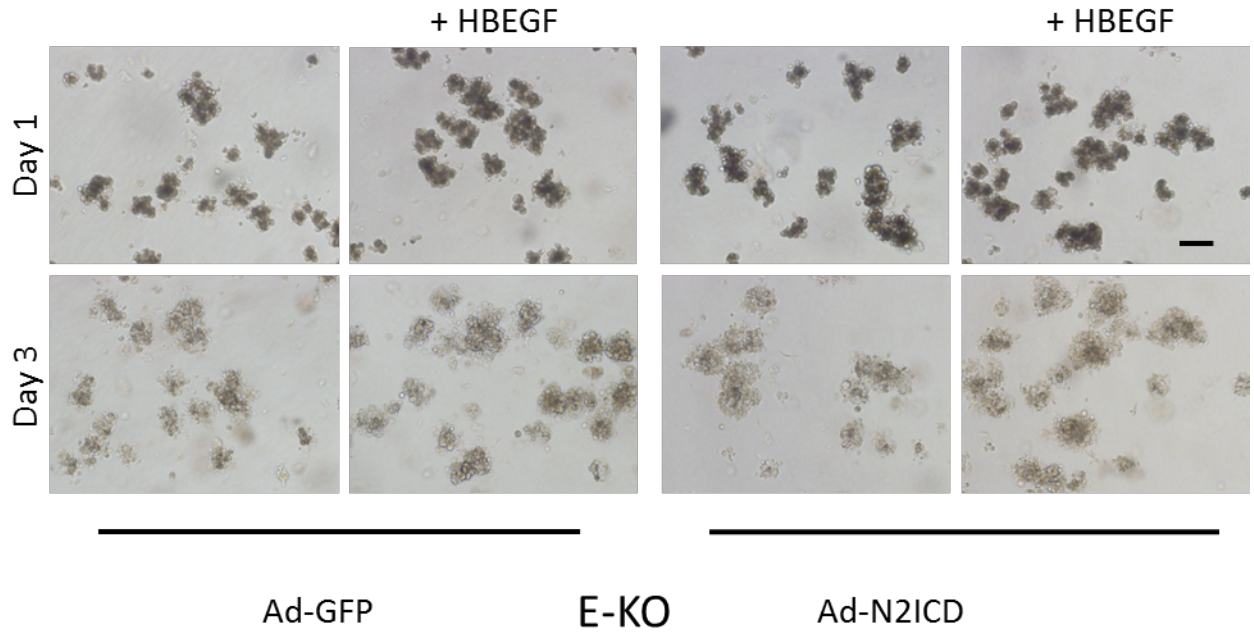
+ HBEGF
+ HBEGF
Day 1
Day 3
Ad-GFP
E-KO
Ad-N2ICD

Figure 30: HB-EGF treatment does not cause ADM in the absence of EGFR. HB-EGF treatment of E-KO acinar cells infected with ad-N2ICD or ad-GFP did not result in ADM by activation of an alternative ErbB receptor. Scale bar = 100μm.

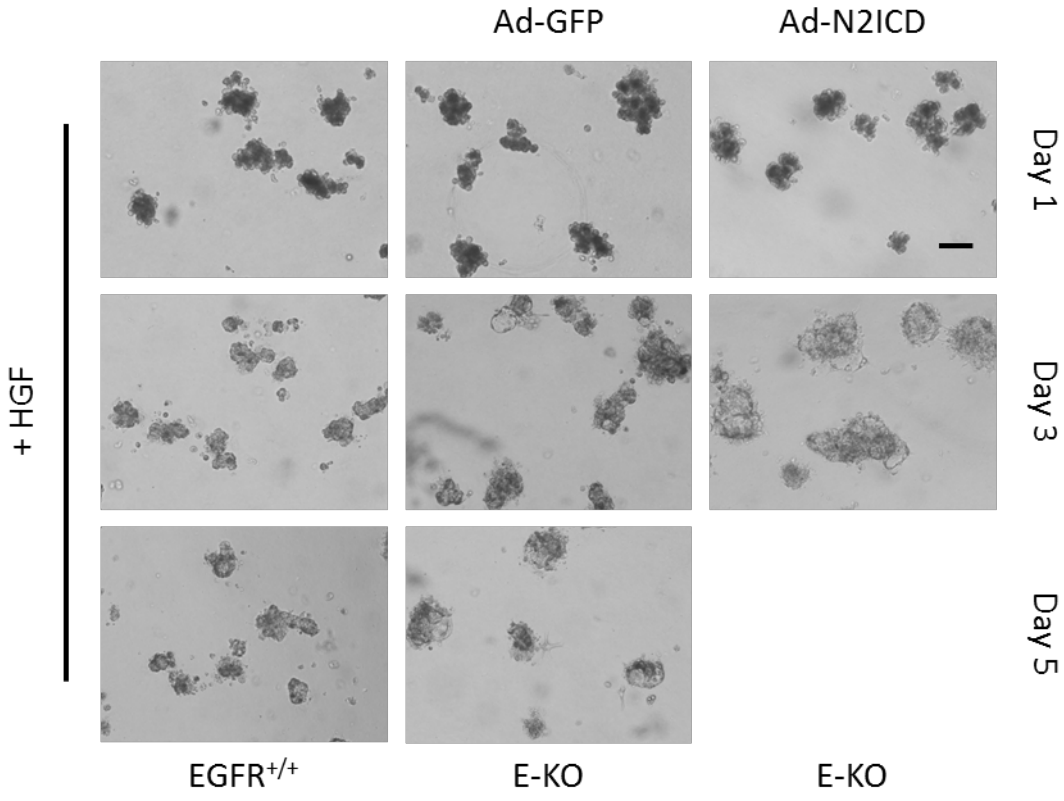
Ad-GFP
Ad-N2ICD
Day 1
Day 3
Day 5
+ HGF
EGFR+/+
E-KO
E-KO

Figure 31: HGF treatment of EGFR null acinar cells can induce ADM and cooperate with Notch driven ADM. WT and E-KO acinar cells which were infected with ad-GFP or ad-N2ICD embedded in collagen then treated with HGF. By day 3 in culture, ad-N2ICD infected E-KO acinar cells transdifferentiated, and occasional acinar clusters in ad-GFP infected E-KO acinar cells were also seen to have undergone ADM. In contrast, WT acinar cells did not appear to undergo ADM even by day 5 in culture, by which point most E-KO acinar clusters developed ductal cysts. Scale bar = 100μm.

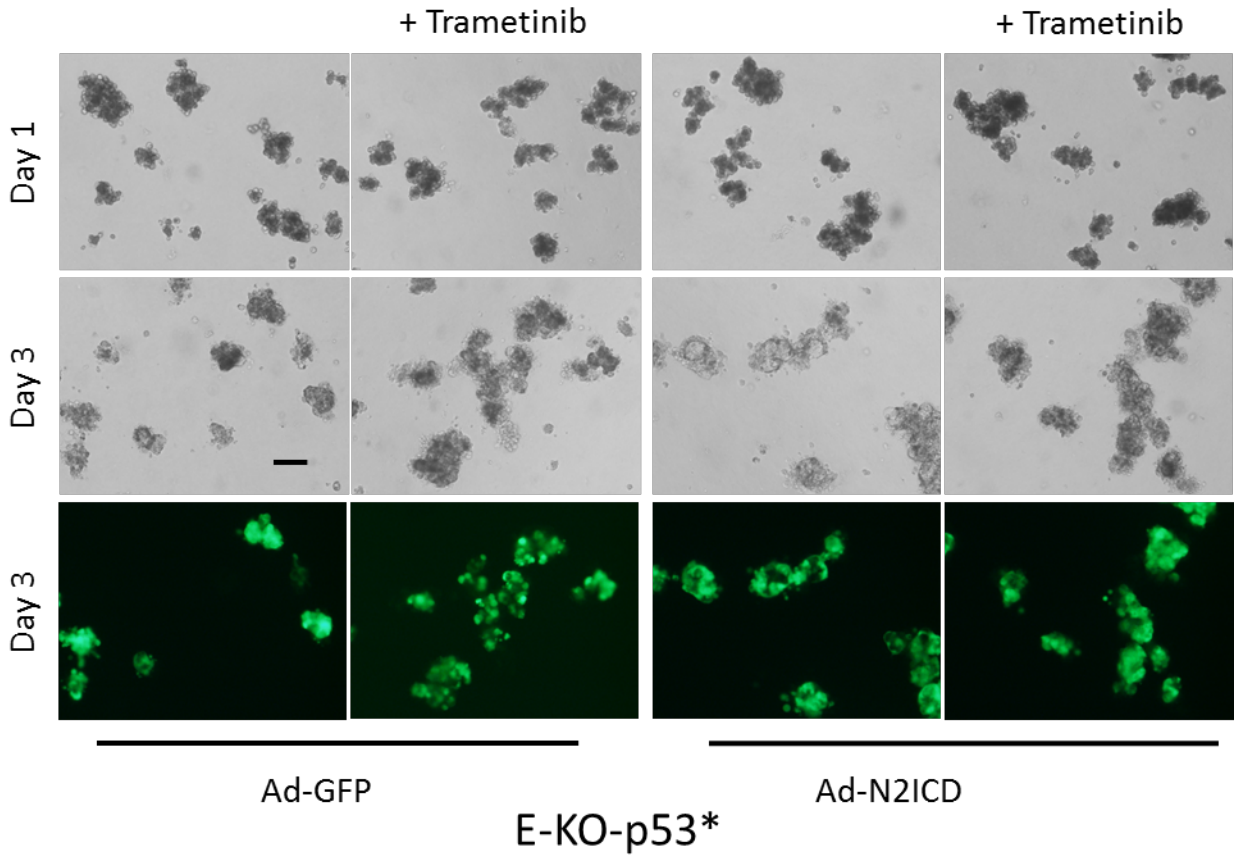
+ Trametinib
+ Trametinib
Day 1
Day 3
Day 3
Ad-GFP
Ad-N2ICD
E-KO-p53*

Figure 32: p53 mutation can rescue N2ICD driven ADM in EGFR null acinar cells. Acinar cells from E-KO mice bearing a $p53^{R172H}$ mutation infected with ad-N2ICD readily undergo ADM by day 3 in collagen culture, which was not seen in ad-GFP infected controls. Treatment of E-KO-p53* acinar cells with 100nM trametinib was able to block N2ICD induced ADM, however the trametinib treated acinar cells expressing N2ICD were still viable at day 3. Scale bar = 100μm.

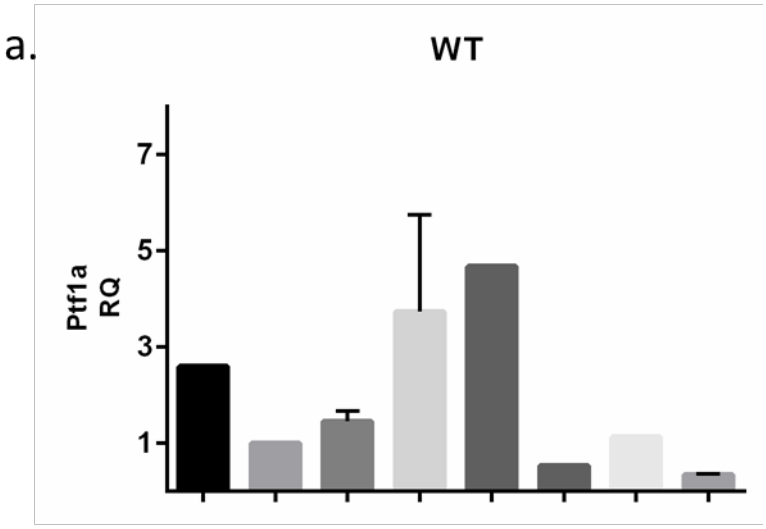
a.
WT
Ptf1a RQ
7
5
3
1
TGF-α - + + + + + + +
DAPT - - + - + + - -
Trametinib - - - + + - + -
Ad-N2ICD - - - - - + + +

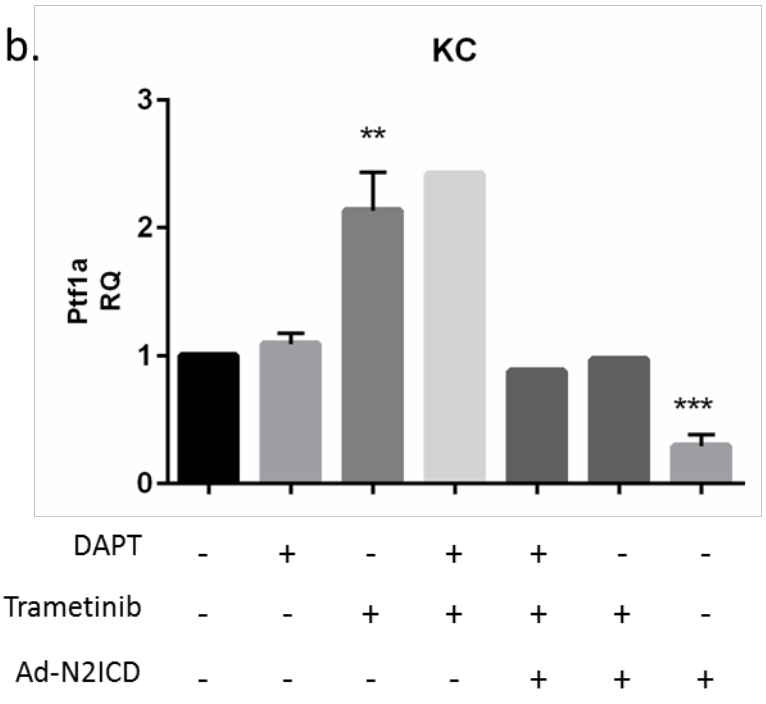
b.
KC
Ptf1a RQ
3
2
1
0
**
***
DAPT - + - + + - -
Trametinib - - + + + + -
Ad-N2ICD - - - - + + +

Figure 33: Both the MAPK and Notch signaling pathways regulate acinar cell de-differentiation. a. TGF-α treatment of WT acinar cells results in a decrease in Ptf1a expression, which is partially blocked by inhibition of gamma-secretase by DAPT, or entirely blocked by MEK inhibition with trametinib treatment. Ad-N2ICD infection of TGF-α acinar cells results in a dramatic decrease in Ptf1a expression levels, which is blocked by trametinib treatment. **b.** KC acinar cell expression of Ptf1a is increased by trametinib treatment, or decreased by N2ICD expression. Trametinib treatment of ad-N2ICD infected KC acinar cells results in the negation of Ptf1a modulation seen by the treatment of either condition alone. n= 3 for all samples which show statistics. Statistics performed using an unpaired student's T test, with p = .0028 (**) and p = .0002(***) respectively.

Chapter 5: Interrogation of Kras signaling by transcriptome sequencing

Background:

The advancement of next-generation sequencing has dramatically increased the scale of data that can be obtained from a sample in terms of both genomic DNA and RNA transcripts, as well as dramatic reduction in cost as the technologies have developed[132]. As the underlying causes of pancreatic cancer are relatively unknown, much effort has been devoted to genome wide association studies (GWAS) to attempt to identify susceptible patient populations. GWAS studies involve a very large cohort of afflicted patient samples compared to a very large amount of normal controls, which therefore requires a large financial investment to sequence and analyze all the samples. A study of 1,896 pancreatic cancer patients compared to 1,939 controls revealed that patients with type O blood may have a lower risk factor for pancreatic cancer[133]. Further study by expanding the cohorts to include 3,851 pancreatic cancer patients and 3,934 control samples identified three new genetic loci enriched in single nucleotide polymorphisms[134]. Broadening the patient pool to 7,683 pancreatic cancer patients and 14,397 controls yielded an additional 4 new loci which were determined to be significantly altered in pancreatic cancer[135].

Given the enormous amount of money, manpower, and time to obtain and sequence the number of samples required for significant results, genome sequencing remains impractical for most research programs. Additionally GWAS data offers no functional argument for the enrichment of the genetic loci found. Transcriptome sequencing, also called RNA-seq, is a technique by which sequencing all the messenger RNA in one sample can be used to identify signaling pathways that are modulated in comparison to a different sample. An early example of the utility of RNA-seq in dissecting key signaling pathways in pancreatic cancer demonstrated that analysis of mRNA from two pancreatic cancer patients compared to normal pancreas RNA

revealed an upregulation of 877 common genes between the two samples and normal pancreas which fit into expected signaling pathways seen in pancreatic cancer[136]. However the use of primary tumor samples as a source of material for sequencing is hampered by the large amount of stromal cells which are inherent in pancreas tumors. While several techniques to minimize stromal contaminations exist, such as growing out primary cells lines or establishment of patient derived xenografts[137], there are inherent problems with both techniques, the most important of which is the removal of the cancer cells from their native environment.

To study the signaling promoted by mutant Kras in the initiation of pancreatic cancer, I decided to take a transcriptome sequencing approach on isolated mouse acinar cells. The purpose of using isolated acinar cells is twofold; first I would be able to remove the stromal contamination prior to sequencing, and secondly the sequencing would be limited to signaling in what has been suggested to be the cell of origin of pancreatic cancer[56]. We have recently published two gene knockout mouse models which are protected from $Kras^{G12D}$ initiated pancreatic tumorigenesis by independent mechanisms[72,85]. By ablating EGFR from the pancreas we find that $Kras^{G12D}$ is unable to initiate ADM to promote PanIN formation[72]. In the second model, we have found that p110α protein expression is required to stabilize ADM, which prevents $Kras^{G12D}$ promotion of ADM to PanIN[85]. By comparing the transcriptome of EGFR or p110α knockout acinar cells to acinar cells expressing $Kras^{G12D}$ or normal acinar cells it could be possible to identify common signaling components required by Kras to initiate tumorigensis that could reveal targets for early detection, prevention, or treatment of pancreatic cancer.

Results:

To generate a cohort of samples for transcriptome sequencing I isolated acinar cells from $Kras^{+/LSL-G12D}$;$Ptf1a^{+/Cre}$ mice (KC), $p110\alpha^{f/f}$;KrasG12D;$Ptf1a^{+/Cre}$ mice (PKC),

$EGFR^{f/f}$;KrasG12D;$Ptf1a^{+/Cre}$ mice(EKC), and a normal mice (WT). For each genotype, three individual mice were used, and the isolated acinar cells were allowed to rest overnight to normalize for any variation in physical stress in the digestion and isolation process. After RNA was isolated, purity was confirmed and only samples with a RIN>7 were carried forward for sequencing. cDNA libraries were then constructed and sequenced on an Illumina platform at 100bp paired reads. The reads were then trimmed back to 50bp for alignment, and differentiation gene expression (DGE) analysis was performed using WT acinar cells as a control for each genotype, generating KC vs. WT, EKC vs. WT, and PKC vs. WT gene sets. Gene sets were then queried to determine genes which were regulated by $Kras^{G12D}$ compared to WT with or without respective p110α or EGFR ablation. 760 genes were differentially expressed ($q<0.05$ and 2 fold increase or decrease) in KC acinar cells as compared to WT acinar cells (Figure 34a). Looking at the requirement of p110α signaling on KC DGE vs. WT, 217 genes were found that were increased or decreased by 2 fold in KC acinar cells with or without p110α. The remaining 543 genes found to be differentially expressed in KC over WT acinar cells were not found to be differentially expressed in PKC vs. WT acinar cells (Figure 34b). Comparing EKC vs. WT gene set to the KC vs. WT gene set, I found that 746 genes that were differentially expressed by 2 fold in KC acinar cells were not differentially expressed in EKC acinar cells. The remaining 14 genes in the KC vs. WT gene set were found to be differentially expressed by 2 fold in EKC acinar cells (Figure 34c).

Performing Gene Ontology (GO) analysis on the KC vs. WT gene set revealed that the majority of genes upregulated in KC acinar cells compared to WT were related to inflammation or immune cell signaling pathways (Figure 35). Closer examination of the gene list revealed several genes that are only expressed in immune cells, such as the macrophage marker EMR1.

While mutant Kras is known to promote the expression of inflammatory cytokines[110,111], at this point we could not rule out that our KC acinar cells did not contain a larger number of contaminating immune cells. To help control for this, I designed a new experiment utilizing recombination of $Kras^{G12D}$ *ex vivo* in $Kras^{+/LSL-G212D}$ acinar cell clusters by infection with adenoviral Cre (ad-Cre). However, having a defined time point of activation of $Kras^{G12D}$ in acinar cells would also allow for a temporal study of signaling pathway activation during ADM.

To validate this, I isolated acinar cells from a $Kras^{+/LSL-G212D}$ mouse and infected with adenoviral GFP (ad-GFP) or ad-Cre. After 24 hours of infection (Day 1), I harvested a sample of both the ad-GFP and ad-Cre, then subsequently harvested ad-Cre infected acinar cells at 48 (Day 2) and 72 (Day 3) hours post infection. Extracting RNA from all of the samples, I analyzed the gene expression of acinar markers Ptf1a and Amylase, Sox9 as a ductal marker, and CyclinD1 as readout of Kras driven Erk activity (Figure 36). None of the markers showed any change of expression between the ad-Cre and ad-GFP infected acinar cells, however by day 2 in the ad-Cre infected acinar cells Amylase and Ptf1a expression dropped dramatically, while Sox9 and CyclinD1 expression increased. The expression of CyclinD1 and Sox9 increased further in the Day3 sample of the ad-Cre infected acinar cells, demonstrating that further Kras induced signaling modifications are occurring at that time point.

I next isolated a cohort of 3 $Kras^{+/LSL-G12D}$ mice and repeated the infection protocol, harvesting the ad-GFP at acinar cells on Day 1 and ad-Cre acinar cells at Day 1, Day 2, and Day 3. RNA was isolated from each sample and sent off for library construction and sequencing after verification of RNA purity. Sequence data was obtained and aligned at 50bp paired reads. DGE counts were then obtained by paired analysis, as each time point could be paired with the others from the same mouse. Using a differential expression cutoff of 2≤fold we identified 21 genes

differentially expressed by Day 1, 1691 genes differentially expressed by Day 2, and 2315 genes differentially expressed by Day 3.

I next subjected the Day 1 ad-GFP and Day 3 ad-Cre to Gene Set Enrichment Analysis (GSEA). Among the top gene sets enriched for genes in the ad-Cre Day 3 gene set were several cancer gene sets, as well as an exocrine progenitor gene set, and an EMT gene set (Figure 37a). As the EMT gene set was particularly interesting, I looked at the gene enrichment plot (Figure 37b) and heat maps of the gene set with the samples (Figure 37c). There was a nearly complete overlap of the gene set, and very consistent expression across the sample cohorts. Further examination of genes typically associated with mesenchymal cells reveal an increase in expression in the ad-Cre infected cells over time (Figure 38a). The expression of genes associated with extracellular matrix modeling was also found to be increased by mutant Kras expression over the time course (Figure 38b). The expression of genes associated with acinar epithelial differentiation were seen to decrease in time with mutant Kras expressions (Figure 39a), however genes in which expression is normally lost during canonical EMT were found to either increase in expression or remain unchanged (Figure 39b). This finding demonstrates that ADM has an "EMT-like" program, in which there is a gain of mesenchymal features, but not a loss of the epithelial features.

Discussion:

The advent of next generation sequencing has a lot of potential to identify targets in pancreatic cancer which would potentially have been overlooked. RNA-seq has proven useful in identifying PDGFR β as a critical signaling pathway in metastasis in p53 mutant pancreatic cancer cells[138] and finding that WNT signaling is enriched in non-adherent human pancreatic tumor spheres and circulating tumor cells[139]. Taking advantage of our ability to harvest and

maintain acinar cells from mice I was able to investigate the gene signature of acinar cells expressing mutant Kras as compared to normal acinar cells, as well as acinar cells expressing mutant Kras which are protected from tumorigenesis by knockout of either EGFR or p110α. As we consider ADM to be a putative source of tumorigenesis, I expected the acinar isolation to provide a relatively pure population of cells in which to study the early signaling events in Kras tumorigenesis. I found 760 genes that were modulated in acinar cells expressing mutant Kras, 746 (98%) of which required EGFR signaling to be differentially expressed, whereas 543 of the 760 genes (71%) required p110α expression to be differentially expressed. The remaining 217 out of 760 genes were modulated by Kras independently of p110α expression, while 14 of the 760 genes were differentially expressed by Kras even in the absence EGFR expression. Of the genes which Kras was able to differentially express, TFF1, PRAP1, 2210407C18RIK, SGPP2, CYP2B10, PKD1L2, and GT(ROSA)26SOR were identified to be independent of both p110α and EGFR expression. Importantly, GT(ROSA)26SOR is a gene locus in which our mice have reporter genes, and should not have a biological function, which leaves the total genes shared between the lists at 6.

Grouping the differentially expressed genes in the KC vs. WT gene set, I discovered that a large number of the genes were related to inflammation and immune cell signals. While I did expect mutant Kras to stimulate an inflammatory signature based on other studies[110,111], several genes that are specific to certain linages of immune cells indicated that isolating acinar cells was not sufficient to completely remove stromal contamination, as KC pancreata are likely to contain more immune cells at rest, even in mice as young as those used in the study. To address this problem I harvested acinar cells from mice with the mutant Kras allele which was not yet recombined and added adenoviral Cre to the cells *ex vivo*. As these acinar cells had mutant Kras

signaling initiated at a specific time harvesting the acinar cells in a time course post infection allowed for interrogating of signaling pathways in response to mutant Kras activation in a stepwise fashion. As expected, the number of differentially expressed genes started out small, 21 genes, and rose dramatically to identify 2315 over the course of the study. Running a GSEA analysis on the Day 3 gene set compared to the GFP infected control cells, several interesting pathways were enriched, however the EMT pathway near the top of the results were of particular interest, as Rhim et al. demonstrated that EMT is actually an early event in pancreatic tumorigenesis[140]. Further investigation into extracellular matrix remodeling and mesenchymal genes traditionally gained during EMT revealed a close overlap with genes upregulated during ADM, however there was no loss of epithelial gene markers despite loss of acinar differentiation. This finding lends strength to the argument that the gain of mesenchymal markers are an early event in pancreatic tumorigenesis, however there is not EMT in the traditional sense with a loss of epithelial identity.

Combining the data gain from these sequencing experiments with the observation that the EGFR-Ras-MAPK and Notch signaling pathways are not configured in a linear fashion allows for a prediction of what the contributions of each pathway may be. First, the repression of acinar differentiation appears to have an absolute requirement for MAPK signaling, which is lost in acinar cells stimulated with TGF-α or by $Kras^{G12D}$ expression when treated with the MEK inhibitor trametinib. However, the inhibition of gamma-secretase with DAPT has not demonstrated significant impairment of the repression of acinar differentiation in acinar cells stimulated with TGF-α or by $Kras^{G12D}$ expression. However, previous studies have extensively shown the role of Notch signaling in the gain of an embryonic progenitor state, therefore the role of Notch signaling could be the upregulation of mesenchymal markers and progenitor markers

that are seen to increase in ADM in the sequencing experiments. Therefore, I believe that the EGFR-Ras-MAPK pathway is required to drive the de-differentiation of acinar cells by repression of PTf1a and other acinar differentiation factors, while the Notch pathway is responsible for the gain of mesenchymal markers and progenitor phenotype in acinar-to-ductal metaplasia, which in the presence of mutant Ras can develop into PanIN lesions.

Future Directions:

As a whole this transcriptome sequencing study has generated a lot of data, however only the tip of the iceberg has been addressed in terms of analysis. I hope to enlist the help of a bioinformatician to assist in further mining the data to try and find a common theme in the pathways activated by Kras, which is difficult to do just by looking at lists of gene names. I have done some preliminary validation of results from the sequencing by qPCR, however it would again be helpful to narrow down the results before spending the time, effort, and cost involved in validation of targets.

I am also interested in following up on the EMT-like phenotype observed during ADM. Some preliminary staining for N-cadherin, a mesenchymal associated adhesion protein led us to buy N-cadherin floxed mice from Jackson labs, and a coworker is currently in the process of breeding those mice to a KC background to determine what role N-cadherin plays in tumorigenesis. It will also be interesting to see the results of the Rhim lab at the University of Michigan who are investigating the requirement of Slug and Snail, EMT associated transcription factors, in Kras induced tumorigenesis. The Simeone lab at the University of Michigan also recently identified the protein ATDC as important contributor to EMT in pancreatic cancer[141]. They are currently in the process of validating ATDC conditional knockout mice, which appear to be protected from $Kras^{G12D}$ tumorigenesis in a relatively aggressive p53 haploinsufficiency

model. I plan to assist them to determine if ATDC as well as CD44, an identified effector protein, are required for acinar cells to undergo or maintain ADM.

Figures for Chapter 5: Interrogation of Kras signaling by transcriptome sequencing

a. **KC genes regulated vs. WT**

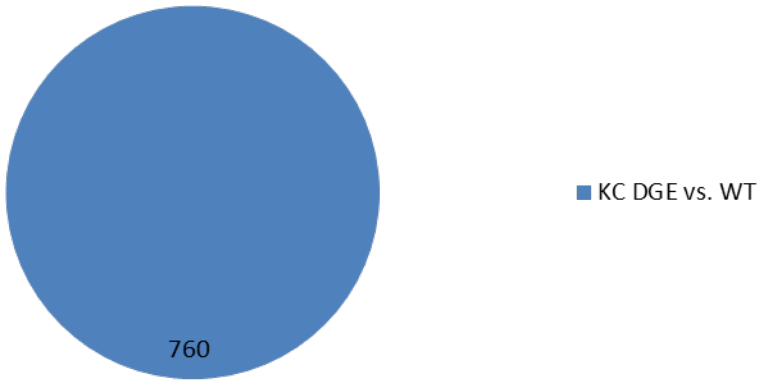

b. **p110α modulation of Kras Signaling**

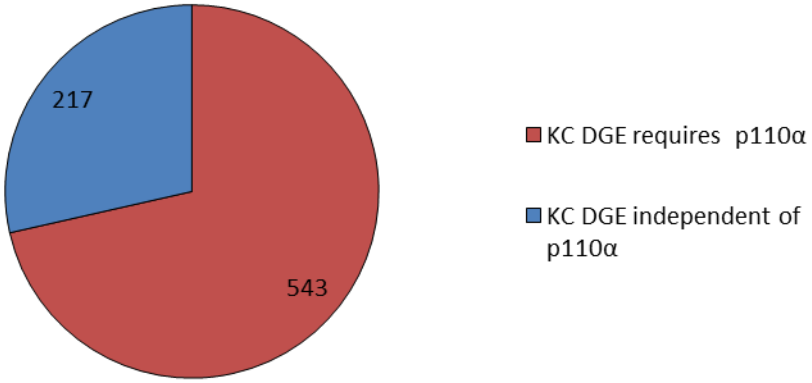

c. **EGFR modulation of Kras Signaling**

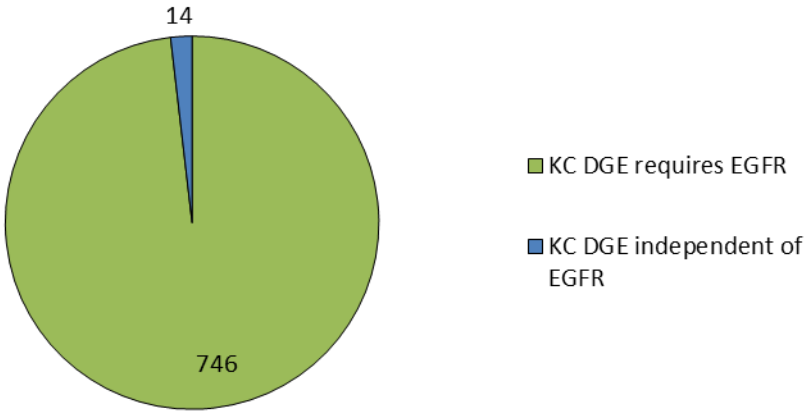

Figure 34: Mutant Kras signaling depends on both p110*α* and EGFR protein expression. **a.** Differential gene expression analysis of KC vs. WT acinar cells revealed 760 genes differentially expressed by 2 fold with a q factor <0.05. **b.** Comparing gene sets from PKC vs. WT and KC vs. WT revealed that 217 genes are differentially expressed by Kras regardless of p110α expression, while 543 genes are only differentially expressed by Kras in the presence of p110α expression. **c.** Comparison of EKC vs. WT and KC vs. WT gene sets reveal that 746 (98%) of genes differentially expressed by Kras require EGFR expression in acinar cells, while 14 are differentially expressed regardless of EGFR expression.

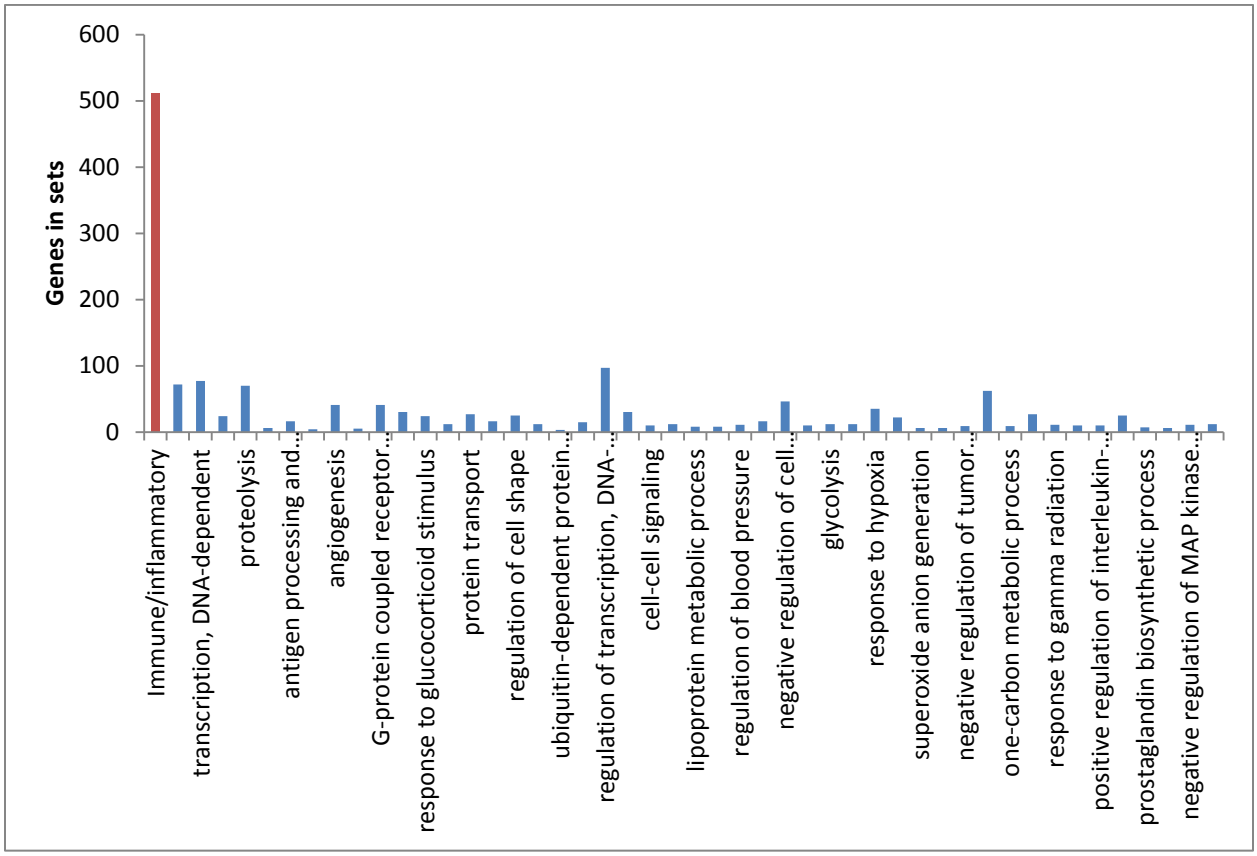
Genes in sets
600
500
400
300
200
100
0
Immune/inflammatory
transcription, DNA-dependent
proteolysis
antigen processing and...
angiogenesis
G-protein coupled receptor...
response to glucocorticoid stimulus
protein transport
regulation of cell shape
ubiquitin-dependent protein...
regulation of transcription, DNA-...
cell-cell signaling
lipoprotein metabolic process
regulation of blood pressure
negative regulation of cell...
glycolysis
response to hypoxia
superoxide anion generation
negative regulation of tumor...
one-carbon metabolic process
response to gamma radiation
positive regulation of interleukin-...
prostaglandin biosynthetic process
negative regulation of MAP kinase...

Figure 35: Gene Ontology analysis reveals an immune/inflammatory Kras gene signature. Grouping all of the immune cell and inflammatory pathway results from gene ontology analysis demonstrates the dominant feature of these gene signatures in mutant Kras signaling in acinar cells.

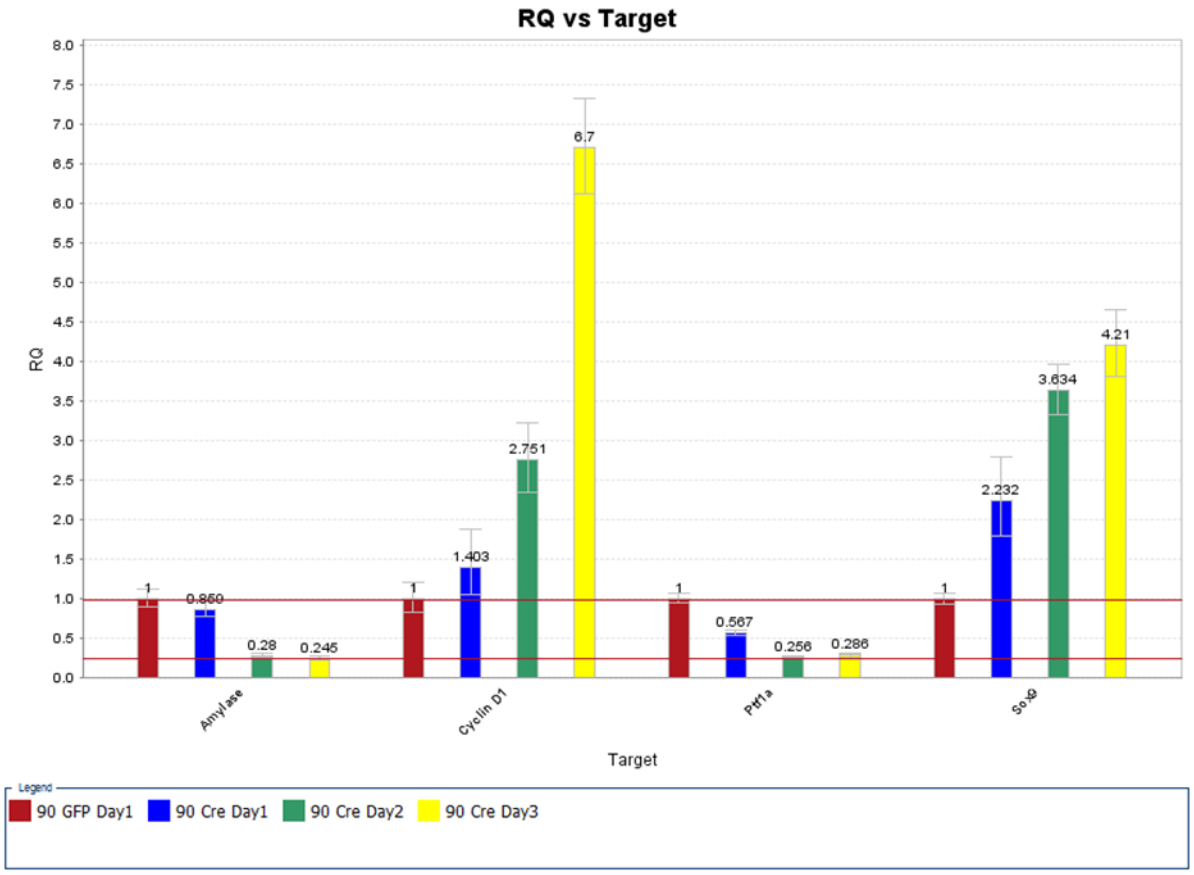
RQ vs Target
RQ
Target
Amylase
Cyclin D1
Ptf1a
Sox9
1
0.850
0.28
0.245
1
1.403
2.751
6.7
1
0.567
0.256
0.286
1
2.232
3.634
4.21
Legend
90 GFP Day1
90 Cre Day1
90 Cre Day2
90 Cre Day3

Figure 36: KrasG12D driven ADM can be tracked kinetically. qPCR results of RNA harvested from $Kras^{+/LSLG12D}$ acinar cells infected with adenoviral GFP or Cre and harvested at 24 hours (Day 1), 28 hours (Day 2), or 72 hours (Day 3) post infection. Acinar cell markers such as Amylase and Ptf1a can be seen to decrease by Day 2, while Sox9 and CyclinD1 expression begin to increase at Day 2 and further increase by Day 3.

a.

NAME
FARMER_BREAST_CANCER_CLUSTER_5
WEBER_METHYLATED_ICP_IN_SPERM_DN
ANASTASSIOU_CANCER_MESENCHYMAL_TRANSITION_SIGNATURE
MODULE_42
CLASPER_LYMPHATIC_VESSELS_DURING_METASTASIS_DN
GNF2_CDH11
BIOCARTA_PLATELETAPP_PATHWAY
REACTOME_COLLAGEN_FORMATION
REACTOME_RESPIRATORY_ELECTRON_TRANSPORT
COLLAGEN
CLAUS_PGR_POSITIVE_MENINGIOMA_DN
MODULE_103
TESAR_JAK_TARGETS_MOUSE_ES_D3_UP
STEGER_ADIPOGENESIS_DN
NADH_DEHYDROGENASE_COMPLEX
KEGG_FATTY_ACID_METABOLISM
REACTOME_RESPIRATORY_ELECTRON_TRANSPORT_ATP_SYNTHESIS_BY_CHEMIOSMOTIC_COU
MODULE_77
MODULE_210
ZHOU_PANCREATIC_EXOCRINE_PROGENITOR

b.

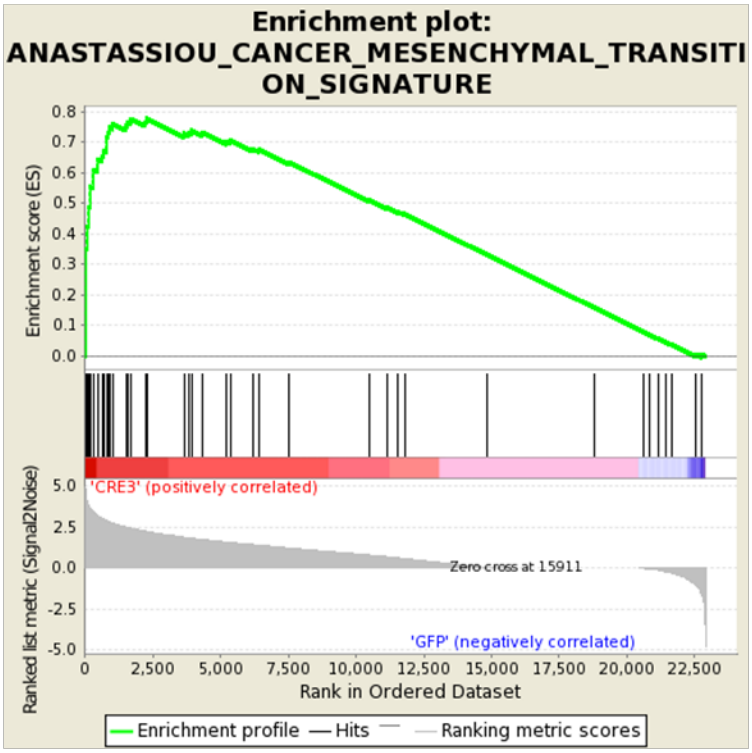

c.

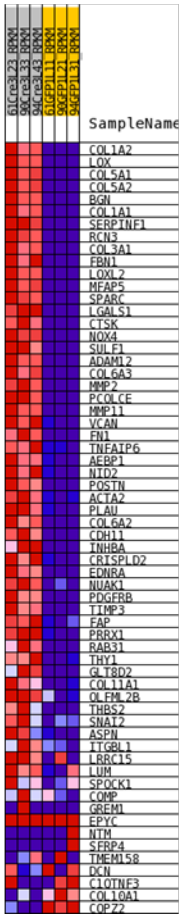

Figure 37: Kras signaling initiates an EMT gene signature in ADM. a. Top 21 results for a GSEA analysis of ad-GFP Day 1 vs. ad-Cre Day 3 gene sets. Several cancer related gene sets, as well as an EMT and a pancreatic progenitor gene set are among the results. **b.** Enrichment plot for the Anastassiou_Cancer_Mesenchymal_Transition_Signature for the ad-Cre Day 3 vs. Ad-GFP day 1 GSEA. **c.** Heat map of Anastassiou_Cancer_Mesenchymal_Transition_Signature genes in both data sets reveals a high overlap, as well as consistency across the sample groups.

a.

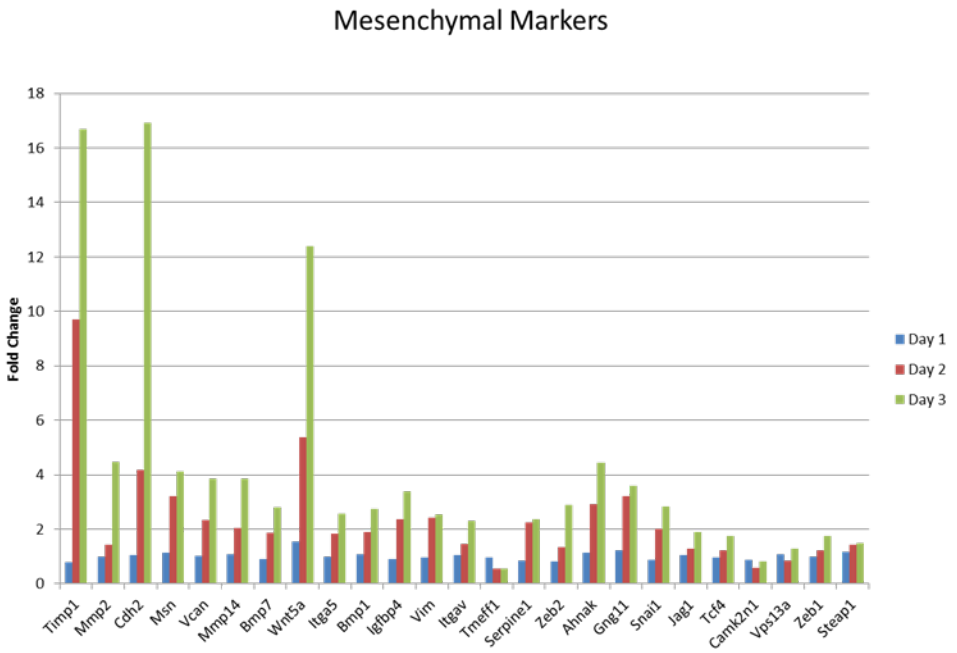
Mesenchymal Markers
Fold Change
18
16
14
12
10
8
6
4
2
0
Timp1
Mmp2
Cdh2
Msn
Vcan
Mmp14
Bmp7
Wnt5a
Itga5
Bmp1
Igfbp4
Vim
Itgav
Tmeff1
Serpine1
Zeb2
Ahnak
Gng11
Snai1
Jag1
Tcf4
Camk2n1
Vps13a
Zeb1
Steap1
Day 1
Day 2
Day 3

b.

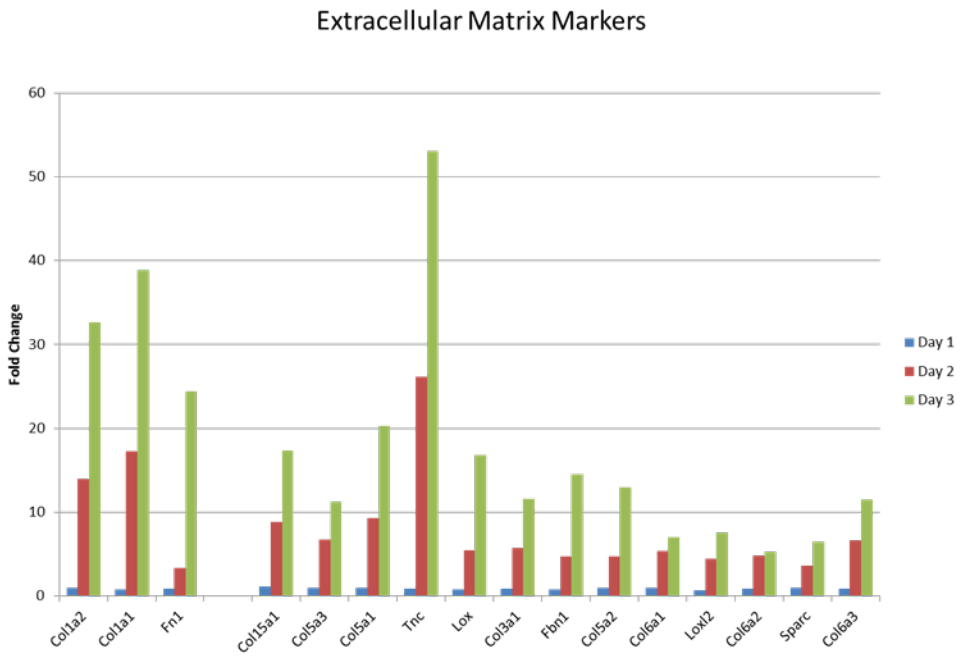
Extracellular Matrix Markers
Fold Change
60
50
40
30
20
10
0
Col1a2
Col1a1
Fn1
Col15a1
Col5a3
Col5a1
Tnc
Lox
Col3a1
Fbn1
Col5a2
Col6a1
Loxl2
Col6a2
Sparc
Col6a3
Day 1
Day 2
Day 3

Figure 38: KrasG12D driven ADM leads to a gain of mesenchymal markers. Expression of genes associated with both mesenchymal cells (**a**) and extracellular matrix remodeling (**b**) are found to increase over time in ad-Cre infected $Kras^{+/LSL\text{-}G12D}$ acinar cells compared to ad-GFP infected $Kras^{+/LSL\text{-}G12D}$ acinar cells.

a.

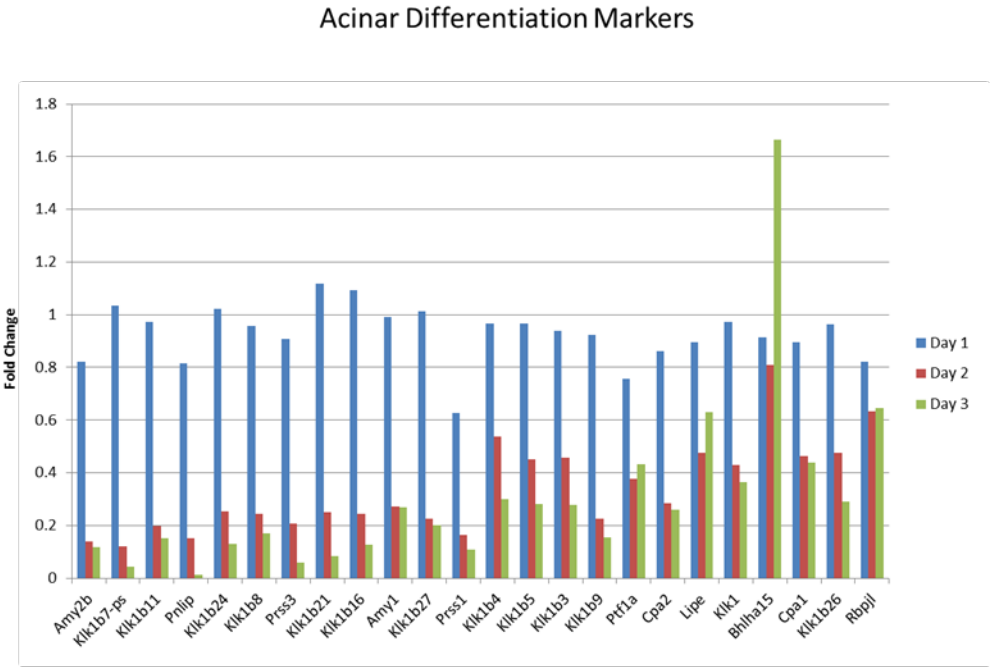
Acinar Differentiation Markers
Fold Change
1.8
1.6
1.4
1.2
1
0.8
0.6
0.4
0.2
0
Amy2b
Klk1b7-ps
Klk1b11
Pnlip
Klk1b24
Klk1b8
Prss3
Klk1b21
Klk1b16
Amy1
Klk1b27
Prss1
Klk1b4
Klk1b5
Klk1b3
Klk1b9
Ptf1a
Cpa2
Lipe
Klk1
Bhlha15
Cpa1
Klk1b26
Rbpjl
Day 1
Day 2
Day 3

b.

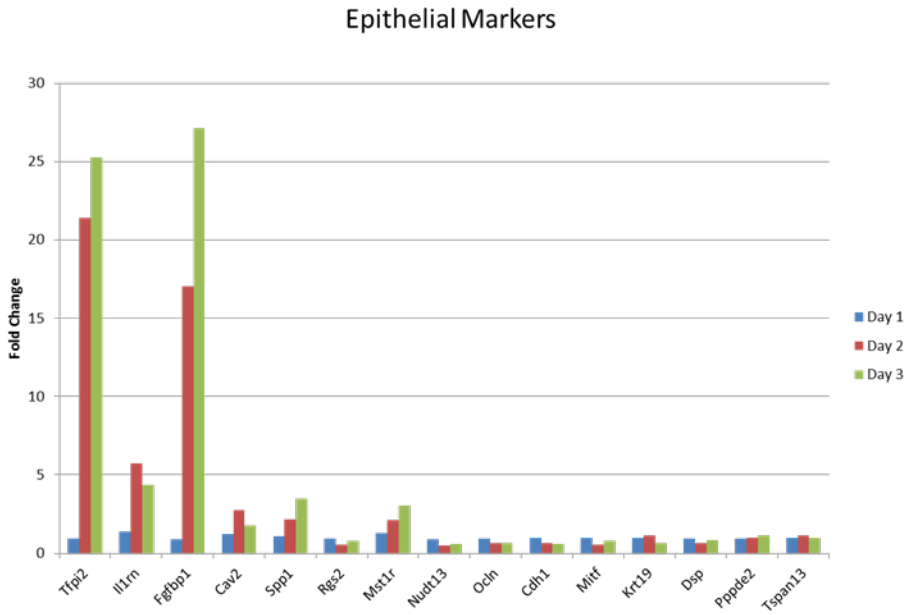
Epithelial Markers
Fold Change
30
25
20
15
10
5
0
Tfpi2
Il1rn
Fgfbp1
Cav2
Spp1
Rgs2
Mst1r
Nudt13
Ocln
Cdh1
Mitf
Krt19
Dsp
Pppde2
Tspan13
Day 1
Day 2
Day 3

Figure 39: KrasG12D driven ADM results in a loss of acinar, but not epithelial, differentiation. a. Expression of acinar cell associated genes were seen to decrease in ad-Cre infected $Kras^{+/LSL\text{-}G12D}$ acinar cells over time as compared to ad-GFP infected $Kras^{+/LSL\text{-}G12D}$ acinar cells. **b.** Expression of genes typically lost in epithelial-to-mesenchymal transition are either increased or not changed during ADM in ad-Cre infected $Kras^{+/G12D}$ acinar cells as compared to ad-GFP infected $Kras^{+/G12D}$ acinar cells.

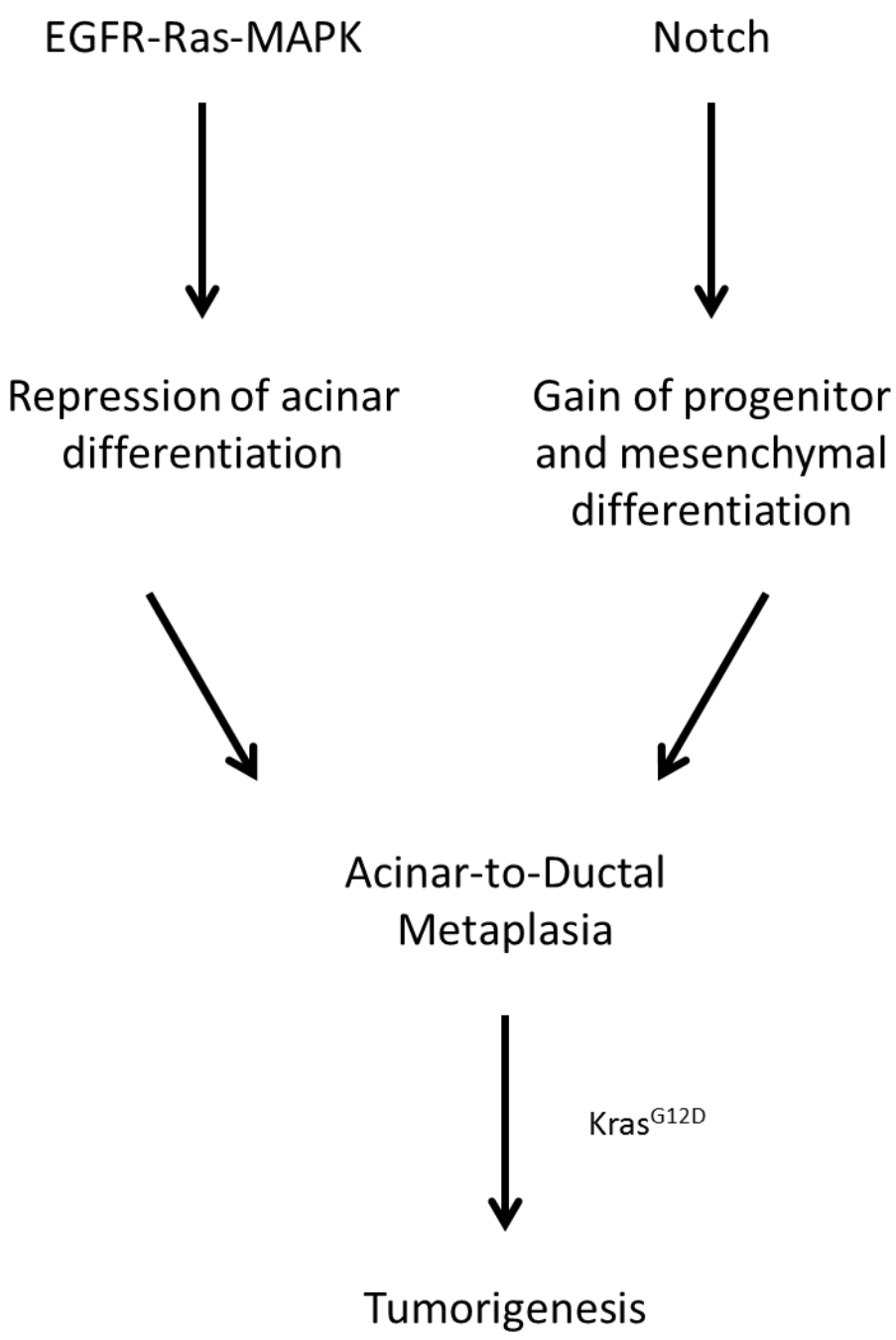
EGFR-Ras-MAPK
Notch
Repression of acinar differentiation
Gain of progenitor and mesenchymal differentiation
Acinar-to-Ductal Metaplasia
Kras^G12D
Tumorigenesis

Figure 40: Proposed Mechanism of ADM and pancreatic tumorigenesis. EGFR-Ras-MAPK signaling is leads to the repression of genes which drive acinar differentiation, while Notch signaling drive the gain of progenitor genes, as well as genes typically associated with a mesenchymal phenotype. Together, these two signals drive ADM, which can be hijacked by mutant Kras to drive tumorigenesis.

References:

1 Slack, J. M. Developmental biology of the pancreas. *Development* **121**, 1569-1580 (1995).

2 Pan, F. C. & Wright, C. Pancreas Organogenesis: From Bud to Plexus to Gland. *Dev Dynam* **240**, 530-565, doi:Doi 10.1002/Dvdy.22584 (2011).

3 Jonsson, J., Carlsson, L., Edlund, T. & Edlund, H. Insulin-Promoter-Factor-1 Is Required for Pancreas Development in Mice. *Nature* **371**, 606-609, doi:Doi 10.1038/371606a0 (1994).

4 Gu, G. Q., Dubauskaite, J. & Melton, D. A. Direct evidence for the pancreatic lineage: NGN3+cells are islet progenitors and are distinct from duct progenitors. *Development* **129**, 2447-2457 (2002).

5 Krapp, A. *et al.* The bHLH protein PTF1-p48 is essential for the formation of the exocrine and the correct spatial organization of the endocrine pancreas. *Gene Dev* **12**, 3752-3763, doi:DOI 10.1101/gad.12.23.3752 (1998).

6 Sellick, G. S. *et al.* Mutations in PTF1A cause pancreatic and cerebellar agenesis. *Nat Genet* **36**, 1301-1305, doi:ng1475 [pii]

10.1038/ng1475 (2004).

7 Kawaguchi, Y. *et al.* The role of the transcriptional regulator Ptf1a in converting intestinal to pancreatic progenitors. *Nat Genet* **32**, 128-134, doi:10.1038/ng959

ng959 [pii] (2002).

8 Masui, T. *et al.* Replacement of Rbpj with Rbpjl in the PTF1 complex controls the final maturation of pancreatic acinar cells. *Gastroenterology* **139**, 270-280, doi:10.1053/j.gastro.2010.04.003

S0016-5085(10)00549-4 [pii] (2010).

9 Seymour, P. A. *et al.* SOX9 is required for maintenance of the pancreatic progenitor cell pool. *P Natl Acad Sci USA* **104**, 1865-1870, doi:DOI 10.1073/pnas.0609217104 (2007).

10 Norgaard, G. A., Jensen, J. N. & Jensen, J. FGF10 signaling maintains the pancreatic progenitor cell state revealing a novel role of Notch in organ development. *Developmental Biology* **264**, 323-338, doi:DOI 10.1016/j.ydbio.2003.08.013 (2003).

11 Murtaugh, L. C., Stanger, B. Z., Kwan, K. M. & Melton, D. A. Notch signaling controls multiple steps of pancreatic differentiation. *P Natl Acad Sci USA* **100**, 14920-14925, doi:DOI 10.1073/pnas.2436557100 (2003).

12 Apelqvist, A. *et al.* Notch signalling controls pancreatic cell differentiation. *Nature* **400**, 877-881 (1999).

13 Esni, F. *et al.* Notch inhibits Ptf1 function and acinar cell differentiation in developing mouse and zebrafish pancreas. *Development* **131**, 4213-4224, doi:10.1242/dev.01280 (2004).

14 Yadav, D. & Lowenfels, A. B. The Epidemiology of Pancreatitis and Pancreatic Cancer. *Gastroenterology* **144**, 1252-1261, doi:DOI 10.1053/j.gastro.2013.01.068 (2013).

15 Bradley, E. L. A Clinically Based Classification-System for Acute-Pancreatitis. *Ann Chir* **47**, 537-541 (1993).

16 Treacy, J. *et al.* Evaluation of amylase and lipase in the diagnosis of acute pancreatitis. *Anz J Surg* **71**, 577-582, doi:DOI 10.1046/j.1445-2197.2001.02220.x (2001).

17 Archer, H., Jura, N., Keller, J., Jacobson, M. & Bar-Sagi, D. A mouse model of hereditary pancreatitis generated by transgenic expression of R122H trypsinogen. *Gastroenterology* **131**, 1844-1855, doi:DOI 10.1053/j.gastro.2006.09.049 (2006).

18 Watanabe, S., Abe, K., Anbo, Y. & Katoh, H. Changes in the Mouse Exocrine Pancreas after Pancreatic Duct Ligation - a Qualitative and Quantitative Histological Study. *Arch Histol Cytol* **58**, 365-374, doi:Doi 10.1679/Aohc.58.365 (1995).
19 Niederau, C., Ferrell, L. D. & Grendell, J. H. Caerulein-Induced Acute Necrotizing Pancreatitis in Mice - Protective Effects of Proglumide, Benzotript, and Secretin. *Gastroenterology* **88**, 1192-1204 (1985).
20 Li, J. *et al.* Does chronic ethanol intake cause chronic pancreatitis? Evidence and mechanism. *Pancreas* **37**, 189-195 (2008).
21 Fortunato, F. & Gates, L. K. Alcohol feeding and lipopolysaccharide injection modulate apoptotic effectors in the rat pancreas in vivo. *Pancreas* **21**, 174-180, doi:Doi 10.1097/00006676-200008000-00011 (2000).
22 Tsukamoto, H., Towner, S. J., Yu, G. S. M. & French, S. W. Potentiation of Ethanol-Induced Pancreatic Injury by Dietary-Fat - Induction of Chronic-Pancreatitis by Alcohol in Rats. *American Journal of Pathology* **131**, 246-257 (1988).
23 DelGiorno, K. E. *et al.* Persistent Salmonellosis Causes Pancreatitis in a Murine Model of Infection. *Plos One* **9**, doi:ARTN e92807

DOI 10.1371/journal.pone.0092807 (2014).
24 Siegel, R., Ma, J. M., Zou, Z. H. & Jemal, A. Cancer Statistics, 2014. *Ca-Cancer J Clin* **64**, 9-29, doi:Doi 10.3322/Caac.21208 (2014).
25 Von Hoff, D. D. *et al.* Increased survival in pancreatic cancer with nab-paclitaxel plus gemcitabine. *N Engl J Med* **369**, 1691-1703, doi:10.1056/NEJMoa1304369 (2013).
26 Ryan, D. P., Hong, T. S. & Bardeesy, N. Pancreatic Adenocarcinoma. *New Engl J Med* **371**, 1039-1049, doi:Doi 10.1056/Nejmra1404198 (2014).
27 Hruban, R. H., Maitra, A. & Goggins, M. Update on pancreatic intraepithelial neoplasia. *Int J Clin Exp Pathol* **1**, 306-316 (2008).
28 Andea, A., Sarkar, F. & Adsay, V. N. Clinicopathological correlates of pancreatic intraepithelial neoplasia: A comparative analysis of 82 cases with and 152 cases without pancreatic ductal adenocarcinoma. *Modern Pathol* **16**, 996-1006, doi:Doi 10.1097/01.Mp.0000087422.24733.62 (2003).
29 Distler, M., Aust, D., Weitz, J., Pilarsky, C. & Grutzmann, R. Precursor Lesions for Sporadic Pancreatic Cancer: PanIN, IPMN, and MCN. *Biomed Research International*, doi:Artn 474905

Doi 10.1155/2014/474905 (2014).
30 Jones, S. *et al.* Core signaling pathways in human pancreatic cancers revealed by global genomic analyses. *Science* **321**, 1801-1806, doi:DOI 10.1126/science.1164368 (2008).
31 Lohr, M., Kloppel, G., Maisonneuve, P., Lowenfels, A. B. & Luttges, J. Frequency of K-ras mutations in pancreatic intraductal neoplasias associated with pancreatic ductal adenocarcinoma and chronic pancreatitis: a meta-analysis. *Neoplasia* **7**, 17-23, doi:10.1593/neo.04445 (2005).
32 Yamano, M. *et al.* Genetic progression and divergence in pancreatic carcinoma. *American Journal of Pathology* **156**, 2123-2133, doi:Doi 10.1016/S0002-9440(10)65083-3 (2000).
33 Luttges, J. *et al.* Allelic loss is often the first hit in the biallelic inactivation of the p53 and DPC4 genes during pancreatic carcinogenesis. *American Journal of Pathology* **158**, 1677-1683, doi:Doi 10.1016/S0002-9440(10)64123-5 (2001).
34 Rocks, O., Peyker, A. & Bastiaens, P. I. Spatio-temporal segregation of Ras signals: one ship, three anchors, many harbors. *Curr Opin Cell Biol* **18**, 351-357, doi:10.1016/j.ceb.2006.06.007 (2006).

35 Johnson, L. *et al.* K-ras is an essential gene in the mouse with partial functional overlap with N-ras. *Gene Dev* **11**, 2468-2481, doi:DOI 10.1101/gad.11.19.2468 (1997).
36 Bos, J. L., Rehmann, H. & Wittinghofer, A. GEFs and GAPs: critical elements in the control of small G proteins. *Cell* **129**, 865-877, doi:10.1016/j.cell.2007.05.018 (2007).
37 John, J. *et al.* Kinetics of interaction of nucleotides with nucleotide-free H-ras p21. *Biochemistry-Us* **29**, 6058-6065 (1990).
38 Traut, T. W. Physiological concentrations of purines and pyrimidines. *Mol Cell Biochem* **140**, 1-22 (1994).
39 Baines, A. T., Xu, D. & Der, C. J. Inhibition of Ras for cancer treatment: the search continues. *Future medicinal chemistry* **3**, 1787-1808, doi:10.4155/fmc.11.121 (2011).
40 Ostrem, J. M., Peters, U., Sos, M. L., Wells, J. A. & Shokat, K. M. K-Ras(G12C) inhibitors allosterically control GTP affinity and effector interactions. *Nature* **503**, 548-551, doi:10.1038/nature12796 (2013).
41 Jeng, H. H., Taylor, L. J. & Bar-Sagi, D. Sos-mediated cross-activation of wild-type Ras by oncogenic Ras is essential for tumorigenesis. *Nat Commun* **3**, 1168, doi:10.1038/ncomms2173 (2012).
42 Grabocka, E. *et al.* Wild-type H- and N-Ras promote mutant K-Ras-driven tumorigenesis by modulating the DNA damage response. *Cancer Cell* **25**, 243-256, doi:10.1016/j.ccr.2014.01.005 (2014).
43 Lemmon, M. A. Ligand-induced ErbB receptor dimerization. *Exp Cell Res* **315**, 638-648, doi:10.1016/j.yexcr.2008.10.024 (2009).
44 Olayioye, M. A. Update on HER-2 as a target for cancer therapy - Intracellular signaling pathways of ErbB2/HER-2 and family members. *Breast Cancer Research* **3**, 385-389, doi:Doi 10.1186/Bcr327 (2001).
45 Hingorani, S. R. *et al.* Preinvasive and invasive ductal pancreatic cancer and its early detection in the mouse. *Cancer Cell* **4**, 437-450, doi:Doi 10.1016/S1535-6108(03)00309-X (2003).
46 Hingorani, S. R. *et al.* Trp53R172H and KrasG12D cooperate to promote chromosomal instability and widely metastatic pancreatic ductal adenocarcinoma in mice. *Cancer Cell* **7**, 469-483, doi:S1535-6108(05)00128-5 [pii]

10.1016/j.ccr.2005.04.023 (2005).
47 Aguirre, A. J. *et al.* Activated Kras and Ink4a/Arf deficiency cooperate to produce metastatic pancreatic ductal adenocarcinoma. *Gene Dev* **17**, 3112-3126, doi:Doi 10.1101/Gad.1158703 (2003).
48 Bardeesy, N. *et al.* Both p16(Ink4a) and the p19(Arf)-p53 pathway constrain progression of pancreatic adenocarcinoma in the mouse. *P Natl Acad Sci USA* **103**, 5947-5952, doi:DOI 10.1073/pnas.0601273103 (2006).
49 Bardeesy, N. *et al.* Smad4 is dispensable for normal pancreas development yet critical in progression and tumor biology of pancreas cancer. *Gene Dev* **20**, 3130-3146, doi:Doi 10.1101/Gad.1478706 (2006).
50 Ijichi, H. *et al.* Aggressive pancreatic ductal adenocarcinoma in mice caused by pancreas-specific blockade of transforming growth factor-beta signaling in cooperation with active Kras expression. *Genes Dev* **20**, 3147-3160, doi:20/22/3147 [pii]

10.1101/gad.1475506 (2006).
51 Brembeck, F. H. *et al.* The mutant K-ras oncogene causes pancreatic periductal lymphocytic infiltration and gastric mucous neck cell hyperplasia in transgenic mice. *Cancer Res* **63**, 2005-2009 (2003).

52 Stanger, B. Z. *et al.* Pten constrains centroacinar cell expansion and malignant transformation in the pancreas. *Cancer Cell* **8**, 185-195, doi:DOI 10.1016/j.ccr.2005.07.015 (2005).
53 Guerra, C. *et al.* Chronic pancreatitis is essential for induction of pancreatic ductal adenocarcinorna by k-Ras Oncogenes in adult mice. *Cancer Cell* **11**, 291-302, doi:DOI 10.1016/j.ccr.2007.01.012 (2007).
54 Habbe, N. *et al.* Spontaneous induction of murine pancreatic intraepithelial neoplasia (mPanIN) by acinar cell targeting of oncogenic Kras in adult mice. *Proc Natl Acad Sci U S A* **105**, 18913-18918, doi:10.1073/pnas.0810097105 (2008).
55 De La, O. J. *et al.* Notch and Kras reprogram pancreatic acinar cells to ductal intraepithelial neoplasia. *Proc Natl Acad Sci U S A* **105**, 18907-18912, doi:10.1073/pnas.0810111105 (2008).
56 Kopp, J. L. *et al.* Identification of Sox9-Dependent Acinar-to-Ductal Reprogramming as the Principal Mechanism for Initiation of Pancreatic Ductal Adenocarcinoma. *Cancer Cell* **22**, 737-750, doi:DOI 10.1016/j.ccr.2012.10.025 (2012).
57 Raff, M. Adult stem cell plasticity: fact or artifact? *Annu Rev Cell Dev Biol* **19**, 1-22, doi:10.1146/annurev.cellbio.19.111301.143037 (2003).
58 Sandgren, E. P., Luetteke, N. C., Palmiter, R. D., Brinster, R. L. & Lee, D. C. Overexpression of TGF alpha in transgenic mice: induction of epithelial hyperplasia, pancreatic metaplasia, and carcinoma of the breast. *Cell* **61**, 1121-1135, doi:0092-8674(90)90075-P [pii] (1990).
59 Jensen, J. N. *et al.* Recapitulation of elements of embryonic development in adult mouse pancreatic regeneration. *Gastroenterology* **128**, 728-741, doi:DOI 10.1053/j.gastro.2004.12.008 (2005).
60 Miyamoto, Y. *et al.* Notch mediates TGF alpha-induced changes in epithelial differentiation during pancreatic tumorigenesis. *Cancer Cell* **3**, 565-576, doi:Doi 10.1016/S1535-6108(03)00140-5 (2003).
61 Means, A. L. *et al.* Pancreatic epithelial plasticity mediated by acinar cell transdifferentiation and generation of nestin-positive intermediates. *Development* **132**, 3767-3776, doi:dev.01925 [pii]

10.1242/dev.01925 (2005).
62 Fendrich, V. *et al.* Hedgehog signaling is required for effective regeneration of exocrine pancreas. *Gastroenterology* **135**, 621-631, doi:DOI 10.1053/j.gastro.2008.04.011 (2008).
63 Desai, B. M. *et al.* Preexisting pancreatic acinar cells contribute to acinar cell, but not islet beta cell, regeneration. *J Clin Invest* **117**, 971-977, doi:10.1172/JCI29988 (2007).
64 von Figura, G., Morris, J. P. t., Wright, C. V. & Hebrok, M. Nr5a2 maintains acinar cell differentiation and constrains oncogenic Kras-mediated pancreatic neoplastic initiation. *Gut* **63**, 656-664, doi:10.1136/gutjnl-2012-304287 (2014).
65 Shi, G. *et al.* Maintenance of acinar cell organization is critical to preventing Kras-induced acinar-ductal metaplasia. *Oncogene* **32**, 1950-1958, doi:Doi 10.1038/Onc.2012.210 (2013).
66 Flandez, M. *et al.* Nr5a2 heterozygosity sensitises to, and cooperates with, inflammation in KRas(G12V)-driven pancreatic tumourigenesis. *Gut* **63**, 647-655, doi:10.1136/gutjnl-2012-304381 (2014).
67 Prevot, P. P. *et al.* Role of the ductal transcription factors HNF6 and Sox9 in pancreatic acinar-to-ductal metaplasia. *Gut* **61**, 1723-1732, doi:10.1136/gutjnl-2011-300266 (2012).
68 Grimont, A. *et al.* SOX9 regulates ERBB signalling in pancreatic cancer development. *Gut*, doi:10.1136/gutjnl-2014-307075 (2014).
69 Sivere, J. T. *et al.* Notch signaling is required for exocrine regeneration after acute pancreatitis. *Gastroenterology* **134**, 544-555, doi:DOI 10.1053/j.gastro.2007.11.003 (2008).

70 Hanlon, L. *et al.* Notch1 Functions as a Tumor Suppressor in a Model of K-ras-Induced Pancreatic Ductal Adenocarcinoma. *Cancer Res.* **70**, 4280-4286, doi:Doi 10.1158/0008-5472.Can-09-4645 (2010).
71 Mazur, P. K. *et al.* Notch2 is required for progression of pancreatic intraepithelial neoplasia and development of pancreatic ductal adenocarcinoma. *P Natl Acad Sci USA* **107**, 13438-13443, doi:DOI 10.1073/pnas.1002423107 (2010).
72 Ardito, C. M. *et al.* EGF receptor is required for KRAS-induced pancreatic tumorigenesis. *Cancer Cell* **22**, 304-317, doi:10.1016/j.ccr.2012.07.024

S1535-6108(12)00337-6 [pii] (2012).
73 Navas, C. *et al.* EGF receptor signaling is essential for k-ras oncogene-driven pancreatic ductal adenocarcinoma. *Cancer Cell* **22**, 318-330, doi:10.1016/j.ccr.2012.08.001 (2012).
74 Collisson, E. A. *et al.* A central role for RAF-->MEK-->ERK signaling in the genesis of pancreatic ductal adenocarcinoma. *Cancer Discov* **2**, 685-693, doi:10.1158/2159-8290.CD-11-0347 (2012).
75 Singh, A. *et al.* A gene expression signature associated with "K-Ras addiction" reveals regulators of EMT and tumor cell survival. *Cancer Cell* **15**, 489-500, doi:10.1016/j.ccr.2009.03.022 (2009).
76 Collins, M. A. *et al.* Oncogenic Kras is required for both the initiation and maintenance of pancreatic cancer in mice. *J Clin Invest* **122**, 639-653, doi:10.1172/JCI59227 (2012).
77 Ying, H. Q. *et al.* Oncogenic Kras Maintains Pancreatic Tumors through Regulation of Anabolic Glucose Metabolism. *Cell* **149**, 656-670, doi:DOI 10.1016/j.cell.2012.01.058 (2012).
78 Kapoor, A. *et al.* Yap1 Activation Enables Bypass of Oncogenic Kras Addiction in Pancreatic Cancer. *Cell* **158**, 185-197, doi:DOI 10.1016/j.cell.2014.06.003 (2014).
79 Collins, M. A., Yan, W., Sebolt-Leopold, J. S. & di Magliano, M. P. MAPK Signaling Is Required for Dedifferentiation of Acinar Cells and Development of Pancreatic Intraepithelial Neoplasia in Mice. *Gastroenterology* **146**, 822-+, doi:DOI 10.1053/j.gastro.2013.11.052 (2014).
80 Vanhaesebroeck, B., Stephens, L. & Hawkins, P. PI3K signalling: the path to discovery and understanding. *Nat Rev Mol Cell Biol* **13**, 195-203, doi:10.1038/nrm3290 (2012).
81 Eser, S. *et al.* Selective requirement of PI3K/PDK1 signaling for Kras oncogene-driven pancreatic cell plasticity and cancer. *Cancer Cell* **23**, 406-420, doi:10.1016/j.ccr.2013.01.023 (2013).
82 Elghazi, L. *et al.* Regulation of pancreas plasticity and malignant transformation by Akt signaling. *Gastroenterology* **136**, 1091-1103, doi:10.1053/j.gastro.2008.11.043 (2009).
83 Mack, N. A., Whalley, H. J., Castillo-Lluva, S. & Malliri, A. The diverse roles of Rac signaling in tumorigenesis. *Cell Cycle* **10**, 1571-1581 (2011).
84 Heid, I. *et al.* Early requirement of Rac1 in a mouse model of pancreatic cancer. *Gastroenterology* **141**, 719-730, 730 e711-717, doi:10.1053/j.gastro.2011.04.043 (2011).
85 Wu, C. Y. *et al.* PI3K regulation of RAC1 is required for KRAS-induced pancreatic tumorigenesis in mice. *Gastroenterology* **147**, 1405-1416 e1407, doi:10.1053/j.gastro.2014.08.032

S0016-5085(14)01071-3 [pii] (2014).
86 Lee, R. C., Feinbaum, R. L. & Ambros, V. The C. elegans heterochronic gene lin-4 encodes small RNAs with antisense complementarity to lin-14. *Cell* **75**, 843-854 (1993).
87 Guo, S. & Kemphues, K. J. par-1, a gene required for establishing polarity in C. elegans embryos, encodes a putative Ser/Thr kinase that is asymmetrically distributed. *Cell* **81**, 611-620 (1995).
88 Fire, A. *et al.* Potent and specific genetic interference by double-stranded RNA in Caenorhabditis elegans. *Nature* **391**, 806-811, doi:10.1038/35888 (1998).
89 Carthew, R. W. & Sontheimer, E. J. Origins and Mechanisms of miRNAs and siRNAs. *Cell* **136**, 642-655, doi:10.1016/j.cell.2009.01.035 (2009).

90 Schwarz, D. S. *et al.* Asymmetry in the assembly of the RNAi enzyme complex. *Cell* **115**, 199-208 (2003).
91 Brummelkamp, T. R., Bernards, R. & Agami, R. A system for stable expression of short interfering RNAs in mammalian cells. *Science* **296**, 550-553, doi:10.1126/science.1068999 (2002).
92 Boden, D. *et al.* Enhanced gene silencing of HIV-1 specific siRNA using microRNA designed hairpins. *Nucleic Acids Research* **32**, 1154-1158, doi:Doi 10.1093/Nar/Gkh278 (2004).
93 Dickins, R. A. *et al.* Probing tumor phenotypes using stable and regulated synthetic microRNA precursors. *Nature Genetics* **37**, 1289-1295, doi:Doi 10.1038/Ng1651 (2005).
94 Olive, K. P. *et al.* Mutant p53 gain of function in two mouse models of Li-Fraumeni syndrome. *Cell* **119**, 847-860, doi:S0092867404010463 [pii]

10.1016/j.cell.2004.11.004 (2004).
95 Premsrirut, P. K. *et al.* A Rapid and Scalable System for Studying Gene Function in Mice Using Conditional RNA Interference. *Cell* **145**, 145-158, doi:DOI 10.1016/j.cell.2011.03.012 (2011).
96 Saborowski, M. *et al.* A modular and flexible ESC-based mouse model of pancreatic cancer. *Genes Dev* **28**, 85-97, doi:10.1101/gad.232082.113 (2014).
97 Galabova-Kovacs, G. *et al.* ERK and beyond: insights from B-Raf and Raf-1 conditional knockouts. *Cell Cycle* **5**, 1514-1518 (2006).
98 Blasco, R. B. *et al.* c-Raf, but not B-Raf, is essential for development of K-Ras oncogene-driven non-small cell lung carcinoma. *Cancer Cell* **19**, 652-663, doi:10.1016/j.ccr.2011.04.002 (2011).
99 Giroux, S. *et al.* Embryonic death of Mek1-deficient mice reveals a role for this kinase in angiogenesis in the labyrinthine region of the placenta. *Current Biology* **9**, 369-372, doi:Doi 10.1016/S0960-9822(99)80164-X (1999).
100 Belanger, L. F. *et al.* Mek2 is dispensable for mouse growth and development. *Molecular and Cellular Biology* **23**, 4778-4787, doi:Doi 10.1128/Mcb.23.14.4778-4787.2003 (2003).
101 Voisin, L. *et al.* Activation of MEK1 or MEK2 isoform is sufficient to fully transform intestinal epithelial cells and induce the formation of metastatic tumors. *Bmc Cancer* **8**, 337, doi:10.1186/1471-2407-8-337 (2008).
102 Scholl, F. A. *et al.* Selective Role for Mek1 but not Mek2 in the Induction of Epidermal Neoplasia. *Cancer Res.* **69**, 3772-3778, doi:Doi 10.1158/0008-5472.Can-08-1963 (2009).
103 Gailhouste, L. *et al.* RNAi-mediated MEK1 knock-down prevents ERK1/2 activation and abolishes human hepatocarcinoma growth in vitro and in vivo. *International Journal of Cancer* **126**, 1367-1377, doi:Doi 10.1002/Ijc.24950 (2010).
104 Lee, C. S. *et al.* MEK2 Is Sufficient but Not Necessary for Proliferation and Anchorage-Independent Growth of SK-MEL-28 Melanoma Cells. *Plos One* **6**, doi:ARTN e17165

DOI 10.1371/journal.pone.0017165 (2011).
105 Catalanotti, F. *et al.* A Mek1-Mek2 heterodimer determines the strength and duration of the Erk signal. *Nat Struct Mol Biol* **16**, 294-303, doi:10.1038/nsmb.1564 (2009).
106 Yoshida, S. *et al.* Pancreatic stellate cells (PSCs) express cyclooxygenase-2 (COX-2) and pancreatic cancer stimulates COX-2 in PSCs. *Mol Cancer* **4**, 27, doi:10.1186/1476-4598-4-27 (2005).
107 Daniluk, J. *et al.* An NF-kappaB pathway-mediated positive feedback loop amplifies Ras activity to pathological levels in mice. *J Clin Invest* **122**, 1519-1528, doi:10.1172/JCI59743 (2012).
108 Boj, S. F. *et al.* Organoid models of human and mouse ductal pancreatic cancer. *Cell* **160**, 324-338, doi:10.1016/j.cell.2014.12.021 (2015).
109 Liou, G. Y. *et al.* Macrophage-secreted cytokines drive pancreatic acinar-to-ductal metaplasia through NF-kappaB and MMPs. *J Cell Biol* **202**, 563-577, doi:10.1083/jcb.201301001 (2013).

110 Liou, G. Y. *et al.* Mutant KRAS-induced expression of ICAM-1 in pancreatic acinar cells causes attraction of macrophages to expedite the formation of precancerous lesions. *Cancer Discov* **5**, 52-63, doi:10.1158/2159-8290.CD-14-0474 (2015).
111 McAllister, F. *et al.* Oncogenic Kras activates a hematopoietic-to-epithelial IL-17 signaling axis in preinvasive pancreatic neoplasia. *Cancer Cell* **25**, 621-637, doi:10.1016/j.ccr.2014.03.014 (2014).
112 Pylayeva-Gupta, Y., Lee, K. E., Hajdu, C. H., Miller, G. & Bar-Sagi, D. Oncogenic Kras-induced GM-CSF production promotes the development of pancreatic neoplasia. *Cancer Cell* **21**, 836-847, doi:10.1016/j.ccr.2012.04.024 (2012).
113 Bayne, L. J. *et al.* Tumor-derived granulocyte-macrophage colony-stimulating factor regulates myeloid inflammation and T cell immunity in pancreatic cancer. *Cancer Cell* **21**, 822-835, doi:10.1016/j.ccr.2012.04.025 (2012).
114 Fellmann, C. *et al.* Functional identification of optimized RNAi triggers using a massively parallel sensor assay. *Molecular cell* **41**, 733-746, doi:10.1016/j.molcel.2011.02.008 (2011).
115 Myburgh, R. *et al.* Optimization of Critical Hairpin Features Allows miRNA-based Gene Knockdown Upon Single-copy Transduction. *Molecular therapy. Nucleic acids* **3**, e207, doi:10.1038/mtna.2014.58 (2014).
116 Kambhampati, S., Park, W. & Habtezion, A. Pharmacologic therapy for acute pancreatitis. *World J Gastroenterol* **20**, 16868-16880, doi:10.3748/wjg.v20.i45.16868 (2014).
117 Grammer, T. C. & Blenis, J. Evidence for MEK-independent pathways regulating the prolonged activation of the ERK-MAP kinases. *Oncogene* **14**, 1635-1642, doi:DOI 10.1038/sj.onc.1201000 (1997).
118 Jeffrey, K. L., Camps, M., Rommel, C. & Mackay, C. R. Targeting dual-specificity phosphatases: manipulating MAP kinase signalling and immune responses. *Nat Rev Drug Discov* **6**, 391-403, doi:10.1038/nrd2289 (2007).
119 Wagner, M. *et al.* Transgenic overexpression of amphiregulin induces a mitogenic response selectively in pancreatic duct cells. *Gastroenterology* **122**, 1898-1912 (2002).
120 Sawey, E. T., Johnson, J. A. & Crawford, H. C. Matrix metalloproteinase 7 controls pancreatic acinar cell transdifferentiation by activating the Notch signaling pathway. *P Natl Acad Sci USA* **104**, 19327-19332, doi:DOI 10.1073/pnas.0705953104 (2007).
121 Liou, G. Y. *et al.* Protein kinase D1 drives pancreatic acinar cell reprogramming and progression to intraepithelial neoplasia. *Nat Commun* **6**, 6200, doi:10.1038/ncomms7200 (2015).
122 Avila, J. L., Troutman, S., Durham, A. & Kissil, J. L. Notch1 is not required for acinar-to-ductal metaplasia in a model of Kras-induced pancreatic ductal adenocarcinoma. *Plos One* **7**, e52133, doi:10.1371/journal.pone.0052133 (2012).
123 Kohn, A. D., Summers, S. A., Birnbaum, M. J. & Roth, R. A. Expression of a constitutively active Akt Ser/Thr kinase in 3T3-L1 adipocytes stimulates glucose uptake and glucose transporter 4 translocation. *J Biol Chem* **271**, 31372-31378 (1996).
124 Fukuda, A. *et al.* Stat3 and MMP7 contribute to pancreatic ductal adenocarcinoma initiation and progression. *Cancer Cell* **19**, 441-455, doi:10.1016/j.ccr.2011.03.002 (2011).
125 Ray, K. C. *et al.* Heparin-binding epidermal growth factor-like growth factor eliminates constraints on activated Kras to promote rapid onset of pancreatic neoplasia. *Oncogene* **33**, 823-831, doi:10.1038/onc.2013.3 (2014).
126 Tremblay, I., Pare, E., Arsenault, D., Douziech, M. & Boucher, M. J. The MEK/ERK pathway promotes NOTCH signalling in pancreatic cancer cells. *Plos One* **8**, e85502, doi:10.1371/journal.pone.0085502 (2013).
127 Schettino, C., Bareschino, M. A., Ricci, V. & Ciardiello, F. Erlotinib: an EGF receptor tyrosine kinase inhibitor in non-small-cell lung cancer treatment. *Expert review of respiratory medicine* **2**, 167-178, doi:10.1586/17476348.2.2.167 (2008).

128 Levitzki, A. & Gazit, A. Tyrosine kinase inhibition: an approach to drug development. *Science* **267**, 1782-1788 (1995).
129 Corcoran, R. B. *et al.* STAT3 plays a critical role in KRAS-induced pancreatic tumorigenesis. *Cancer Res* **71**, 5020-5029, doi:10.1158/0008-5472.CAN-11-0908 (2011).
130 Lesina, M. *et al.* Stat3/Socs3 activation by IL-6 transsignaling promotes progression of pancreatic intraepithelial neoplasia and development of pancreatic cancer. *Cancer Cell* **19**, 456-469, doi:10.1016/j.ccr.2011.03.009 (2011).
131 Criscimanna, A., Coudriet, G. M., Gittes, G. K., Piganelli, J. D. & Esni, F. Activated macrophages create lineage-specific microenvironments for pancreatic acinar- and beta-cell regeneration in mice. *Gastroenterology* **147**, 1106-1118 e1111, doi:10.1053/j.gastro.2014.08.008 (2014).
132 van Dijk, E. L., Auger, H., Jaszczyszyn, Y. & Thermes, C. Ten years of next-generation sequencing technology. *Trends in genetics : TIG* **30**, 418-426, doi:10.1016/j.tig.2014.07.001 (2014).
133 Amundadottir, L. *et al.* Genome-wide association study identifies variants in the ABO locus associated with susceptibility to pancreatic cancer. *Nat Genet* **41**, 986-990, doi:10.1038/ng.429 (2009).
134 Petersen, G. M. *et al.* A genome-wide association study identifies pancreatic cancer susceptibility loci on chromosomes 13q22.1, 1q32.1 and 5p15.33. *Nat Genet* **42**, 224-228, doi:10.1038/ng.522 (2010).
135 Wolpin, B. M. *et al.* Genome-wide association study identifies multiple susceptibility loci for pancreatic cancer. *Nat Genet* **46**, 994-1000, doi:10.1038/ng.3052 (2014).
136 Liang, W. S. *et al.* Genome-Wide Characterization of Pancreatic Adenocarcinoma Patients Using Next Generation Sequencing. *Plos One* **7**, doi:ARTN e43192

DOI 10.1371/journal.pone.0043192 (2012).
137 Mardis, E. R. Applying next-generation sequencing to pancreatic cancer treatment. *Nat Rev Gastroenterol Hepatol* **9**, 477-486, doi:10.1038/nrgastro.2012.126 (2012).
138 Weissmueller, S. *et al.* Mutant p53 Drives Pancreatic Cancer Metastasis through Cell-Autonomous PDGF Receptor beta Signaling. *Cell* **157**, 382-394, doi:DOI 10.1016/j.cell.2014.01.066 (2014).
139 Yu, M. *et al.* RNA sequencing of pancreatic circulating tumour cells implicates WNT signalling in metastasis. *Nature* **487**, 510-U130, doi:Doi 10.1038/Nature11217 (2012).
140 Rhim, A. D. *et al.* EMT and dissemination precede pancreatic tumor formation. *Cell* **148**, 349-361, doi:10.1016/j.cell.2011.11.025 (2012).
141 Wang, L. D. *et al.* Oncogenic Function of ATDC in Pancreatic Cancer through Wnt Pathway Activation and beta-Catenin Stabilization. *Cancer Cell* **15**, 207-219, doi:DOI 10.1016/j.ccr.2009.01.018 (2009).